Photo source: NHC

Yukon Regional Flow Frequency Analysis and Empirical Equation Development
Final Report

Prepared by:

Northwest Hydraulic Consultants Ltd.
30 Gostick Place
North Vancouver, BC V7M 3G3
Tel: (604) 980-6011
www.nhcweb.com

NHC Project Contact:
Piotr Kuraś, PEng
Principal

Prepared for:

Government of Yukon
Box 2703
Whitehorse, Yukon, Y1A 2C6

May 9, 2023
Final Report, Rev. 0

NHC Reference 3007020

Document Tracking

Date	Revision No.	Reviewer(s)	Issued for
2022-06-07	R0	Piotr Kuraś	25% draft client review
2022-10-04	R0	Piotr Kuraś	50% draft client review
2023-03-01	R0	Jane Bachman, Malcolm Leytham, Piotr Kuraś	75% draft client review
2023-04-26	R0	Piotr Kuraś	95% draft client review
2023-05-09	R0	Piotr Kuraś	Final Report

Report prepared by:

Genevieve Brown
May 3, 2023

Genevieve Brown, MASc, PEng (BC)
Hydrologist

L Bawagan May 3, 2023

Lucia Marie Bawagan, MWS, GIT (BC)
Hydrologist

Mariza Costa Cabral
May 3, 2023

Mariza Costa Cabral, PhD
Senior Climate Change Scientist

Report reviewed by:

PROFESSIONAL ENGINEER
YUKON TERRITORY
PIOTR KURAŚ
1889
20230503

Piotr Kuraś, MASc, PEng (YT, BC)
Principal Hydrologist

PERMIT TO PRACTICE
NORTHWEST HYDRAULIC CONSULTANTS
SIGNATURE
Date May 4th 2023
PERMIT NUMBER PP043
Association of Professional Engineers of Yukon

DISCLAIMER

This report has been prepared by **Northwest Hydraulic Consultants Ltd.** for the benefit of **Government of Yukon** for specific application to the **Yukon Regional Flow Frequency Analysis Project**. The information and data contained herein represent **Northwest Hydraulic Consultants Ltd.** best professional judgment in light of the knowledge and information available to **Northwest Hydraulic Consultants Ltd.** at the time of preparation, and was prepared in accordance with generally accepted engineering and geoscience practices.

Except as required by law, this report and the information and data contained herein are to be treated as confidential and may be used and relied upon only by **Government of Yukon**, its officers and employees. **Northwest Hydraulic Consultants Ltd.** denies any liability whatsoever to other parties who may obtain access to this report for any injury, loss or damage suffered by such parties arising from their use of, or reliance upon, this report or any of its contents.

CREDITS AND ACKNOWLEDGEMENTS

The authors would like to thank the Government of Yukon (YG) for initiating this study and for the support provided during the project, in particular:

- Tyler Williams — Water Resources Scientist, Water Resources Branch, YG
- Holly Goulding — Senior Scientist – Hydrology, Water Resources Branch, YG
- Benoit Turcotte — Senior Research Professional - Hydrology, Yukon University
- Darryl Cann — Environmental Coordinator, Transportation Engineering, YG
- Alexandre Mischler — Hydrology Technologist, Water Resources Branch, YG
- Jonathan Kolot — Hydrology Technologist, Water Resources Branch, YG
- Anthony Bier — Senior Hydrologist, Water Resources Branch, YG

The following NHC personnel (sorted alphabetically) participated in the study:

- Elizabeth Baird — Hydrologist, NHC
- Lucia Marie Bawagan — Hydrologist, NHC
- Genevieve Brown — Hydrologist, NHC
- Mariza Costa Cabral — Senior Climate Change Scientist, NHC
- Lance Costain — Water Resources Engineering Technologist, NHC
- Joe Drechsler — GIS Analyst, NHC
- Piotr Kuraś — Principal Hydrologist, NHC
- Anjali Kuruppu — Engineering Co-op Student, NHC

NHC partnered with EDI Environmental Dynamics Inc. and Klondike H2O Sampling on basin delineation:

- Pat Tobler — Regional Director/Senior Biologist, EDI
- Haylee Beeman — Environmental Technician, Klondike H2O Sampling
- Simon Nagano — Klondike H20 Sampling

EXECUTIVE SUMMARY

The objective of this study is to provide an updated methodology for estimating the magnitude of peak flows across the Yukon to support the design and assessment of transportation infrastructure, water crossings, conveyance structures, and other water resource projects. Streamflow records within the Yukon are sparse. In the absence of observed records, regionalization methods developed as part of this study can be used to estimate peak flows at ungauged locations.

The scope of work for this study includes:

- Compilation of streamflow data and basin characteristics across the Yukon and extending into British Columbia, Alaska, and the Northwest Territories
- Frequency analysis of peak flows for gauged locations
- Development of peak flow regions and methods for estimating peak flows based on regression analysis and basin drainage area scaling
- Guidance for considering climate change and the potential impact of climate change on peak flows.

Streamflow data through 2021 was compiled for gauges from the Water Survey of Canada, United States Geological Survey and Yukon Government Water Resources Branch with at least 10 years of instantaneous or daily data. When applicable, gaps in the instantaneous data were infilled based on the daily to instantaneous relationship at a gauge or area-based scaling of upstream gauges. Flood frequency estimates were calculated for 253 gauges based on two related distributions depending on the length of available record. A Log-Normal distribution was used when there was less than 20 years of available data, whereas a Log-Pearson Type III distribution was used when there was more than 20 years.

Six primary peak flow regions were developed for the study area based on North American Ecoregion Level 3 regions. Regional regression equations for each peak flow region were developed using explanatory basin characteristics including physical and climatic variables. An ordinary least square regression was used to determine the combination of basin characteristics for each peak flow region. Final equations were developed using generalized least squares regression. Results from the Northern Region and Interior Mountains should be used with caution due to the limited number of stations available to develop peak flow regressions. Fitted skews from stations with more than 25 years of data were explored by peak flow region and in space. Given the sparsity of data within the study area, a regional skew adjustment was not included in this study. An analysis of area scaling coefficients was also undertaken, with a range of appropriate coefficients provided for the six peak flow regions.

Climate change projections and potential impacts to peak flows were examined. Overall, climate change has the potential to significantly alter peak flows within the Yukon. This is due to the complexity of how changes in precipitation and temperature impact streamflow, which is not only due to changes in snowmelt and rainfall but also landscape changes such as permafrost thaw.

The outcomes of this work are:

- The results of hydrological, statistical, and GIS analyses to estimate daily and instantaneous peak flows for gauged and ungauged sites.

- Guidance on limits to future applicability of peak flow frequency analyses and regional equations due to the projected effects of climate change including methods to help understand potential changes to peak flows, and
- A spreadsheet tool for users to apply the regional frequency analysis.

It is recommended that users of the results of this study rely on a qualified Registrant for the interpretation and application of the study results. The results of this study have a limited lifetime, with a review recommended in 5 years and an update in 10 years.

TABLE OF CONTENTS

LIST OF TABLES IN TEXT

LIST OF FIGURES IN TEXT

APPENDICES

ABBREVIATIONS

Acronym / Abbreviation	Definition
BC	British Columbia
CMIP6	Coupled Model Intercomparison Project Phase 6
DEM	Digital Elevation Model
EMA	Expected Moments Algorithm
FLNRORD	Ministry of Forests, lands, Natural Resource Operations and Rural Development
GLS	Generalized Least Squares
LN	Log-Normal
LP3	Log-Pearson Type III
MAP	Mean Annual Precipitation
MAT	Mean Annual Temperature
NHD	National Hydrography Dataset
NHN	National Hydro Network
OLS	Ordinary Least Squares
RP	Return Period
SSP	Shared Socioeconomic Pathway
SWE	Snow Water Equivalent
USGS	United States Geological Survey
WREG	Weighted Multiple Linear Regression
WSC	Water Survey of Canada
YG WRB	Yukon Government Water Resources Branch

1 INTRODUCTION

Estimates of the magnitude and frequency of peak flows are required across the Yukon to support the design and assessment of transportation infrastructure, water crossings, conveyance structures, and other water resource projects. Peak flow statistics can be computed directly for a stream or river where a stream gauge with a suitable record length exists. Such stream gauges are sparse across the Yukon, leaving large areas underrepresented. For ungauged locations or locations with short streamflow records, regional regression equations can be developed based on basin characteristics to provide estimates of the magnitude and frequency of peak flows at those locations.

This report provides a methodology and associated resources for estimating peak flow statistics across the Yukon at both gauged and ungauged sites. The work builds on previously completed studies that cover all, or portions of the Yukon, using up-to-date streamflow data, spatial information, and computational techniques to estimate peak flow statistics and consider the potential impacts of climate change.

It is recommended that users of the results of this study rely on a qualified Registrant for the interpretation and application of the study results. The user should refer to limitations of the study which are discussed in Section 3.3, 4.7, and 5.4.

1.1 Objectives and Scope

The objective of this work is to provide an updated methodology and computational resources for estimating the magnitude and frequency of peak flows across the Yukon. The outcome of this work includes:

- The results of hydrological, statistical, and GIS analyses to estimate daily and instantaneous peak flows for gauged and ungauged sites.
- Guidance on limits to future applicability of peak flow frequency analyses and regional equations due to the projected effects of climate change and methods to help understand potential changes to peak flows.
- A spreadsheet tool for users to apply the regional frequency analysis.

The study results include peak instantaneous and daily estimates up to the 200-year peak flow, where data record length allows. Approved historical data and preliminary data up until the end of 2021 (as available) is considered in the analysis.

Within the study region, peak water levels do not necessarily correspond to peak discharge levels. The formation and breakup of river ice along with events that can restrict flow (e.g., beaver dams, landslides etc.) can result in water levels higher than what would be associated with open, unimpeded discharge. For this study, hydrometric data is limited to peak instantaneous and daily discharge records, mainly associated with rain and snowmelt runoff, and not water levels.

1.2 Study Area

The primary area of focus for this study is the Yukon Territory, Canada. The study boundaries include portions of the Northwest Territories, northern British Columbia, and Alaska. When defining peak flow regions, there is no physical justification to constrain regions to political boundaries. The hydrologic boundary for the project is based on Water Survey of Canada (WSC) subdrainage areas which cross the Yukon border or are adjacent to it. The location and extent of the study area are shown in Figure 1.1. The study area covers portions of the major drainage basins of the Yukon River (including the Porcupine River), Liard River, Mackenzie River, Peel River, Alsek River, and Copper River.

The study area covers more than 1.3 million km^2 and encompasses many diverse physical and climatic settings which directly influence the local hydrologic responses throughout the study area. Topography within the study area ranges from the low relief Yukon Coastal Lowland along the Beaufort Sea to the high elevation mountains of the Coast, St. Elias, and Alaska ranges in the southwest. A number of lowlands, plateaus, and mountain ranges separate these two extremes (Smith et al., 2004).

The climate over the study area varies with location and physiography (Wang et al., 2012). The Coast Mountains in the southwest receive the greatest amount of precipitation, with some areas receiving over 3,000 mm of annual precipitation. The central Yukon basin and northern portions of the study area receive much less precipitation with mean annual precipitation in the range of 200 to 300 mm in low lying areas and increasing over the Ogilvie and Mackenzie mountains to 500 to 800 mm. Mean annual temperature varies with latitude and elevation with mean annual temperatures ranging from 0°C on the southwest coast to -10°C at the northern extents.

Permafrost occurs throughout the entire study region, ranging from the extensive continuous permafrost zone (>90% areal coverage) in the north to the sporadic discontinuous zone (10-50% areal coverage) and isolated patches (<10% areal coverage) in the south (Obu et al., 2019). Streamflow response to the presence of permafrost and permafrost thaw is complex but plays an important role in the hydrologic response of the study area (Hinzman et al., 2003; Janowicz, 2008; Janowicz et al., 2016). The permafrost extent as well as active layer thickness can control the peak response, with the presence of permafrost contributing to a high runoff ratio due to diminished subsurface storage (Kane and Yang, 2004; McNamara et al., 1998).

Given the wide range of physical and climatic settings, several different processes generate peak flows within the study area including snowmelt, glacial melt, rain on snow, and rainfall. In most of the study basins, annual peak flows occur in the late spring and early summer due to snowmelt (freshet). In basins with glacier coverage, annual peak flows can occur later in the summer due to increased melt from high elevation snow cover and glaciers. Peak flows due to glacial melt are a different process than glacial outbursts which are a sudden release of water due to the failure of a moraine or ice-dam glacial lake. Rainfall related peaks can occur in the summer and fall, especially in smaller and more mountainous basins. Within the study area, ice jams and icing (or aufeis) can cause peak annual water levels; however, these are typically associated with a lower discharge and are therefore not considered in this study.

Yukon

nhc
northwest hydraulic consultants

WSC Subdrainage Area
Yukon Boundary
Study Area

DATA SOURCES: WSC Sub Drainage Areas (2016), Background - ESRI World Topographic Map

SCALE - 1:6,309,138
0 100 200 km
N

Coordinate System: NAD 1983 CSRS BC ENVIRONMENT ALBERS

Job: 3007020 | *Date: 04-MAY-2023*

YUKON REGIONAL FLOW ANALYSIS
Location and Extent of Study Area

FIGURE 1.1

ABC: \\mainfile-van\Projects\Active\3007020 Yukon Regional Flow Analysis\95 GIS\3007020_GMWB_FinalRptFigures.aprx

Projected changes in seasonal mean and extreme values of temperature and precipitation will affect watershed hydrology and the generation of peak flows. Changes in temperature and precipitation have already been observed across the Yukon over the past 50 years. The average air temperature in the winter season has increased markedly over the past five decades, by an estimated 4°C. Mean temperature rise was less in the other seasons, and the estimated mean annual rise is about 2°C (Perrin and Jolkowski, 2022).

Annual precipitation is also expected to increase by 10 to 20% by the end-of-century with increases also expected in extreme rainfall events (Perrin and Jolkowski, 2022) . Degradation of permafrost, continued loss of glacier mass, changes in the ratio of snowfall to rainfall, and changes in melt timing and magnitude will all influence the hydrologic response across the study area, leading to conditions outside the range of historical observations.

1.3 Previous Studies

Several peak flow studies have been previously completed that cover portions of the study area. This section provides an overview of these previous studies to provide context and background to this report.

Peak flow studies that focused specifically on the Yukon were conducted by Janowicz (1986, 1989). Both studies focused on the area south of the Ogilvie Mountains, as available data further north was limited and indicated a different hydrologic response than the southern basins, presumably due to underlying permafrost. The studies were based on gauges with at least 6 years of data primarily in the Yukon with select gauges from British Columbia and Alaska included in the analysis. The single station frequency analysis fit a two-parameter lognormal distribution to each station. Regionalization in the two studies varied slightly. Janowicz (1986) defined two regions: the Interior region and Western Mountains region, which included both the Coast and St. Elias Mountains. During development of the regional peak flow equations, basins with significant storage due to lakes or wetlands were found to contribute to the outliers and were grouped into a third “region”. Equations for estimating peak flows from the mean annual flood to the 100-year peak flow were developed using watershed area and a storage factor. Janowicz (1989) simplified the regionalization with only an Interior and Mountain region defined. Instead of spatial location, regions were defined based on stream channel slopes greater or less than 4.5%. A relationship between peak flow and drainage area was developed for peaks flows of different return periods, from the mean annual flood to the 100-year peak flow.

The USGS has also completed multiple peak flow studies for Alaska and conterminous basins in Canada (Curran et al., 2003, 2016; Jones and Fahl, 1994). The latest study (Curran et al., 2016) builds on work from 2003 (Curran et al., 2003) and uses hydrometric data up until 2012. The study region includes the Yukon River basin and portions of the Coast Mountains and northern Brooks Range. Regionalization of previous studies from the USGS was examined, but ultimately all data was grouped together into one large region. Single station frequency analysis was performed for each station with at least 10 years of record that were not substantially influenced by regulation or urbanization. A Log-Pearson Type III (LP3) distribution was fit to each station using the expected moments algorithm (EMA) (Cohn et al., 1997) which incorporated censored flows (potentially influential low floods, zero flows etc.) and historical flows when available. Regional skew coefficients which help improve the accuracy of the skew estimator

for a gauge were developed for two regions within the study area which had an adequate density of stations with at least 25-years of data. The two regions cover portions of central Alaska and the southwest coast. For gauges outside of the regional skew areas, only the single station skew coefficient was used for computation of the frequency analysis. Regional regressions were developed for peak flow estimates from the 2-year to 500-year flows based on drainage area and mean annual precipitation. On the Yukon River where the drainage area exceeded 80,500 km^2, regressions were not recommended for peak flow estimation. Instead, station-based estimates and area scaling should be used for peak flow estimation.

More recently, the British Columbia (BC) Ministry of Forests, Lands, Natural Resource Operations and Rural Development (FLNRORD) – now the BC Ministry of Forests – completed the British Columbia Extreme Flood Project (NHC, 2021). The project extents cover British Columbia and portions of southern Yukon and Alaska as well as Alberta, Washington, Idaho, and Montana. Regionalization was based on the Ecoprovince boundaries from the Ecological Land Classification (Statistics Canada, 2017) and resulted in eight regions. Single station frequency analysis was performed on 1-, 3-, 5-, and 10-day peak flow data for stations with at least 10-years of data. Three distributions (Log-Normal (LN), LP3, and mixed LP3) were fit to the data using EMA to incorporate censored flows and historical flows when available. A regional skew correction was not used in the analysis. Regional regressions were developed for peak flow estimates from the 10-year up to the 200-year based on drainage area, mean annual precipitation, and median basin elevation. Scaling exponents for area-based scaling from proxy basins were also provided for each region.

2 DATA COMPILATION

Streamflow data was compiled for the study area along with basin characteristics and supporting analysis including determining the degree of regulation and infilling streamflow data sets. The following section summarizes the data sources and methods used.

2.1 Streamflow Gauge Data

Hydrometric data within the study area is available from the following sources:

- Water Survey of Canada (WSC)
    - WSC collects and disseminates surface water quantity data in the Yukon and Canada through cooperative partnerships with territorial and provincial governments.
- Yukon Government Water Resources Branch (YG WRB)
    - The YG WRB performs numerous roles, including water quality and quantity monitoring and research in the Yukon.
- United States Geological Survey (USGS)
    - The USGS is the United States national authority responsible for the collection and dissemination of water resource data in Alaska.

The peak flow analysis uses annual daily maximum[1] and annual instantaneous maximum data from the different sources. Initially, gauges with at least 10 years of daily or instantaneous data were included for analysis, resulting in 275 gauges (Figure 2.1). Within the study region, peak water levels do not necessarily correspond to peak discharge. For this study, the analysis is limited to peak instantaneous and daily discharge records and not water levels. Annual peak data is based on the calendar year, which is due to the standard format that the WSC provides instantaneous peak data. The inclusion of gauges in the single station frequency analysis and regional frequency analysis is further discussed in Section 3.1.

[1] WSC's annual daily maximums are based on a calendar day, not a rolling average

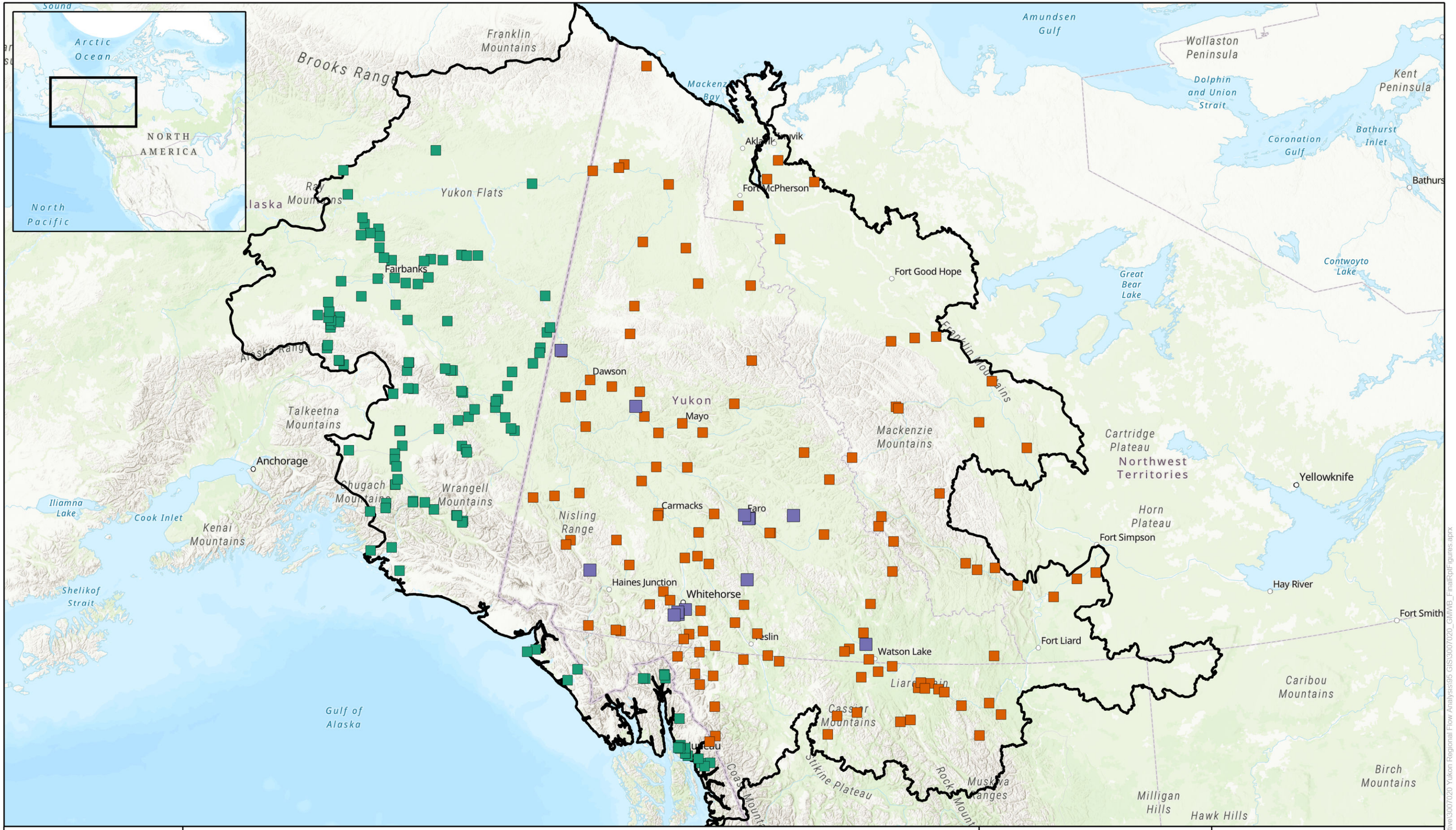

Yukon

nhc
northwest hydraulic consultants

Study Gauges

- USGS
- WSC
- YG WRB
- Study Area

DATA SOURCES:
Background - ESRI World Topographic Map

SCALE - 1:6,309,138
0 100 200 km
N

Coordinate System: NAD 1983 CSRS BC ENVIRONMENT ALBERS

Job: 3007020 | Date: 04-MAY-2023

YUKON REGIONAL FLOW ANALYSIS
Study Gauges for Single Station Frequency Analysis

FIGURE 2.1

ABC: \\mainfile-van\Projects\Active\3007020 Yukon Regional Flow Analysis\95 GIS\3007020_GMWB_FinalRptFigures.aprx

Data for the WSC was obtained from the WSC hydat database (WSC, 2022) using the 'tidyhydat' package (Albers, 2017) in the statistical programming language R. Annual instantaneous peaks are reported by the WSC within the HYDAT database. The annual statistics provided by WSC were used to determine the annual daily peaks for each gauge. Provisional data for gauges up until December 2021 was obtained directly from the WSC. All data was reviewed for any anomalous values and any zero values were removed. Annual maxima that had been flagged as ice affected ('B') were removed from the data set.

Data for the USGS was obtained using the USGS hydrologic data package 'dataRetrieval' (De Cicco et al., 2018). Annual instantaneous peaks are reported directly by the USGS; while annual daily peaks were obtained for each gauge based on the available daily flow data. Unlike the WSC which uses a calendar year reporting system, the instantaneous peaks reported by the USGS are reported on a water-year basis (October 1 to September 30). The dates of the instantaneous peaks from the USGS were converted to a calendar year basis. In some instances, two water year peaks can occur within the same calendar year. In these cases, the larger of the two peaks was taken as the annual maximum peak. The daily data was reviewed visually for years with incomplete records. If it could not be determined that the annual daily maximum was in fact the annual maximum (i.e., short gauging period that year, gauge starting on a peak) the annual maximum for that year was removed. The data was reviewed for any anomalous values and any data points flagged by the USGS as affected by dam failure were removed from the analysis. Instantaneous peak flows which the USGS had replaced with the daily peak flow (Code 1) were examined to check if the comparative values were similar to recorded instantaneous and daily peaks at that gauge.

Flow data for the YG WRB gauges was provided directly by the YG WRB. The instantaneous and daily data was analyzed to determine the annual instantaneous peak and annual daily peak. Where overlapping periods of instantaneous and daily data was provided, daily values were recalculated from the instantaneous data. The daily data was reviewed visually for years where data had been recalculated based on the instantaneous data and for years where a daily dataset was also provided by the YG WRB. If overlap between the YG WRB daily data and the recalculated daily annual peaks was present in the same year, the larger of the two peaks was taken as the maximum annual daily peak. Since most YG WRB gauges operate seasonally, NHC undertook an overview-level review of the peak flow data. Years where the true peak was potentially not captured by the gauge (e.g., gauge record started after spring freshet) were excluded from the analysis. Streamflow data is not a variable that is directly measured by the USGS, WSC or YG WRB. Instead, stage is measured and related to flow through a stage-discharge relationship. All aspects of the calculation of flow, from the stage and flow measurements to the development of the stage-discharge relationship (i.e., rating curve), introduce a level of uncertainty into the streamflow data. While data uncertainty is qualified by the USGS, WSC, and YG WRB, the level of uncertainty associated with the calculated streamflow time series data is not quantified. To better understand the potential uncertainty in the underlying peak flow data, the data flags which were assigned to the streamflow data by the agency were maintained and indicated in the single station frequency analysis. Table 2.1 summarizes the data codes from the various agencies.

Table 2.1 Summary of agency data flags

Agency	Code	Description
WSC	E	Estimate – no available information for day or period, streamflow was estimated using alternative methods (interpolation, extrapolation, comparison with other streams, or by correlation to meteorological data, etc.)
	A	Partial Day – daily mean streamflow was estimated despite gaps of more than 120 minutes in the data string, or missing data was not significant enough to warrant use of an E flag
	B	Ice Conditions – streamflow value was estimated due to the presence of ice in the stream
USGS	1	Discharge is a Maximum Daily Average
	2	Discharge is an Estimate
	3	Discharge affected by Dam Failure
	4	Discharge less than indicated value which is Minimum Recordable Discharge at this site
	5	Discharge affected to unknown degree by Regulation or Diversion
	6	Discharge affected by Regulation or Diversion
	7	Discharge is a Historic Peak
	8	Discharge greater than indicated value
	9	Discharge due to Snowmelt, Hurricane, Ice-Jam or Debris Dam breakup
	Bd	Day of occurrence is unknown or not exact
	Bm	Month of occurrence is unknown or not exact
	A	Year of occurrence is unknown or not exact
	e	Only annual maximum peak available for this year
	P	Provisional data that is subject to revision
	R	Revised – a revision, correction, or addition has been made to the historical discharge database after 1 January 1989
YG WRB	2	Estimated
	-1/0	Unspecified or undefined– data periods have not been graded
	3	Low quality data grade based roughly on BC RISC hydrometric standards
	4	Medium quality data grade based roughly on BC RISC hydrometric standards
	99/-6	Incomplete Record – High water not captured (data grade prior to 2020 data)

2.2 Basin Characteristics

Basins used in the peak flow analysis were characterized to provide explanatory variables for the regional analysis (Section 4).

Where available, existing basin delineation was used from Environment and Climate Change Canada, (2020), USGS (Falcone, 2011), and BC FLNRORD (NHC, 2021). Basins without existing drainage areas were delineated by NHC using a 10 m DEM (Government of Canada, 2022; U.S. Geological Survey, 2020) to create a set of fundamental drainage areas in ArcHydro. Fundamental drainage areas are small subbasins derived from a stream network. Fundamental drainage areas upstream of each gauge were selected and merged into a single basin for that gauge. Where the resolution of the fundamental drainage area was coarser than the gauge drainage area or where the area extended downstream of the gauge, manual delineation techniques were instead used. When the gauge drainage area value provided by the gauge owner (WSC, USGS, or YG WRB) varied from the delineated polygon area by more than 10%, the drainage area was manually checked for discrepancies. In some cases, the gauge location did not match the outlet of the fundamental drainage area exactly. If the difference in drainage area was expected to be greater than 10% of the drainage area due to a mismatched gauge location, it was corrected to the actual gauge location. At the end of this process, 11 gauges of 275 have drainage areas that vary by more than 10% of the originally recorded area by the gauge owner (Table 2.2). In these instances, the drainage areas developed by NHC were adopted. A large difference (40%) was noted for Sloko River near Atlin. In this case, NHC contacted WSC directly and confirmed the location of the gauge from notes and drawings provided by WSC.

Table 2.2 Summary of gauges with drainage areas that vary by more than 10% from the owner delineated area

Gauge Owner	Gauge ID	Gauge Name	Owner Area (km^2)	NHC Area (km^2)	Relative Difference (%)
USGS	15470000	Chisana R at Northway Jct AK	7,666	8,553	12%
USGS	15516050	Jack R nr Cantwell AK	790	703	-11%
USGS	15541600	Globe C nr Livengood AK	59.8	67.4	13%
USGS	15472100	Porcupine C nr Tetlin Junction AK	21.1	23.3	11%
USGS	15201100	L Nelchina R tr nr Eureka Lodge AK	21.5	18.3	-15%
USGS	15476049	Tanana R Tr nr Cathedral Rapids AK	7.3	8.1	11%
USGS	15305920	Wf tr nr Tetlin Junction AK	2.6	2.9	12%
WSC	10LD002	Jackfish Creek near Fort Good Hope	62.9	69.8	11%
WSC	08BB002	Sloko River near Atlin	427	254	-40%
YGRB	29AD003	Rose River	942	843	-11%
YGRB	30BE003	Cosh Creek	33.0	28.3	-14%

For each drainage area, characteristics expected to influence the peak flow were compiled. Basin characteristics and their associated data sources are summarized in Table 2.3. In some cases, multiple data sources were used to extend the data into Alaska.

Table 2.3 Spatial data sources for basin characteristics (Canada and Alaska)

Basin Characteristic	Data Source
Median elevation, dominant aspect, average slope	Canadian DEM, US 3D Elevation Program
Land Cover (Forest, Wetland, Shrubland/Grassland/Tundra, Barren)	North America Land Cover Dataset (30 m resolution)
Permafrost Region (Continuous – 90-100%, Discontinuous 50-90%, Sporadic 10-50%, Isolated <10%)	(Obu, Jaroslav et al., 2018)
Surface Water Coverage (Lakes)	National Hydro Network (NHN), National Hydrography Dataset (NHD)
Glacial coverage	National Snow and Ice Data Center
Ecoregions	(Commission for Environmental Cooperation, 1997; Smith et al., 2004; Statistics Canada, 2017)
Mean annual precipitation	(Wang et al., 2016)
Monthly precipitation	(Wang et al., 2016)
Winter precipitation (November to March)	(Wang et al., 2016)
Mean annual temperature	(Wang et al., 2016)
Monthly temperature	(Wang et al., 2016)

2.3 Degree of Regulation

WSC, USGS, and YG WRB classify rivers as regulated if a dam or control structure is present in the channel upstream of the gauge location. The degree of regulation will depend on the purpose of the structure which could include peak flow control, water supply, power generation, or a combination of purposes. Regulation can typically result in the alteration of the annual hydrograph with peak flows dampened, especially when the reservoir storage is large relative to the runoff volume (Graf, 1999). Regulation affects the natural flow regime and violates key assumptions for the application of frequency analysis.

An analysis was undertaken to determine the impact of regulation on gauges where regulation was present. Gauges were identified as potentially being regulated based on the regulation status (WSC), data flags (UGSS), and gauge description (YG WRB). Gauge names were also searched for keywords potentially associated with regulation such as “Dam”, “Outlet”, or “Powerhouse”. Dam locations were identified based on aerial imagery with the help of spatial water licence information. For each regulated gauge, the percent of watershed area controlled by regulation was determined as indicated:

$$\%\ of\ watershed\ area\ controlled\ by\ regulation = \sum^{i=n} \frac{AC_i}{AG}$$

where *AC* is the drainage basin area controlled by dam *i, AG* is the drainage area of the gauge, and *n* is the total number of dams. Gauging stations were considered impacted by regulation if the percent of basin area controlled by the dam was greater than 20% of the total basin area (NHC, 2021).

Regulation due to placer operations was also identified at some locations. Since placer operations are not typically expected to significantly impact peak flows the gauges were flagged as regulated, but a degree of regulation was not calculated.

2.4 Nonstandard and Historical Peak Flow Data

Flood frequency analyses commonly rely on the systematic flood record, consisting of measured annual peak discharge data collected at a hydrometric gauge site. EMA (Cohn et al., 1997) allows for other data sources including nonstandard and historical peak flow data to be incorporated into a frequency analysis, extending the record of a gauge or infilling record data gaps.

Non-standard data includes information during years for which it was known no peak equalled or exceeded a specific threshold value. This may be the result of streamflow measured at a crest stage gauge where the annual peak flow is known to not have exceeded the crest base at the gauge and the peak annual discharge is therefore less than the flow of the crest base. In other cases, a hydrometric gauge may have been overtopped, and the magnitude of the discharge above the maximum gauge measurement may not be known. Non-standard data can also include ranges of flows, where there is uncertainty in the measured peak.

Historical peak flow data are observations of peak flow outside of the systematic gauge record. This is typically used to describe estimates of peak flow prior to the establishment of a gauging station or after the decommissioning of a gauge. Historical peak flow data is also used to describe knowledge that no flood during a period (for example during a gap in a gauge record) exceeded some historical peak flow.

Both non-standard data and historical peak flow data are incorporated into an EMA flood frequency analysis using flow intervals and perception thresholds. Flow intervals consist of a lower (Q_L) and upper (Q_U) bound which describes the magnitude of discharge. For example, there may be uncertainty in a flow measurement and the true value is thought to lie between some lower (Q_L) and upper (Q_U) value. Perception thresholds are used to define the information in each year of the record in which a peak flow value would have been observed or recorded and are defined by a lower (T_L) and upper (T_U) threshold. For example, if during a gap in the gauge record, the flow is known to not have exceeded some large flood peak (e.g., 500 m^3/s), the perception thresholds during the gap could be set between a minimum flow value (T_L) and 500 m^3/s (T_U).

The WSC does not incorporate non-standard and historical peak flow data within their peak streamflow record; however, the USGS does provide such information. Annual peak flows may be indicated as a historical flow (Peak Code 7), as having a discharge less the indicated value, which is the minimum

recordable discharge at that site (Peak Code 4), or as having an actual discharge greater than the indicated value (Peak Code 8) (Table 2.1).

For all USGS gauges with peak flows indicated as less than or greater than the indicated value (Peak Code 4 and 8), flow intervals and perception thresholds were developed. USGS gauges with historical flows (Peak Code 7) were reviewed individually, prior to the development of flow intervals and perception thresholds. The historical peak flow code is potentially misleading as it not only refers to flows of particularly large floods but also to opportunistic gauging recorded outside of a streamflow record (Curran et al., 2016). All discharges with a historic peak flow code were reviewed and were omitted from the analysis if it could not be determined that the historic flow was large enough to potentially inform periods of missing data.

2.5 Data Infilling

Within a streamflow record, instantaneous annual peaks may not be reported while a daily annual peak is provided for a year. To supplement the instantaneous record the relationship between other recorded daily and instantaneous annual peaks can be used to estimate the instantaneous peak for the missing year. The analysis of the relationship between daily and instantaneous annual peaks was limited to stations with at least 10-years of concurrent data. Data was considered from the same event if the daily and instantaneous value occurred within 5 days of each other.

While instantaneous peaks can be infilled based on the relationship between recorded daily and instantaneous peaks, there is often uncertainty in this relationship. EMA can be used along with flow intervals to provide a range of flow when uncertainty in an estimated flow is high (England Jr. et al., 2019). For each gauge, the coefficient of variation was used to determine which stations have high uncertainty in the relationship between daily and instantaneous peaks. Where the coefficient of variation was greater than 25%, a range of flows was specified for infilled years. The upper flow range was based on the 95% prediction intervals from the relationship between instantaneous and daily peaks, while the lower flow range was based on the daily value (i.e., the instantaneous value can not be less than the daily value). Where the coefficient of variation was less than 25%, the infilled year was based on the slope fit (peaking factor) between the instantaneous and daily data (i.e., no flow intervals). The flow intervals for higher uncertainty points could then be incorporated into the frequency analysis using EMA.

For example, the Wolf Creek at Coal Lake gauge (YG WRB 29AB005) reports daily annual peaks from 1996 to 2021. However, instantaneous peaks are only recorded from 2010 to 2021 as shown in Figure 2.2. A linear relationship was obtained by linear regression of instantaneous peaks and daily peaks in the overlapping period from 1996 to 2021 with a 95% prediction interval (Figure 2.3). The prediction intervals along with the linear relationship based on observed instantaneous and daily peaks were then used to estimate the range of the unknown instantaneous peaks (Figure 2.4).

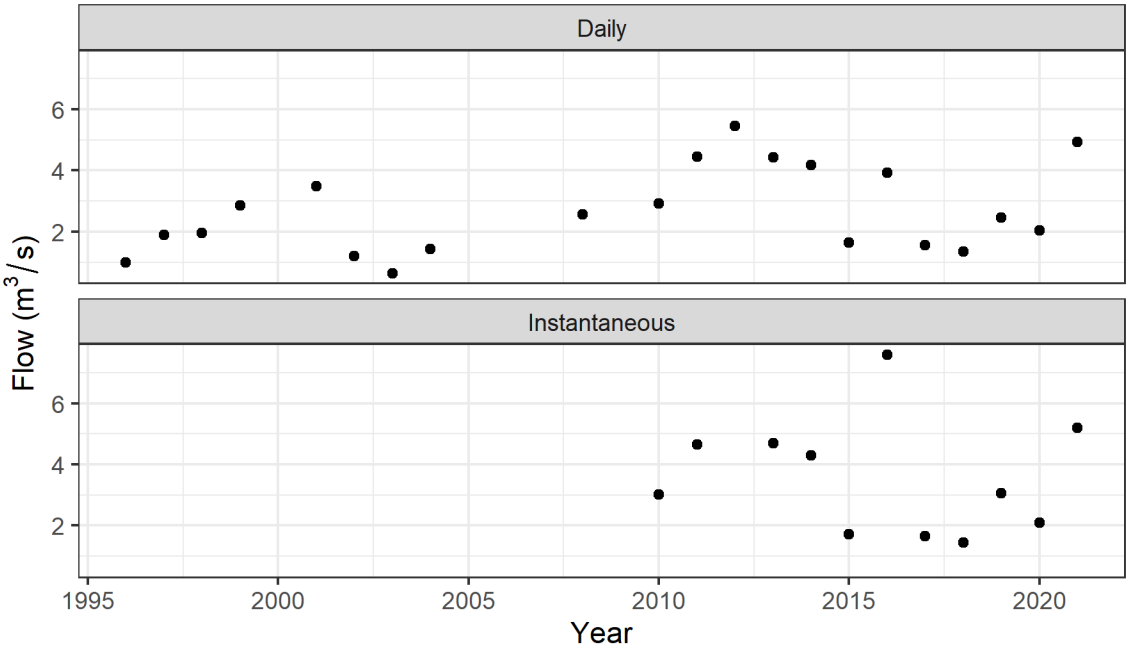

Figure 2.2 Annual daily and instantaneous peaks at Wolf Creek at Coal Lake (29AB005)

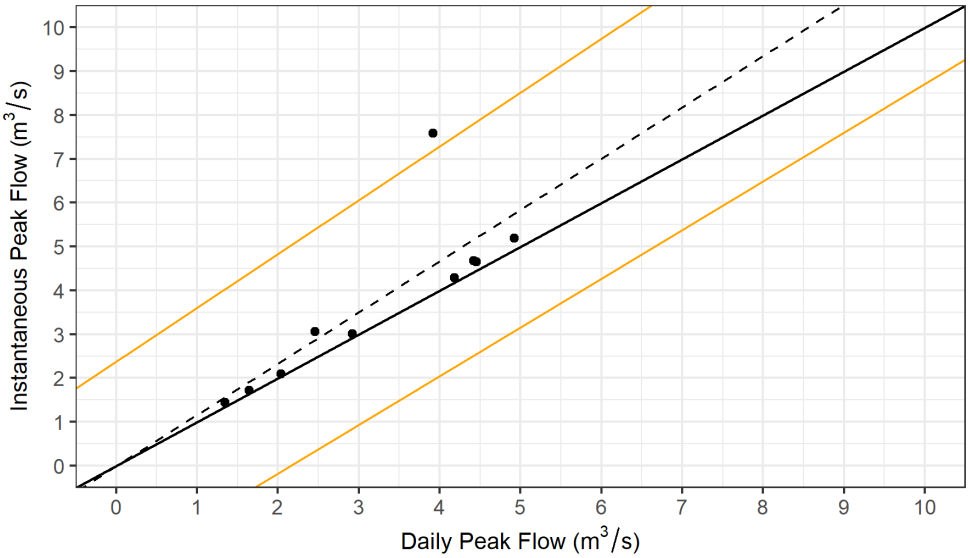

Figure 2.3 Relationship between recorded daily and instantaneous peaks at 29AB005. The dashed line indicates the linear relationship between the daily and instantaneous peaks, the orange lines indicate 95% prediction intervals, and the solid black line is the 1:1 relationship.

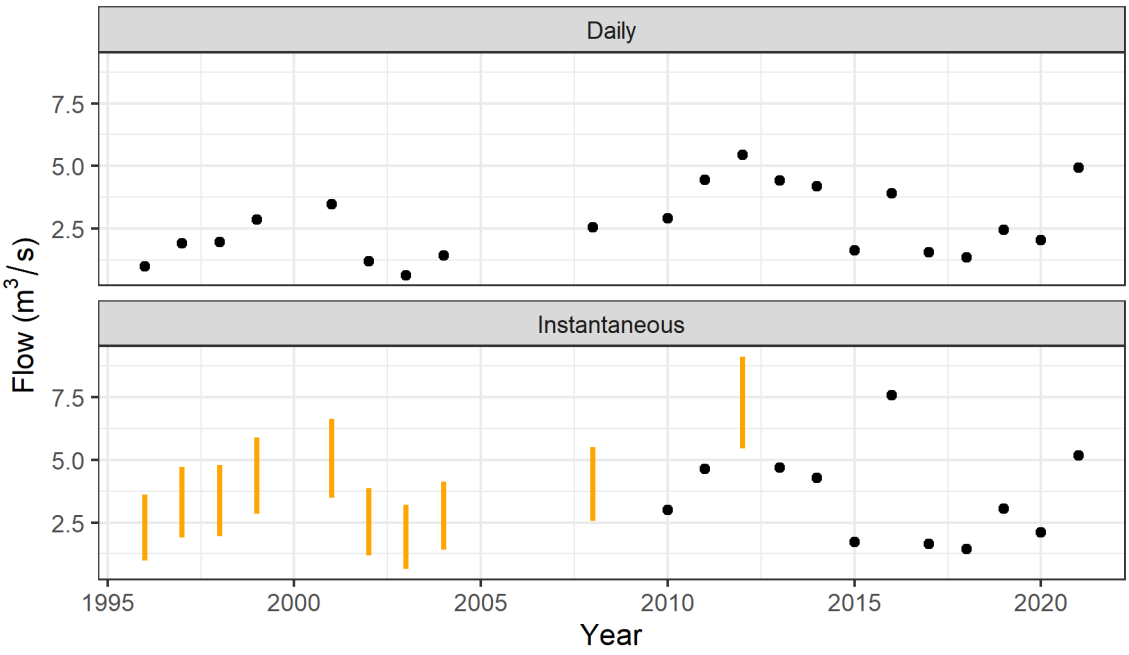

Figure 2.4 Annual daily peaks and infilled instantaneous peaks at 29AB005. Vertical orange lines indicate the range of possible discharge for the infilled instantaneous peaks.

Additional infilling of peak flows was included for nested gauges. Gauges which were nested (i.e., upstream and downstream of each other) were identified based on gauge name and location. Where the upstream gauge had a period of record different from the downstream gauge, the upstream gauge was used to infill the downstream gauge based on a simple area scaling relationship:

$$Q_{downstream} = Q_{upstream} \frac{A_{downstream}}{A_{upstream}}^{b}$$

where b was initially set at 1 but later updated based on the results from Section 4.6, depending on the region of the gauges.

3 FREQUENCY ANALYSIS AT GAUGED SITES

3.1 Gauge Inclusion

A single station frequency analysis was performed for 253 gauged locations. The criterion for inclusion in the single-station frequency analysis was having a record of at least 10 years of daily or instantaneous annual peaks. Gauges with drainage areas greater than 100,000 km^2 (primarily stations on the Liard and Yukon Rivers) were excluded from the single station frequency analysis (5 gauges) along with gauges that were greater than 20% regulated (14 gauges). Other gauges which were excluded from the single-station analysis were USGS 15209800, which appears to be an effluent discharge, and USGS 15201900, which has conflicting information on the gauge location and gauge area (Curran et al., 2003).

The WSC Tom Creek at Kilometre 43.9 Robert Campbell Highway (10AA002) station was also excluded from the single station frequency analysis. The YG WRB Tom Creek station (30AA003) is an extension of this WSC station after the YG WRB took over the original station operated by WSC. Only results from 30AA003, including the extended record, are provided in this study.

The WSC Kluane River at Outlet of Kluane Lake (09CA002) was included in the single station frequency analysis. The hydrologic response of the watershed has changed since 2016 following the diversion of the Slims River from Kluane Lake to Kaskawulsh River due to glacier retreat. Peak flows from the recent record are much lower than the previous historic record following the diversion, and data after 2016 is excluded from the frequency analysis. Historic data from 1953, 1967, 1970, and 1989 were also excluded from the frequency analysis as diversions to Kaskawulsh River as a result of ice (Loukili and Pomeroy, 2018). Data from this frequency analysis should be used with caution, with an understanding that the historic data no longer represents the current conditions.

3.2 Statistical Tests

Traditional flood frequency analysis assumes the series of annual peak flows is random, independent, stationary, and homogeneous. Statistical tests were used on the annual peak flows at each gauge to determine whether the peak flows were independent and stationary:

- Independence was tested by determining the lag-1 autocorrelation of each peak flow series. The lag-1 autocorrelation corresponds to the correlation between the values in a time series and the values in the same time series lagged by one time step (one year, in this case).
- Stationarity was tested using the Mann-Kendall test (Kendall, 1975) to determine whether the data follows a statistically significant monotonic trend with time. A significance of 0.05 was used to determine whether the Mann-Kendall statistic (tau) was significantly different from zero. Mann-Kendall's tau ranges from -1 to 1 and approaches 0 when no trend exists. A negative tau value indicates a declining trend whereas a positive tau value indicates a rising trend.

A significant trend in peak flows was observed at 21 of the 254 instantaneous annual peak series with 14 gauges showing a positive trend and 7 gauges showing a negative trend. It is difficult to attribute trends in the data to a single source. A trend may occur in the peak flow data due to changes in the basin such as regulation, land cover or land use change. Trends may also occur due to shorter term changes in

climate associated with natural climatic variability. Some trends may also be due in part to a changing climate. Type II errors may also result in the detection of trends because of limited sample length and large sample variance. Figure 3.1 shows the location of the gauges with significant trends within the study area. No underlying cause of any trend is apparent when considering the basin's spatial distribution and characteristics.

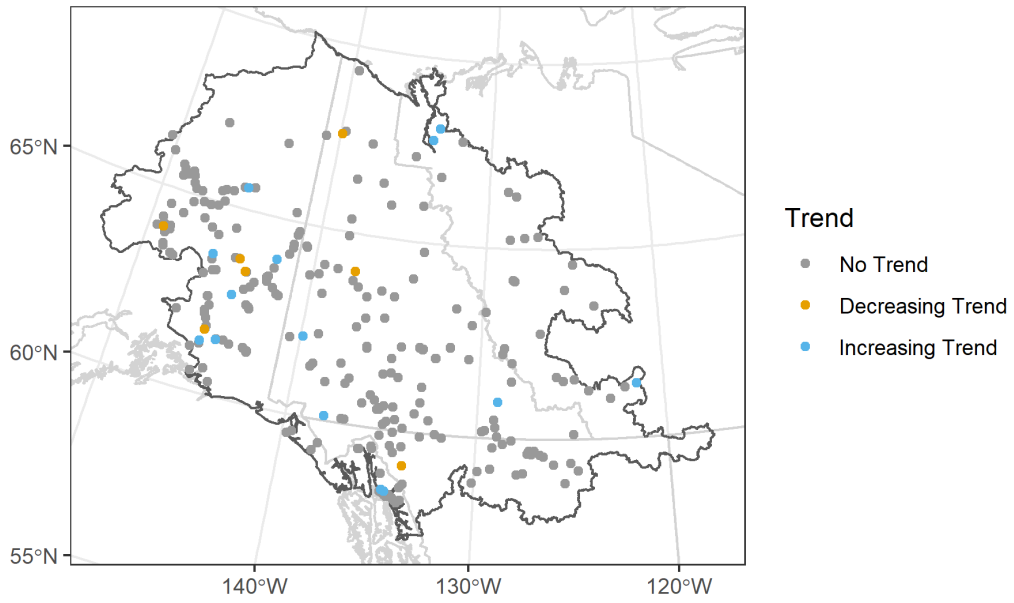

Figure 3.1 Study gauges with a significant Mann-Kendall trend (p-value <0.05)

No correction or exclusion was applied based on the lag-1 autocorrelation or Mann-Kendall tau; however, the correlation and Mann-Kendall statistic and p-value are provided in the results of the single station frequency analysis (Appendix A). It is recommended that additional analysis be undertaken by a user when the single station frequency analysis of gauges with a significant trend is used.

Outliers in the peak flow data were also identified as part of the single station analysis. The multiple Grubbs-Beck test for low outliers (Cohn et al., 2013) was applied to identify and mask low outliers from the single station frequency analysis for gauges with record lengths longer than 25-years. The single sided Grubbs-Beck test for low outliers (Grubbs and Beck, 1972) was applied for gauges with record lengths shorter than 25-years. High outliers were identified using the single sided Grubbs-Beck test regardless of the series length, but no high outlier results were masked from the analysis.

3.1 Seasonality of Peak Flows

Throughout the study area, peak flows can occur from several different processes including snowmelt, rainfall, and glacial melt. Studies in other regions which have considered mixed regimes (NHC, 2021), were able to clearly define mixed regimes based on the date of occurrence, with rainfall peak floods

occurring in the fall and snowmelt driven peaks occurring in the spring. Within the Yukon, however, the timing of different peak mechanisms is not distinct. For example, a peak in early July could be snowmelt, rainfall or glacial driven. As a result, a mixed regime frequency analysis was not considered for any gauges as a gauge specific assessment of that level is beyond the scope of this study.

An analysis of the seasonality of peak flows was instead undertaken to better understand the potential for mixed regimes and different peak flow processes. A seasonality indicator ($\bar{r}$) of annual peak flows about the mean date of the mean annual peak flow (Burn, 1997) was used to understand the variability of the timing of peak flows. The measure of variability ranges from 0 to 1, with 1 indicating that the annual peak flow occurs on the same day every single year and values closer to zero indicating a larger variability of date of occurrence of peak flows. Therefore, lower values of $\bar{r}$ potentially indicate a more mixed regime.

Figure 3.2 shows the measure of variability based on instantaneous station peak flow data, with basins that are glacierized shown. Basins with a mean date of peak flow within July to September tend to be glacierized. The figure indicates that there are a limited number of stations with a mean date of peak flow in the fall and winter months (September to December) and that these stations tend to have a higher variability of the date of occurrence of peak flows (i.e. a mixed flow regime).

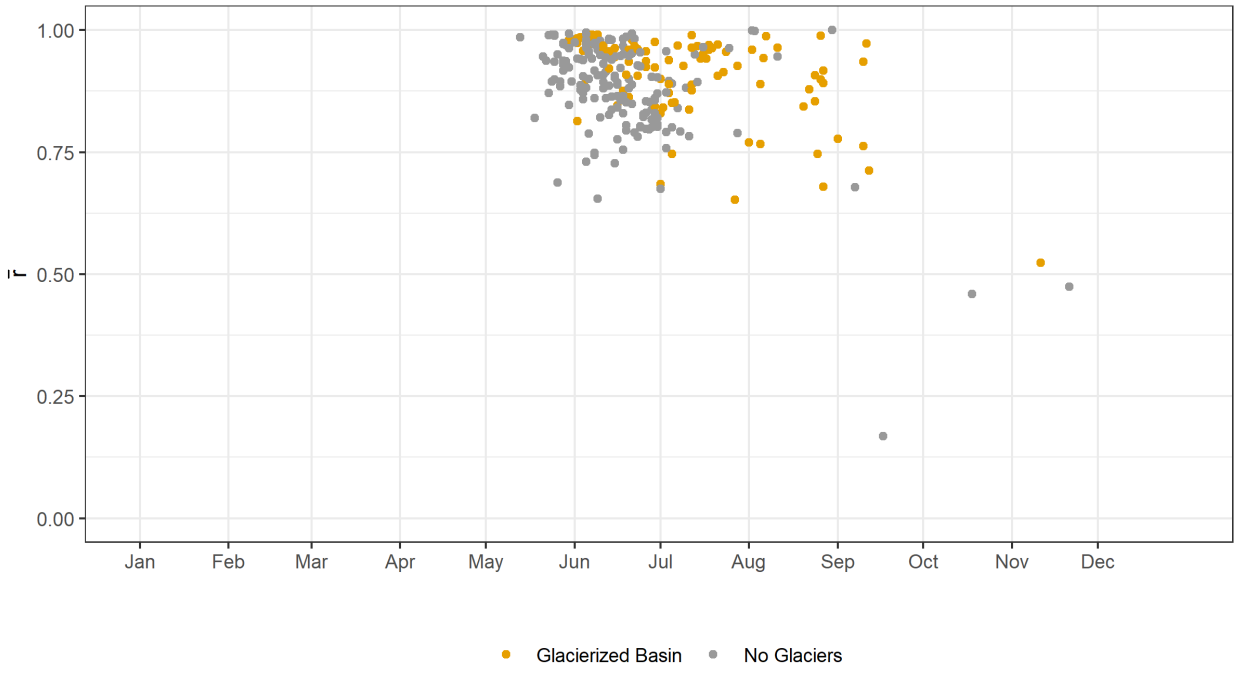

Figure 3.2 Seasonality of peak flows based on instantaneous station data

Figure 3.3 shows the relationship between drainage area and the measure of variability. Larger basins (greater than 5,000 km^2) tend to have lower variability in the peak flow date than smaller basins. Smaller basins are expected to have a greater likelihood of generating peak flows from different mechanisms (i.e., snowmelt and rainfall) due to their size.

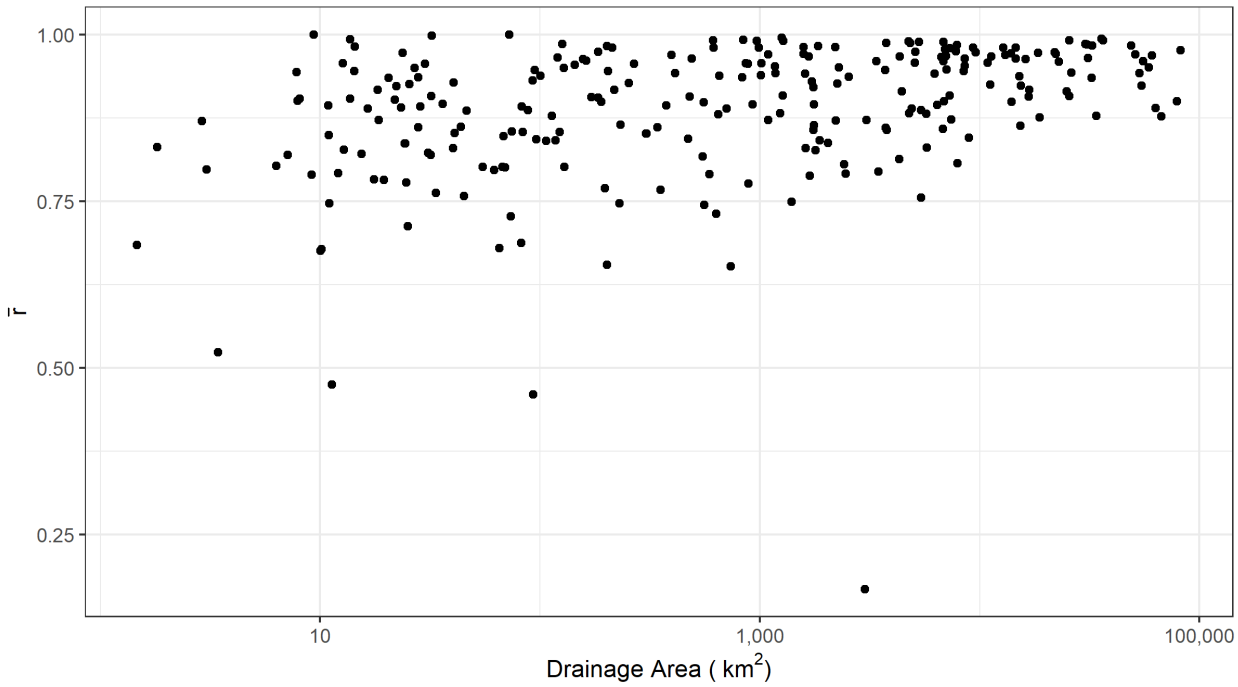

Figure 3.3 Variability of mean peak flow date compared to basin drainage area

3.2 Single Station Frequency Analysis

Frequency analyses were completed for both daily and instantaneous peaks for each gauge. Depending on the data record length, different peak flow distributions were used. Results are included in Appendix A as “gauge reports”.

3.2.1 Peak Flow Distributions and Algorithms

The following peak flow distributions were used for the single station frequency analysis:

- A LP3 distribution was fit to the data when the period of record was longer than or equal to 20 years.
- A LN distribution was fit to the data when the period of record was shorter than 20-years.
- When information was available on nonstandard or historical peak flow data, data infilling with high uncertainty was utilized, or multiple low outliers were present, an LP3 distribution was fit using EMA. This allowed for the use of perception thresholds and flow intervals to describe the nonstandard and historical flow data.

For each gauge, three frequency analyses were performed using the instantaneous peak series, daily peak series, and infilled instantaneous series. The same distribution type was not necessarily used for both instantaneous and daily data at a single gauge. A frequency analysis was only performed if there were more than 10 data points in the peak flow series.

The LP3 distribution uses the $\log_{10}$ transformation of the available maximum flows. The sample mean, standard deviation, and skew of the transformed data are denoted μ, S, and C_s, respectively. The statistics describe the midpoint, slope, and overall curvature of the flow frequency curve. Estimates of the transformed peak value (Q_p) for a given non-exceedance probability (p) are calculated from (USGS, 1982):

$$Q_p = \mu + K_p S$$

Where K_p is a function of C_s and p. The skew coefficient (C_s), through its influence on K_p plays a major role as it describes the shape of the upper tail. When the skew coefficient is positive, the distribution skews upwards such that estimates are unbounded. When the skew coefficient is negative, the upper end of the distribution appears to have an upper bound. The case where the skew coefficient is equal to 0 corresponds to the LN distribution.

Given its large influence on peak estimates it is important to estimate the skew coefficient accurately, which requires a long time series of annual maximum flows. Skew coefficients tend to be an unreliable estimator when gauges have short records (USGS, 1982). The LN distribution only has two parameters – mean and standard deviation – which describe the center and spread of the distribution.

EMA was applied to the study using the source code from the USGS' PeakFQ 7.0 Program (Veilleux et al., 2014), applied in batch format using the statistical programming language R. When EMA was not required (there were no historical peaks or data infilling), the LP3 distribution and LN distribution were fit using the method of L-moments (Asquith, 2011).

In the "gauge reports" (Appendix A), the reported average recurrence intervals or return periods for each gauge vary based on the length of record. Gauges with more than 20-years of data report the 2-, 5-, 10,-, 25-, 50-, 100-, and 200-year return periods. Gauges with 10 to 20 years of data report only up to the 100-year return period, and gauges with less than 10-years of data report only up to the 25-year return period.

Results from the single station flood frequency analysis are an approximation. The frequency analysis assumes an underlying probability distribution and an adequate representation of the probability distribution in the data record. 95% confidence intervals have been included on the single-station frequency analysis plots and tables and should be considered when examining the results of a single gauge. The confidence intervals are an indication of the uncertainty of the fit of the selected probability distribution and do not include other sources of uncertainty or error.

3.2.2 Results

Results of the single station frequency analysis are provided in "gauge reports" (Appendix A). The gauge reports contain the following information:

- Page 1 – Gauge and basin meta data:
  - Map of the basin and gauge location within the study area
  - Gauge metadata (coordinates and elevation)

- Basin characteristics (land use distribution, climate statistics, topography etc.)
- Period of observation (first and last year, total number of years with flow observations)
- Regulation
  - Regulation Status – considered regulated based on WSC regulation status, inclusion of regulation data flag by USGS, and identified by YG WRB
  - Degree of regulation (%)

- Page 2 and 3 – Frequency analysis results for the instantaneous, daily, and instantaneous infilled annual maximum flow series
  - Plots of flood frequency distribution fits
  - Tabulated peak flow quantiles including lower and upper confidence interval limits
  - Distribution and associated parameters
    - Method (EMA or L-Moments)
    - Distribution (LP3 or LN)
    - Parameters (mean, standard deviation, skew (LP3 only))
  - Statistical tests
    - Mann-Kendall's tau statistic and p-value
    - Lag-1 autocorrelation value
  - Plot showing the relationship between daily and instantaneous maximum flow (when data infilling occurred)

3.3 Limitations

There is inherent uncertainty in frequency analysis which stems from data collection through to analysis. Key limitations and sources of uncertainty of the single station frequency analysis and gauge reports in this study include:

- NHC performed a cursory review of the YG WRB data. QAQC of the approved and provisional data from the WSC and USGS gauge data was not performed beyond simple checks described in Section 2.1. The user is advised to review specific gauge data prior to use, with particular attention to extreme, estimated, and provisional values.
- The single station frequency analysis is dependent on streamflow data. Streamflow is not measured directly by WSC, USGS, or YG WRB. Instead, stage-discharge curves are used to estimate streamflow based on stream stage. The quality of calculated high flow data is dependent on the quality and reliability of the stage-discharge relationship and can involve considerable extrapolation above the largest manual discharge measurement.
- In delineating basins for each gauge, some discrepancies were noted (Section 2.2). A manual review of all drainage basins was not undertaken as part of this study and the user should verify the gauge location, basin outline, and drainage area included in the gauge report.

- The degree of regulation indicated on each gauge report is based on the methodology described in Section 2.3. Incorrect or unavailable data may lead to the degree of regulation being misrepresented.
- When considering the flood frequency curve and the associated return period estimates, the user should consider sample size. The minimum sample size used to estimate each return period estimate is noted in Section 3; however, the user must determine whether these sample sizes suffice for their specific applications.
- The flood frequency curve is an approximation. It is based on an assumption of the underlying probability distribution and adequate representation of the distribution through random sampling. 95% confidence limits have been included for the flood frequency curves and should be considered by users when utilizing the gauge reports. These confidence limits are only based on fitting the distribution to the sample data (sample size and variability) and do not include other sources of error and uncertainty.
- It is recommended that additional analyses be undertaken by the user when using gauges for which trends have been identified.
- Information reported on the gauge reports is based on historical land cover / land-use conditions and historical climate data. Changes to land cover / land-use and to climate (Section 5), or new information on the gauges or data would require an update to the analyses and results of this study. Due to sparsity of climate stations within the project area the gridded climate datasets used to develop climatic variables are inherently uncertain.

4 REGIONALIZATION

Regional hydrologic data can be used to supplement or improve streamflow statistics at locations which are ungauged or have insufficient data lengths. Regionalization of data involves grouping data of similar hydrologic responses such that peak flow information within the region can be combined to supplement or improve site specific data. Ideally, hydrologic regions contain data that is hydrologically homogeneous while also containing enough data to provide an effective estimate for the flood statistics. Typically, there is a trade-off between the amount of data and the homogeneity of a region. This trade-off becomes greater in more data-sparse regions such as the Yukon.

The most common approaches for regionalization of flood frequency data are the index peak flow approach and multiple-regression method. The index peak flow approach involves scaling a dimensionless peak flow frequency curve by the index peak flow (Grover et al., 2002). This method requires the study regions to be homogeneous and for there to be a good relationship between the index-peak flow and physiographic and climatic variables (Wang, 2000). The multiple regression method involves developing a regression-based relationship between the peak flows of different return periods and physiographic or climatic parameters through various regression procedures. This study uses the multiple regression method, building upon previous studies that cover the study area (Curran et al., 2016; Janowicz, 1986, 1989; NHC, 2021).

4.1 Gauge Inclusion

Gauges were excluded from the regionalization and regression analysis based on the following factors:

- Degree of regulation greater than 20%
- Drainage area greater than 10,000 km^2
- Nested gauges with a drainage area ratio less than 5 (Curran et al., 2016). Nested gauges with similar sizes and basin characteristics can be redundant in a regression analysis and place a stronger weight on the results from these gauges. For nested gauges with a drainage area ratio less than 5, the gauge with the longer or more recent record was kept as part of the analysis.

Gauges were not excluded from the analysis if they had a significant trend as the underlying cause of the trends is currently not well understood and given the limited availability of data for regionalization. Only eleven gauges with significant trends were included in the analysis, with three showing a negative trend and five showing a positive trend. The gauges with significant trends included in the regionalization are summarized in Table 4.1.

Table 4.1 Gauges with significant trends included in regionalization

Peak Flow Region	Gauge ID	Gauge Name	Record Length (Years)	Start Year	End Year	Drainage Area (km^2)	Mann-Kendall Tau	Relative Sen Slope
Alaska Range	15199000	Copper R Tr Nr Slana Ak	29	1963	1992	11	0.4	0.09
Alaska Range	15518100	L Panguingue C Nr Lignite Ak	10	1965	1974	9	-0.6	-0.11
Coast Mountains	15052000	Lemon C Nr Juneau Ak	41	1952	2022	32	0.5	0.04
Coast Mountains	15052500	Mendenhall R Nr Auke Bay Ak	48	1966	2022	220	0.3	0.01
Coast Mountains	15208000	Tonsina R At Tonsina Ak	33	1950	2006	1090	-0.3	-0.01
Interior Alaska	15305950	Taylor C Nr Chicken Ak	25	1967	1991	105	0.3	0.07
Interior Alaska	15439800	Boulder C Nr Central Ak	50	1964	2013	84	0.2	0.02
Yukon Boreal	09EA005	Little South Klondike River Below Ross Creek	14	1983	2018	860	-0.5	-0.06

4.2 Peak Flow Regions

Previous peak flow studies within the study area have differed in their regionalization of streamflow (Section 1.3). This study investigated several different possible regionalization schemes but predominately focused on the definition of ecoregions for regionalization. Ecoregions have been defined across the Yukon (Smith et al., 2004), Canada (Agriculture and Agri-Food Canada, 2013) and North America (Commission for Environmental Cooperation, 1997), which define areas of similar geology, climate, soils, and vegetation. Because these factors are also dominant controls on the hydrology of a region, this system was used for defining peak flow regions as previously done for the province of British Columbia (NHC, 2021). Since the project area extends into the U.S. and given that the ecoregions have similar boundaries across the three different scales of available data (territory, country, and continent), the North American Ecoregions were used for this study.

There are three different resolutions of the North American Ecoregions. Level 1 regions, which are the largest, divide the continent into 15 broad regions. Level 2 ecoregions provide a more detailed description of the ecological areas nested within Level 1. And Level 3 ecoregions provide the finest discretization. The Level 2 ecoregions were found to be too coarse for use in this study, resulting in only three primary peak flow regions; therefore, the Level 3 ecoregions were used for the analysis. Figure 4.1 shows the Level 3 ecoregions for the project area and Table 4.2 summarizes the number of gauges within each ecoregion with at least 10 years of instantaneous peak flow data. The region associated with

each gauge was determined not based on the coordinates of the gauge, but by which region the majority of the associated gauge's drainage area was located within.

Table 4.2 Number of gauges with at least 10 years of instantaneous peak flow data by Level 3 ecoregion

Ecoregion – Level 3	Number of gauges
Alaska Range	30
Amundsen Plains	0
Arctic Coastal Plains	0
Arctic Foothills	0
Brooks Range/Richardson Mountains	1
Coastal Western Hemlock-Sitka Spruce Forests	2
Copper Plateau	7
Great Bear Plains	5
Hay and Slave River Lowlands	3
Interior Bottomlands	1
Interior Forested Lowlands and Uplands	9
Interior Highlands and Klondike Plateau	30
Mackenzie and Selwyn Mountains	15
Ogilvie Mountains	4
Pacific Coastal Mountains	23
Peel River and Nahanni Plateaus	2
Watson Highlands	39
Wrangell and St. Elias Mountains	10
Yukon Flats	0
Yukon-Stikine Highlands/Boreal Mountains and Plateaus	21

Yukon

nhc
northwest hydraulic consultants

DATA SOURCES:
Level 3 Ecoregions - Commission for Environmental Cooperation ; Background - ESRI World Topographic Map

SCALE - 1:7,009,138
0 100 200
km

N

Coordinate System: NAD 1983 CSRS BC ENVIRONMENT ALBERS

Job: 3007020 | Date: 04-MAY-2023

YUKON REGIONAL FLOW ANALYSIS
North American Level 3 Ecoregions

FIGURE 4.1

The Level 3 regions were combined such that six primary peak flow regions were formed (Table 4.3 and Figure 4.2). Ideally each region would have a minimum of 30 gauges; however, data limitations in the more northern portion of the study resulted in the Interior Mountains and Northern Region having less than 20 gauges. These two regions were originally combined into a single region, but based on differing hydrologic responses, it was separated into two regions. Results from these regions should be used with caution given the limited number of gauges. The Arctic Foothills and Arctic Coastal Plain did not contain any gauges and were excluded from the peak flow regions. These areas are poorly drained and have unique terrain features which may result in a unique hydrologic response (Gallant et al., 1995) . The Yukon Flats did not contain any gauges but the results from the Northern region could be considered for this region by the user with caution. The Amundsen Plains and Great Bear Plains, primarily located within the Northwest Territories, were not included in the peak flow region definition due to limited number of gauges and different hydrologic characteristics than the Northern Region and Interior Mountains.

Only five of the six peak flow regions cover the Yukon territory. The Alaska Range is completely outside of the Yukon territory; however, regression analysis was still completed for this peak flow region. A summary of basin characteristics within each peak flow region is shown in Figure 4.3.

Table 4.3 Summary of peak flow regions for regional analysis

Peak Flow Region	Level 3 Ecoregions	Number of Gauges with > 10 Years of Instantaneous Peak Data	Number of Gauges with > 10 Years of Daily Peak Data
Alaska Range	Alaska Range, Copper Plateau	32	12
Coast Mountains	Wrangell and St. Elias Mountains, Pacific Coastal Mountains, Coastal Western Hemlock-Stika Spruce Forests	33	26
Interior Alaska	Interior Bottomlands, Interior Highlands and Klondike Plateau	30	11
Interior Mountains	Mackenzie and Selwyn Mountains, Peel River and Nahanni Plateaus	16	19
Northern Region	Brooks Range/Richardson Mountains, Interior Forested Lowlands and Uplands, Ogilvie Mountains	14	7
Yukon Boreal	Hay and Slave River Lowlands, Watson Highlands, Yukon-Stikine Highlands/Boreal Mountains and Plateaus	54	57

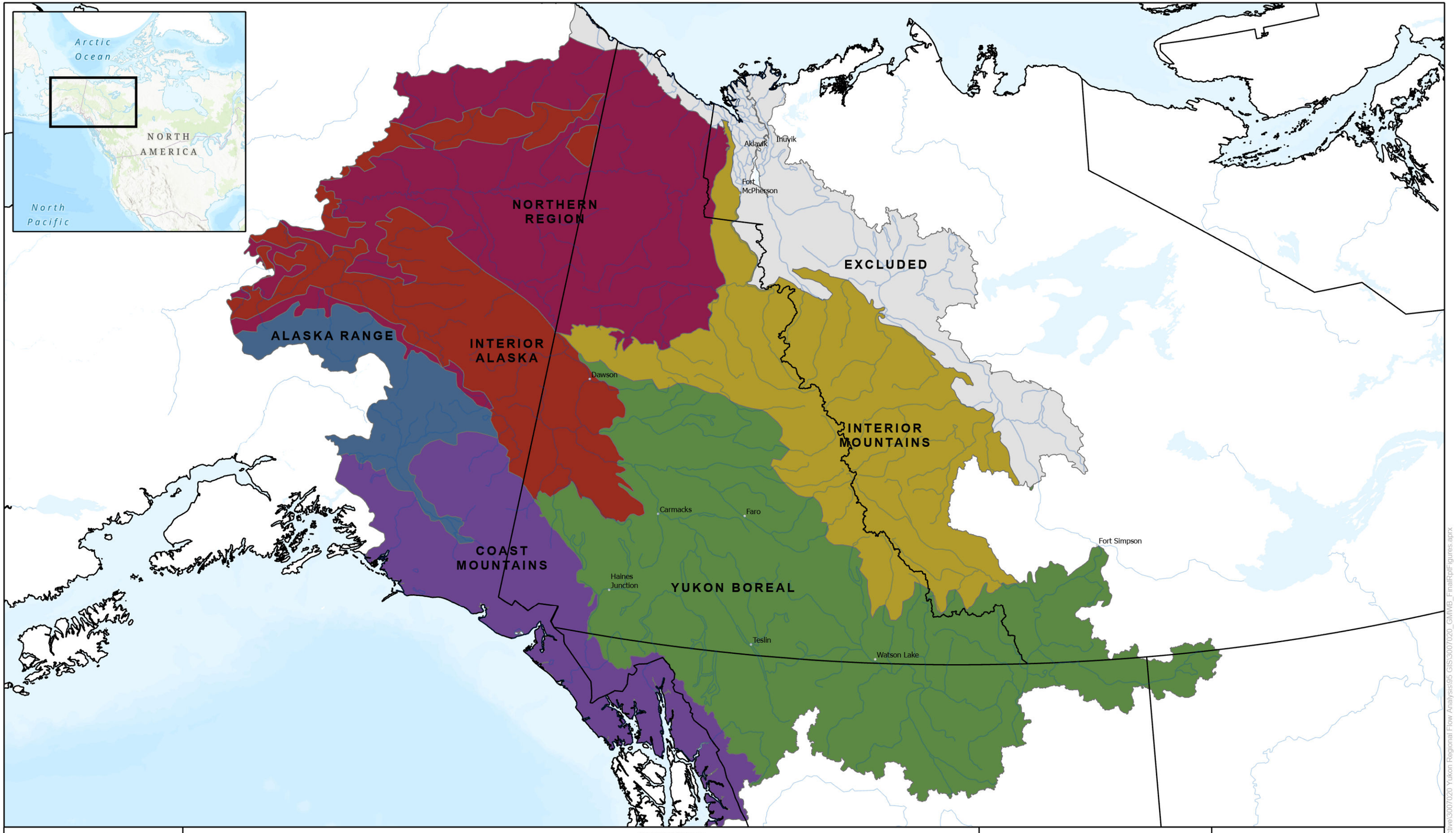

Yukon

nhc
northwest hydraulic consultants

Peak Flow Region

- Alaska Range
- Coast Mountains
- Excluded
- Interior Alaska
- Interior Highlands
- Interior Mountains
- Northern Region
- Yukon Boreal

DATA SOURCES:
Background - ESRI World Topographic Map

SCALE - 1:6,309,138
0 100 200 km
N

Coordinate System: NAD 1983 CSRS BC ENVIRONMENT ALBERS

Job: 3007020 | *Date: 04-MAY-2023*

YUKON REGIONAL FLOW ANALYSIS

Peak Flow Regions

FIGURE 4.2

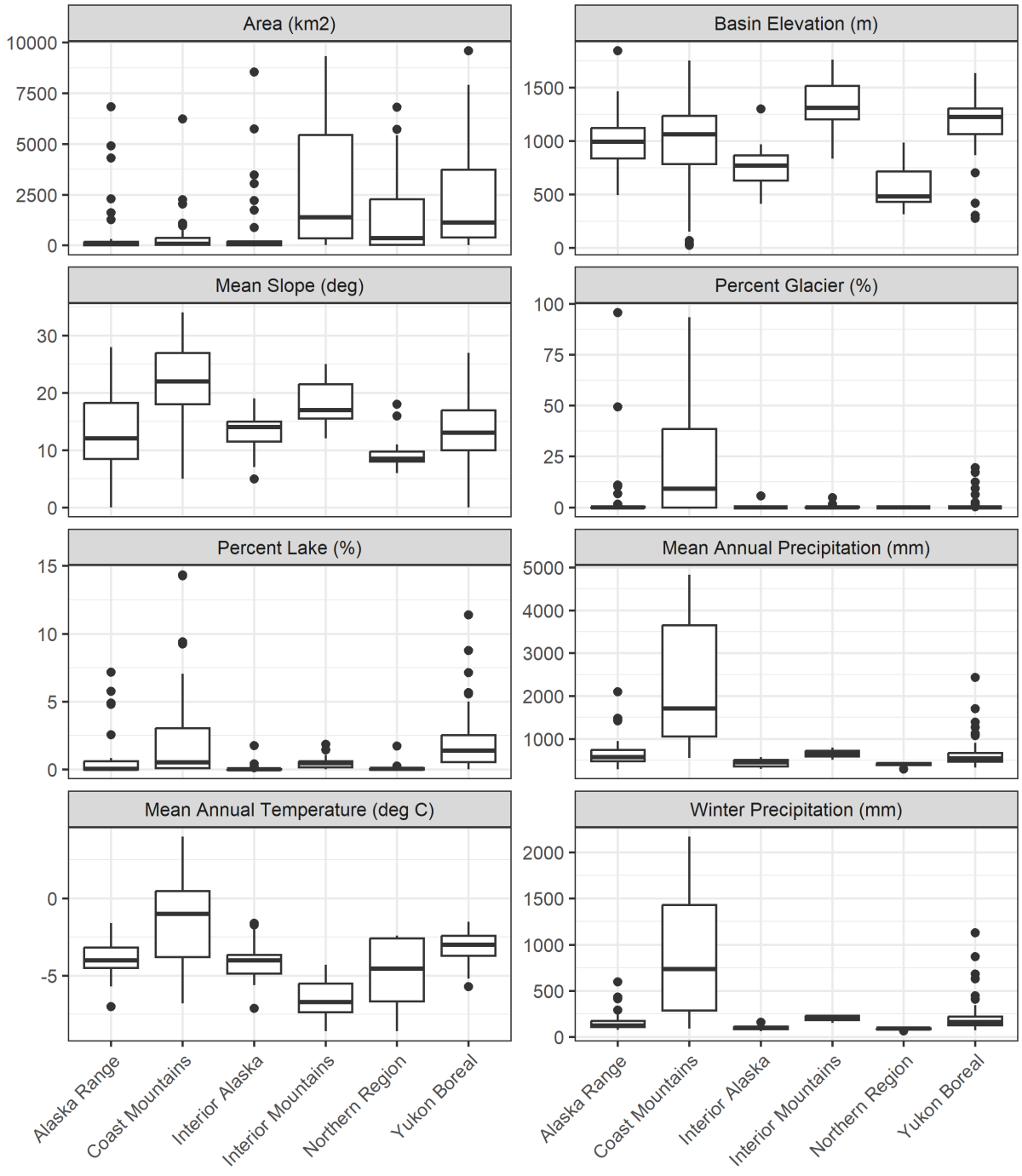

Figure 4.3 Key basin characteristics within each peak flow region.Each boxplot displays the 25th, 50th, and 75th percentile represented by three horizontal lines. The minimum and maximum values of the whiskers indicate the 25th and 75th percentile plus or minus 1.5 times the interquartile range. Observations outside of the minimum and maximum whisker values, indicated as dots, are considered outliers.

The validity of the peak flow regions based on the Level 3 ecoregions was tested using the homogeneity test developed by Langbein (Dalrymple, 1960). The homogeneity test determines whether records differ from one another by amounts that cannot reasonably be expected by chance by examining the variation in the ratio of the 10-year to 2.33-year events. While the true position of a frequency graph can differ from the position indicated by the plotted points, the chances it will lie within certain distances from the plotted position can be calculated. Langbein defined the acceptable range of variation as two standard deviations of the most probable value of the recurrence interval. Figure 4.4 shows the results of the Langbein test with each point representing the predicted 10-year peak for a station based on the 2.33-year peak multiplied by the regional ratio of the 10-year to the 2.33-year events. The grey bands in Figure 4.4 indicate the acceptable variation defined by Langbein. Points outside the grey bands indicate potential outliers. Overall, the regions show good homogeneity with a limited number of outliers within each region.

The Langbein test has been shown to have limited power in identifying homogeneous regions (Fill and Stedinger, 1995) so other homogeneity tests were also explored including the homogeneity test of Hosking and Wallis (1997). The homogeneity test of Hosking and Wallis (1997) is based on L-moment ratios of the region in comparison to the variation that would be expected in a homogeneous region derived from a kappa distribution of the L-moments. The heterogeneity measure (HW_1) is regarded as homogeneous if it is less than 1, possibly heterogeneous between 1 and 2, and heterogenous if greater than 2. In all peak flow regions, the HW_1 measure was greater than 2. Attempts to create homogeneous regions based on the Hosking and Wallis measure resulted in regions with a very limited number of stations, limiting the overall applicability of the regionalization. This highlights the trade-off that must be made between homogeneous regions and adequate data to develop practical regression equations. Given the scarcity of data within the study area, the peak flow regions were considered appropriate, with the individual stations further examined as part of the regionalization to identify those that have high influence and leverage on the regression equations.

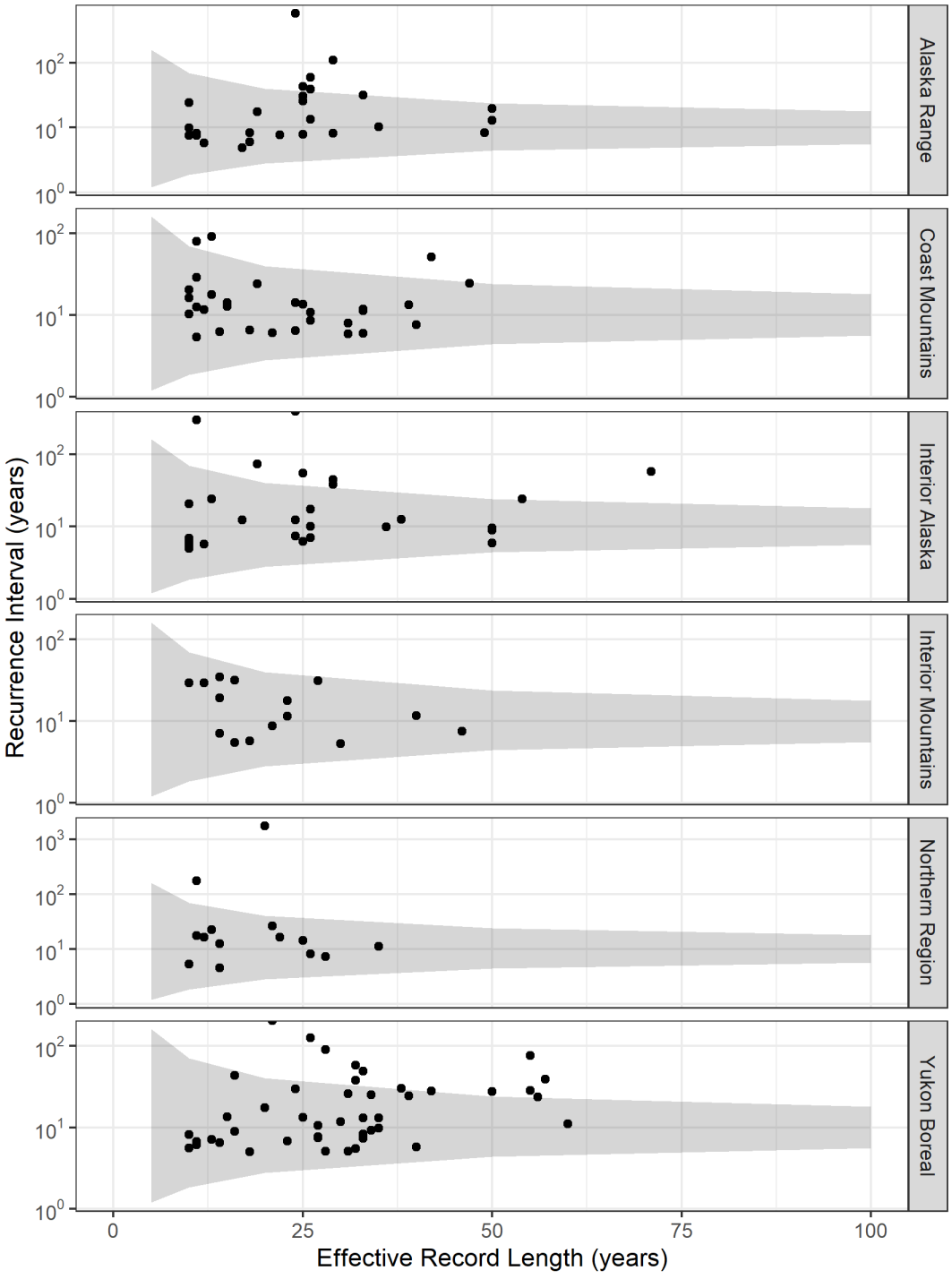

Figure 4.4 **Results of the Langbein homogeneity test applied to peak flow regions within the study area. The y-axis indicates the actual recurrence interval of the predicted 10-year peak based on the 2.33-year peak multiplied by the 10-year to 2.33-year average ratio from each region. The x-axis indicates the record length. The grey bands represent the acceptable variation in recurrence interval.**

4.3 Regression Analysis

Prior to developing the regional regression equations, an exploratory analysis of the regressions was performed using ordinary least squares (OLS). OLS is a simple form of multiple linear regression which is useful for determining the general form of the equations. Generalized Least Squares (GLS) is a more sophisticated technique of regression analysis and can improve the regression equations by accounting for time sampling error and the cross correlation of annual peak flows between stream gauges and was used to finalize the regression equations (Farmer et al., 2021).

4.3.1 Exploratory Analysis

Regional regression equations equate peak flow with basin predictor variables. This method was used in Alaska (Curran et al., 2016) where basin area and mean annual precipitation were used as predictors to fit estimates from the 2-year to 500-year peak flow and in previous studies for the Yukon, where basin area was the primary predictor (Janowicz, 1986, 1989).

Prior to model fitting, collinearity between potential predictors was examined. Collinearity between multiple predictors restricts the ability of a regression analysis to evaluate the importance of the individual variables. The two variables which showed collinearity were mean annual precipitation and winter precipitation (Figure 4.5). Winter precipitation was calculated as the sum of monthly precipitation between November and March. Based on the strong relationship between the two variables, winter precipitation was excluded from the initial analysis. Following regression analysis using mean annual precipitation, winter precipitation was substituted into the equations in place of annual precipitation (where applicable) to test if winter precipitation as a predictor improved the overall fit of the regression. Mean annual precipitation was found to be a better predictor than winter precipitation for all regions.

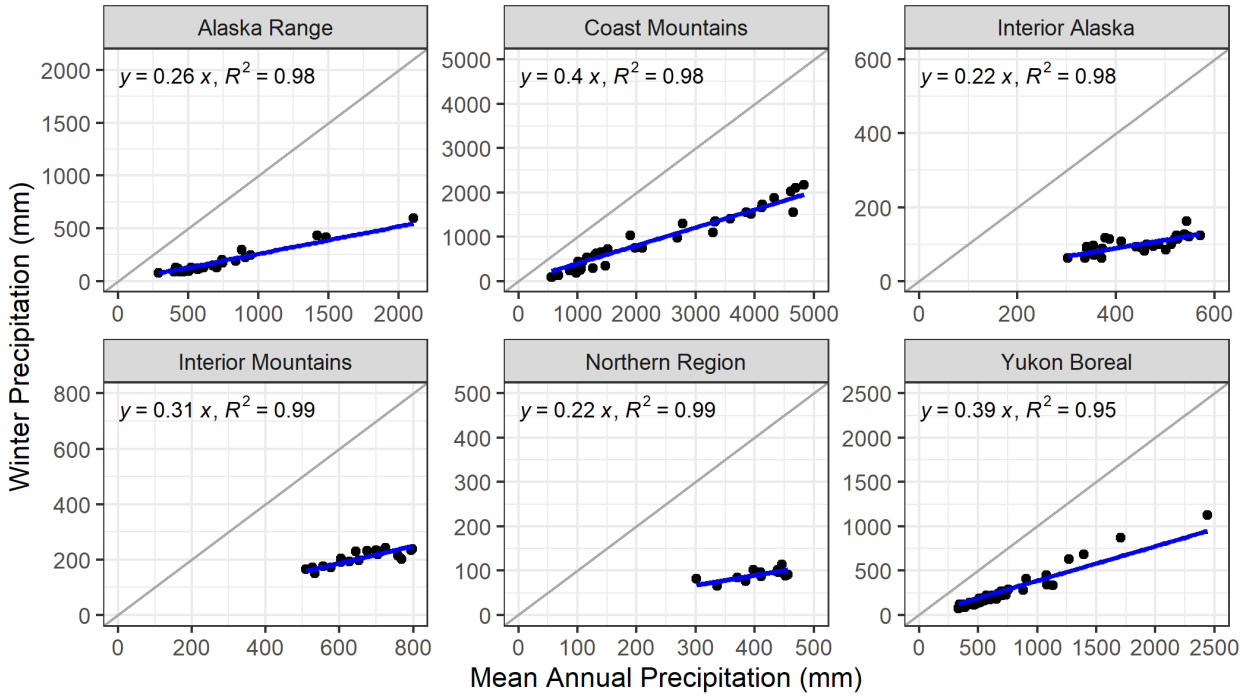

Figure 4.5 Correlation between mean annual precipitation and winter precipitation (November to March) by peak flow region. Grey line represents the 1:1 line.

The predictor variables were log transformed prior to regression analysis, as is commonly done to achieve a linear relationship between peak flow and basin characteristics. Since the logarithm of zero and negative numbers is undefined, datasets containing these values were transformed first. A value of 1 was added to any variables which are expressed as a percentage of basin area (e.g., percent lake). A value of 100 was added to all mean annual temperatures.

The regression analysis was performed using a backward elimination stepwise approach. This involved starting with all candidate predictor variables, and iteratively removing statistically insignificant variables until all predictor variables were statistically significant (p value less than 0.1). The process was completed for each peak flow region, maintaining the same predictor variables across all return periods but not across all peak flow regions. During each step of model definition, the residuals were assessed for normality and homoscedasticity.

Unusual gauges were also identified and assessed based on their leverage and influence. Leverage is a measure of how far away a basin's predictor variables are from the centroid of all other observations and is an indication that a particular basin is an outlier when compared to the others. Influence is a measure of the sensitivity of regression parameters to any single basin. Basins which showed high influence and high leverage were examined as part of the analysis to determine whether they should be excluded from the regression analysis. For example, the three gauges which were located within the Hay River and Slave Lowlands (10ED003, 10ED007, 10ED009) all showed high influence and high leverage. Given that this region is predominantly outside of the Yukon territory, these gauges were excluded from the development of regression equations. Stations with large predictive errors were also examined to

determine if they should be included within a region, moved to a different region, or excluded from the analysis.

Table 4.4 summarizes the predictor variables which were statistically significant for each peak flow region. The daily regressions for the Alaska Range, Northern Region, and Interior Alaska all used less than ten stations and therefore are excluded from the results.

Table 4.4 Explanatory variables for regression equations

Region	Type	Drainage Area (km^2)	Mean Annual Precipitation (mm)	Mean Annual Temperature (°C)	% Lake
Alaska Range	Instantaneous	✓			
Coast Mountains	Instantaneous	✓	✓	✓	✓
	Daily	✓	✓	✓	✓
Interior Alaska	Instantaneous	✓	✓	✓	
Interior Mountains	Instantaneous	✓			
Northern Region	Instantaneous	✓			
Yukon Boreal	Instantaneous	✓	✓	✓	✓
	Daily	✓	✓	✓	✓

4.3.2 Regression Equations

Following the OLS regression analysis to develop the general form of the equations, a GLS regression analysis was used to develop the final equations. The USGS weighted multiple linear regression (WREG) program was implemented in the statistical language R (Farmer, 2021). The significance of regression coefficients for each region were reviewed along with diagnostic plots of residuals, leverage, and influence. The final regional regression equations for the five peak flow regions along with performance statistics are shown in Table 4.5 through Table 4.10 – the performance metrics are described in Section 4.4. Table 4.11 provides the applicability limits of the equations within each region. The 10-year, 50-year and 100-year regression results are shown in Figure 4.6 through Figure 4.8.

A limited number of stations were used for the development of the instantaneous regressions for the Northern Region (n=14) and Interior Mountains (n=15) regression equations, and these should be used with caution given the limited number of stations available.

Table 4.5 Regression Equations for the Alaska Range, by return period (RP), with coefficients *a* and *b*, sample size (n), and performance metrics (R^2, R^2_{Pseudo}, SEP_{AVG}, and R^2_{Pred}) described in Section 4.4.

Peak Flow	RP	*a*	*b*	n	R^2	R^2_{Pseudo}	SEP_{AVG}	R^2_{Pred}
Instantaneous	*Equation Form: $Q = 10^a Area^b$*							
	2	-0.467	0.761	23	0.820	0.814	65.9	0.926
	5	-0.185	0.732	23	0.825	0.819	61.9	0.931
	10	-0.034	0.716	23	0.818	0.811	62.1	0.930
	25	0.132	0.699	23	0.796	0.792	64.9	0.926
	50	0.242	0.687	23	0.771	0.766	69.7	0.920
	100	0.343	0.675	23	0.738	0.734	75.7	0.908
	200	0.437	0.665	23	0.700	0.693	84.0	0.885

Table 4.6 Regression Equations for the Coast Mountains, by return period (RP), with coefficients *a* through *d*, sample size (n), and performance metrics (R^2, R^2_{Pseudo}, SEP_{AVG}, and R^2_{Pred}) described in Section 4.4.

Peak Flow	RP	*a*	*b*	*c*	*d*	n	R^2	R^2_{Pseudo}	SEP_{AVG}	R^2_{Pred}
Instantaneous	*Equation Form: $Q = Area^a MAP^b (MAT+100)^c (1+\%Lake/100)^d$*									
	2	0.964	1.450	-2.513	-8.930	30	0.904	0.895	68.3	0.844
	5	0.945	1.347	-2.248	-9.362	30	0.900	0.89	68.6	0.800
	10	0.938	1.300	-2.120	-9.651	30	0.897	0.886	69.8	0.768
	25	0.932	1.254	-1.991	-10.008	30	0.892	0.881	71.3	0.726
	50	0.929	1.227	-1.912	-10.267	30	0.888	0.876	73.1	0.693
	100	0.928	1.205	-1.844	-10.519	30	0.883	0.871	75.0	0.660
	200	0.927	1.185	-1.784	-10.764	30	0.878	0.864	77.9	0.625
Daily	*Equation Form: $Q = Area^a MAP^b (MAT+100)^c (1+\%Lake/100)^d$*									
	2	0.951	1.261	-2.223	-7.705	23	0.907	0.893	65.1	0.81
	5	0.931	1.184	-2.011	-7.827	23	0.909	0.895	63.1	0.773
	10	0.920	1.131	-1.877	-7.918	23	0.909	0.895	62.8	0.739
	25	0.908	1.064	-1.715	-8.036	23	0.907	0.893	63.4	0.686
	50	0.900	1.015	-1.600	-8.124	23	0.903	0.888	65.1	0.643
	100	0.893	0.967	-1.489	-8.210	23	0.899	0.883	66.9	0.596
	200	0.887	0.920	-1.381	-8.296	23	0.893	0.876	69.7	0.547

Table 4.7 Regression Equations for Interior Alaska, by return period (RP), with coefficients *a* through *c*, sample size (n), and performance metrics (R^2, R^2_{Pseudo}, SEP_{AVG}, and R^2_{Pred}) described in Section 4.4.

Peak Flow	RP	*a*	*b*	*c*	n	R^2	R^2_{Pseudo}	SEP_{AVG}	R^2_{Pred}
Instantaneous	*Equation Form: $Q = Area^a MAP^b (MAT+100)^c$*								
	2	0.863	2.331	-3.476	26	0.969	0.969	38.1	0.963
	5	0.822	2.133	-3.047	26	0.969	0.969	36.0	0.958
	10	0.798	1.972	-2.744	26	0.961	0.962	39.0	0.947
	25	0.770	1.761	-2.363	26	0.945	0.945	46.0	0.930
	50	0.752	1.602	-2.087	26	0.929	0.926	53.1	0.916
	100	0.735	1.444	-1.817	26	0.909	0.907	59.4	0.900
	200	0.719	1.288	-1.552	26	0.886	0.883	66.8	0.884

Table 4.8 Regression Equations for the Interior Mountains, by return period (RP), with coefficients *a* and *b*, sample size (n), and performance metrics (R^2, R^2_{Pseudo}, SEP_{AVG}, and R^2_{Pred}) described in Section 4.4.

Peak Flow	RP	*a*	*b*	n	R^2	R^2_{Pseudo}	SEP_{AVG}	R^2_{Pred}
Instantaneous	*Equation Form: $Q = 10^a Area^b$*							
	2	-0.613	0.890	15	0.967	0.967	26.6	0.824
	5	-0.537	0.907	15	0.961	0.960	30.1	0.708
	10	-0.495	0.916	15	0.955	0.952	33.3	0.644
	25	-0.449	0.926	15	0.943	0.940	38.2	0.579
	50	-0.418	0.933	15	0.933	0.929	42.7	0.539
	100	-0.389	0.940	15	0.921	0.917	47.1	0.505
	200	-0.363	0.946	15	0.909	0.902	52.2	0.476

Table 4.9 Regression Equations for the Northern Region, by return period (RP), with coefficients *a* and *b*, sample size (n), and performance metrics (R^2, R^2_{Pseudo}, SEP_{AVG}, and R^2_{Pred}) described in Section 4.4.

Peak Flow	RP	a	b	n	R^2	R^2_{Pseudo}	SEP_{AVG}	R^2_{Pred}
Instantaneous	*Equation Form: $Q = 10^a Area^b$*							
	2	-0.706	0.918	14	0.983	0.983	32.6	0.956
	5	-0.366	0.868	14	0.968	0.967	44.8	0.946
	10	-0.200	0.846	14	0.953	0.952	53.4	0.941
	25	-0.034	0.826	14	0.933	0.931	65.2	0.933
	50	0.070	0.814	14	0.916	0.914	73.8	0.924
	100	0.159	0.805	14	0.899	0.895	83.5	0.910
	200	0.239	0.797	14	0.881	0.876	93.2	0.889

Table 4.10 Regression Equations for the Yukon Boreal, by return period (RP), with coefficients *a* through *d*, sample size (n), and performance metrics (R^2, R^2_{Pseudo}, SEP_{AVG}, and R^2_{Pred}) described in Section 4.4.

Peak Flow	RP	*a*	*b*	*c*	*d*	n	R^2	R^2_{Pseudo}	SEP_{AVG}	R^2_{Pred}
Instantaneous	*Equation Form: $Q = Area^a MAP^b (MAT+100)^c (1+\%Lake/100)^d$*									
	2	0.958	1.218	-2.197	-17.113	46	0.934	0.931	40.0	0.885
	5	0.920	1.103	-1.892	-19.273	46	0.932	0.929	39.0	0.901
	10	0.900	1.053	-1.746	-20.518	46	0.928	0.924	39.7	0.900
	25	0.878	1.008	-1.600	-21.931	46	0.917	0.914	41.7	0.887
	50	0.864	0.984	-1.512	-22.891	46	0.906	0.902	44.5	0.869
	100	0.851	0.965	-1.435	-23.785	46	0.892	0.888	47.8	0.845
	200	0.839	0.950	-1.368	-24.628	46	0.876	0.869	52.1	0.816
Daily	*Equation Form: $Q = Area^a MAP^b (MAT+100)^c (1+\%Lake/100)^d$*									
	2	0.985	1.264	-2.328	-15.129	49	0.939	0.936	41.6	0.889
	5	0.950	1.154	-2.038	-16.939	49	0.934	0.931	41.6	0.906
	10	0.931	1.101	-1.893	-17.887	49	0.928	0.926	42.3	0.907
	25	0.912	1.048	-1.742	-18.903	49	0.917	0.914	45.1	0.898
	50	0.899	1.016	-1.647	-19.565	49	0.907	0.902	48.1	0.886
	100	0.887	0.988	-1.563	-20.164	49	0.894	0.89	50.9	0.869
	200	0.876	0.964	-1.487	-20.716	49	0.88	0.874	55	0.848

Table 4.11 Range of explanatory variables used to develop regression equations

Peak Flow Region	Area (km^2)	Mean Annual Precipitation (mm)	Mean Annual Temperature (°C)	% Lake
Alaska Range	7 – 4314	289 – 1485	(-5.7) – (-1.6)	0 – 7
Coast Mountains	2 – 6233	555 – 4832	(-6.8) – (4.0)	0 – 14[1]
Interior Alaska	3 -5737	302 – 571	(-7.1) – (-1.6)	0
Interior Mountains	163 – 9320	510 – 798	(-8.6) – (-4.3)	0 – 2
Northern Region	12 -6807	301 – 456	(-8.6) – (-2.4)	0 – 2
Yukon Boreal	73 – 9593	331 – 1708	(-5.7) – (-1.5)	0 – 6[2]

Notes:

1. For the Coast Mountains, daily estimates may exceed instantaneous estimates where % lake is greater than 4% and the mean annual precipitation is less than 600 mm
2. For the Yukon Boreal, daily estimates may exceed instantaneous estimates where drainage area is greater than 1000 $km^2$and % lake is greater than 5%

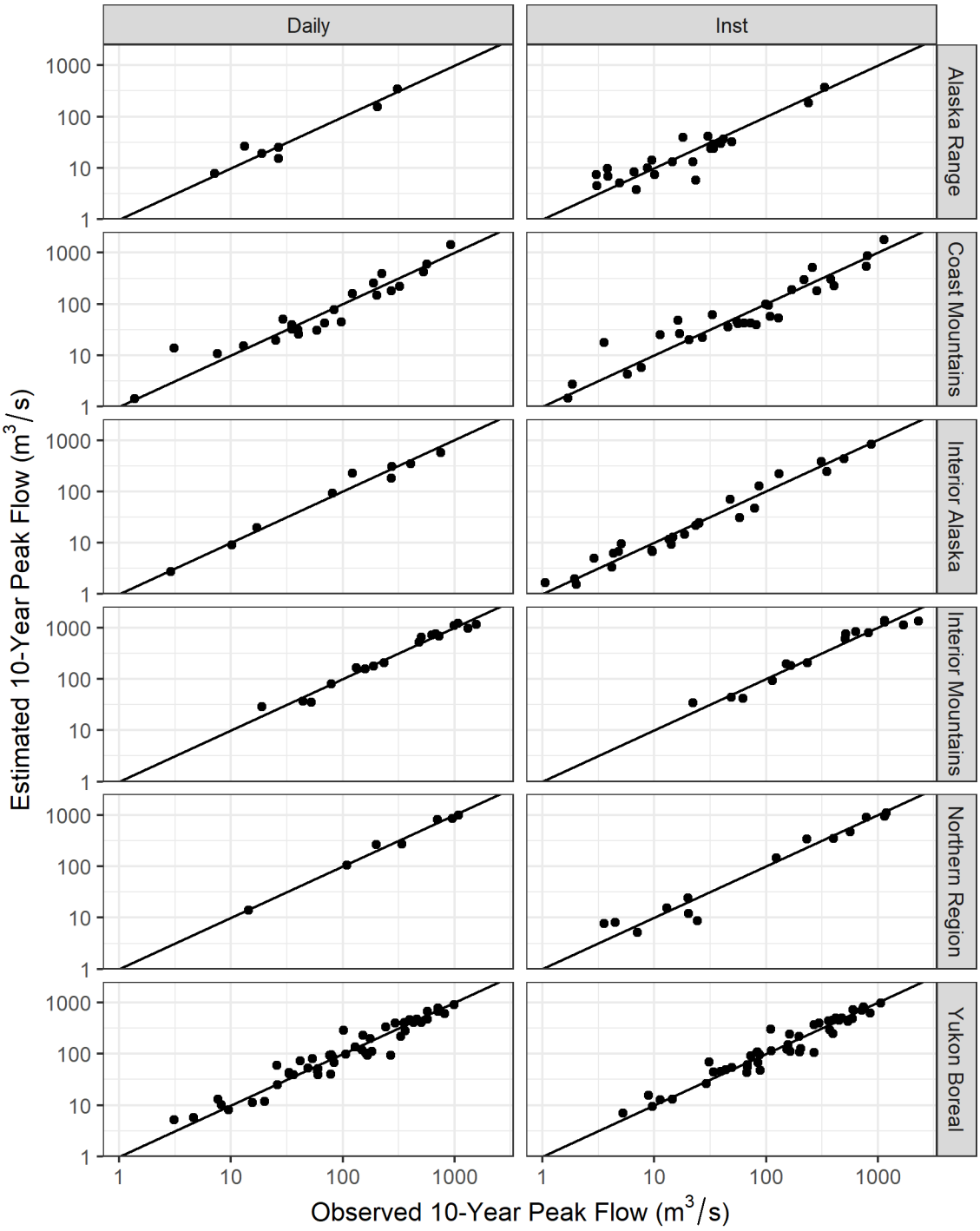

Figure 4.6 Multiple regression model results for prediction of the 10-year return period for daily and instantaneous peak flows for all peak flow regions. Diagonal black line indicates a 1:1 fit between the at-site calculated value and the regional prediction.

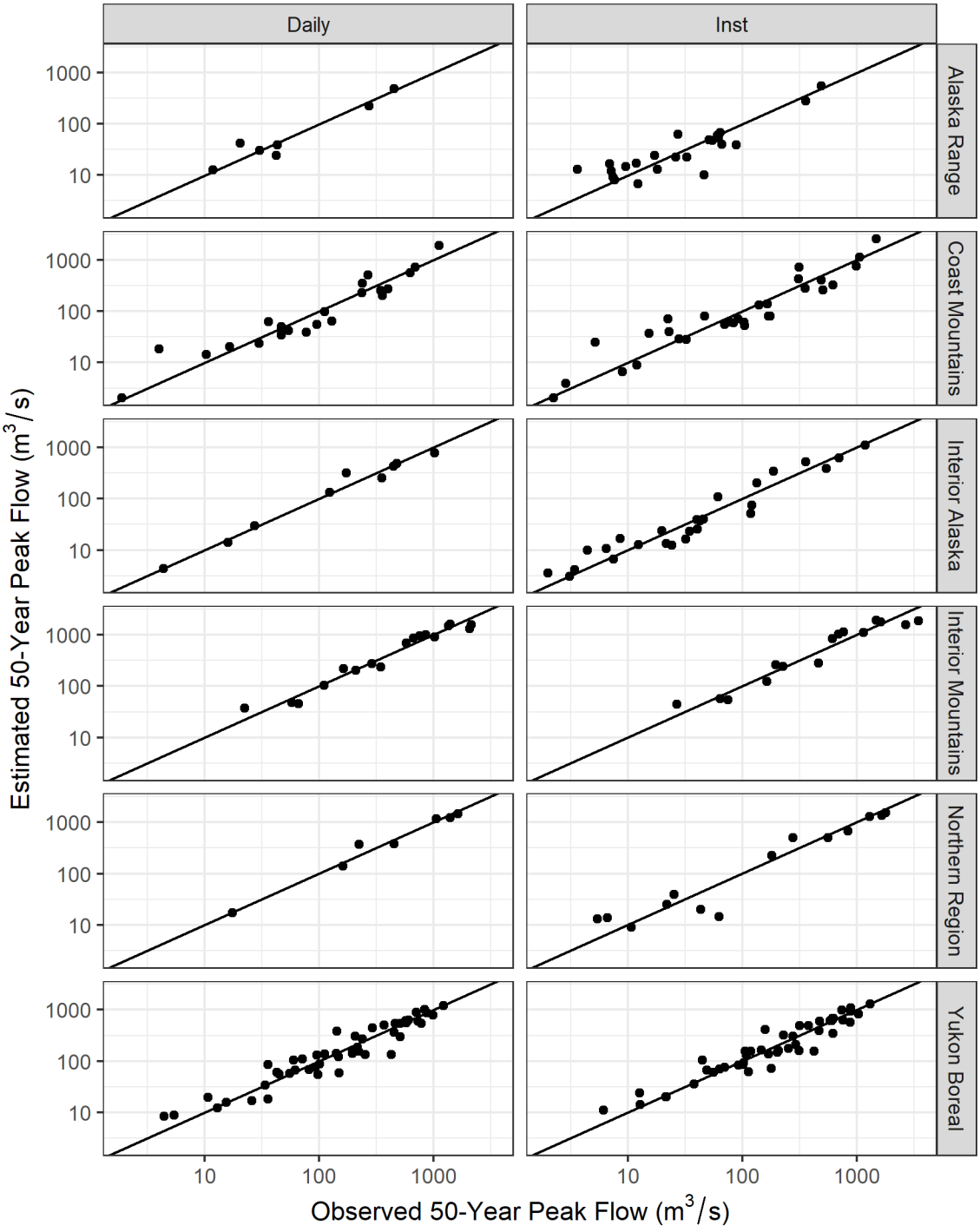

Figure 4.7 Multiple regression model results for prediction of the 50-year return period for daily and instantaneous peak flows for all peak flow regions. Diagonal black line indicates a 1:1 fit between the at-site calculated value and the regional prediction.

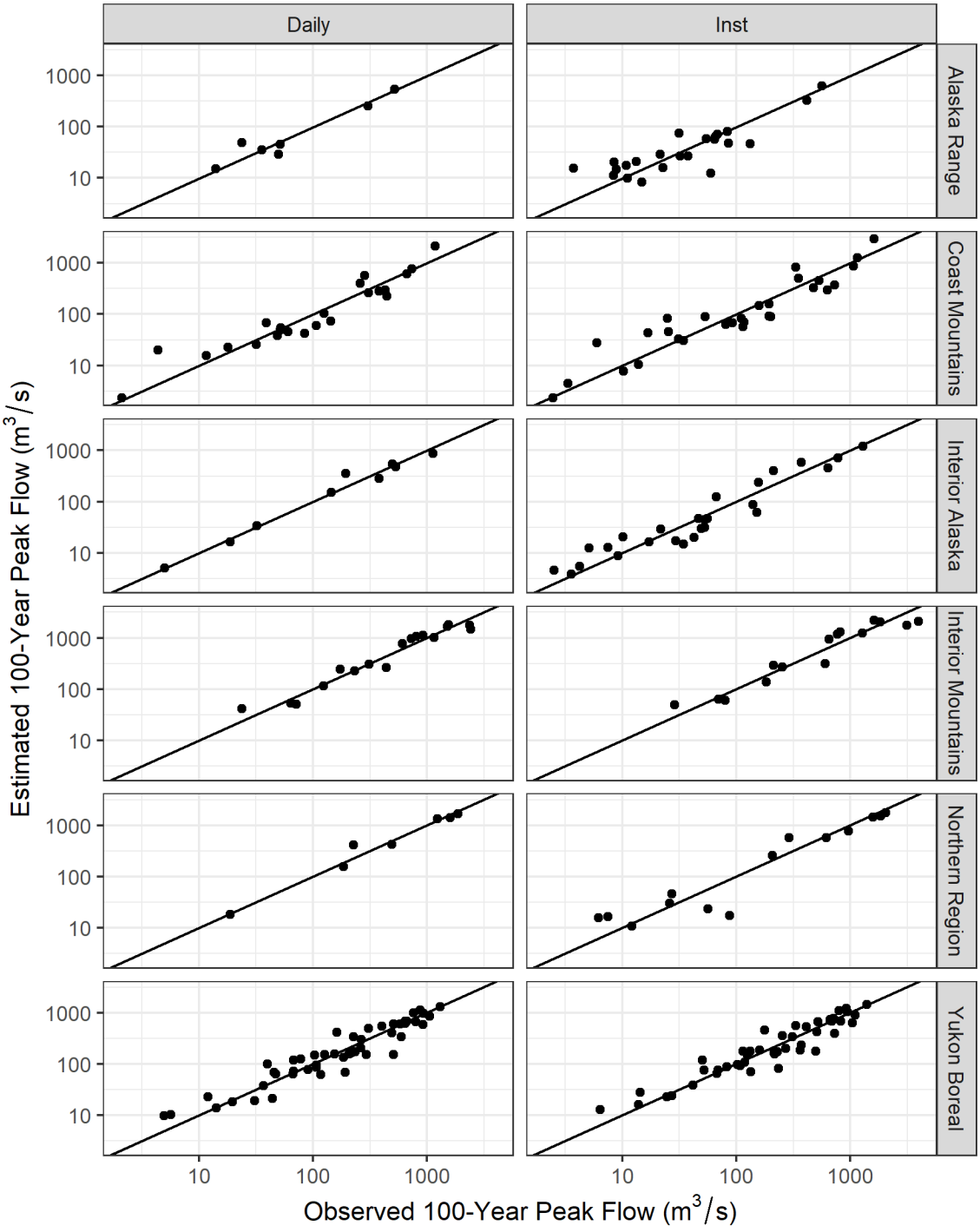

Figure 4.8 Multiple regression model results for prediction of the 100-year return period for daily and instantaneous peak flows for all peak flow regions Diagonal black line indicates a 1:1 fit between the at-site calculated value and the regional prediction.

4.4 Model Performance and Uncertainty

The results from the regional frequency analysis are based on empirical models that relate peak flows to the physical and climatic characteristics of each region's gauged basins. These statistical relationships are uncertain due to the uncertainty in data collection and analysis methodologies (i.e., single station frequency analysis and regional regression development). To support an understanding of the regression performance and uncertainty a number of metrics and uncertainty measures can be used.

4.4.1 Model Performance

Model performance is summarized in Table 4.5 through Table 4.10 by the coefficient of determination, the pseudo coefficient of determination, the standard error of prediction, and the leave-one-out cross-validation error.

The coefficient of determination, or R^2, is a common metric of regression performance ranging from 0 to 1. The metric describes how well the variability of discharge is explained by the regression model and is defined as (Farmer et al., 2021):

$$R^2 = 1 - \frac{SS_E}{SS_A} = \frac{\sum_{i=1}^{N}(Y_i - \widehat{Y}_i)^2}{\sum_{i=1}^{N}(Y_i - \overline{Y}_i)^2}$$

where SS_E is the residual sum of square errors , SS_A is the total sum of squares, N is the number of observations, Y_i is the observed value, $\widehat{Y}_i$ is the estimated value, and $\overline{Y}_i$ is the mean of the observed values.

The pseudo coefficient of determination, or R^2_{pseudo}, is a suggested metric for GLS regressions (Griffis and Stedinger, 2007). The metric is based on the modelling error variance and describes the variability of the response variable (i.e., discharge) explained by the regression after the effect of time sampling error is removed (Farmer et al., 2021). It is as defined as:

$$R^2_{psuedo} = 1 - \frac{\sigma^2_{\delta|M}}{\sigma^2_{\delta|0}}$$

where $\sigma^2_{\delta|M}$ is the modelling error from a GLS regression with M explanatory variables and $\sigma^2_{\delta|0}$ is the modelling error from a GLS regression with no explanatory variables.

The average standard error of prediction (SEP_{AVG}) is another way to express the accuracy of the regression equation. The average standard error of prediction is the square root of the average variance of prediction (AVP), transformed to percent units (Farmer et al., 2021):

$$AVP = \sigma^2_{\delta} + \frac{1}{N}\sum_{i=1}^{N}\sigma^2_{\eta,i}$$

$$SEP_{AVG} = 100\left[e^{(ln10)^2 AVP} - 1\right]^{0.5}$$

where σ^2_δ is the model error variance, and $\sigma^2_{\eta,i}$ is the sampling mean square error for site *i* of *N* gauges.

Leave-one-out cross-validation, is a cross validation method in which the regressions are developed using a calibration set that consists of all but one gauge from the original analysis. The results from this regression are then used to predict the flow for the gauge which had been excluded. This is completed for *N* gauges such that a set of truly predicted values ($\breve{Y}_i$) is developed. A prediction coefficient of determination (R^2_{pred}) can then be determined from the prediction residual error sum of squares (SS_P) (Farmer et al., 2021):

$$R^2{}_{pred} = 1 - \frac{SS_P}{SS_A} = \frac{\sum_{i=1}^{N}(Y_i - \breve{Y}_i)^2}{\sum_{i=1}^{N}(Y_i - \overline{Y}_i)^2}$$

Model performance of the regional regressions was compared to previous work. In general, the regressions show improved or similar performance (R^2_{pseudo} and SEP_{avg}) compared to the regional regressions developed for Alaska (Curran et al., 2016). The regressions from this Alaska study were for instantaneous data. All data were grouped into one peak flow region, with the regressions described by drainage area and mean annual precipitation. The R^2_{pseudo} for the 2-year to 200-year return periods varied from 0.91 to 0.84 and the SEP_{avg} varied from 70% to 81%. For the current study, the R^2_{pseudo} values are within a similar range across all study regions. The Alaska Range shows slightly worse performance at the 200-year with a R^2_{pseudo} of 0.69. The standard error of prediction was lower for a key region in the Yukon (Yukon Boreal), only ranging from 39% to 55%.The peak flow regions primarily outside of the Yukon (Coast Mountains, Alaska Range, Interior Alaska) had similar standard error of predictions as that from Curran et al. (2016). Although the R^2_{pseudo} of the Interior Mountains and Northern Region are of similar performance as that from Curran et al. (2016), the standard error of prediction is high for the Northern Region (93%). Additionally, the low R^2_{pred} at higher return periods for the Interior Mountains and Daily Coastal Mountains are indicative of potentially poor performance at higher return periods. This may be due to poor estimation of peak flows for higher return periods at single stations (i.e. limited data to predict the 200-year peak flow). These two regions were developed with limited stations in a relatively large area and the use of the equations is cautioned.

The R^2 from this study are also similar to the previous peak flow studies for the Yukon (Janowicz, 1986, 1989). Direct comparison is difficult as both the number of stations used in each regression and the number of explanatory variables influence the coefficient of determination. Considering both Janowicz studies, R^2 generally varied from 0.81 to 0.97, similar to the results achieved in this study.

The regional regression equations were also compared directly to results produced from the regressions provided by Curran et al. (2016) and Janowicz (1989). Figure 4.9 and Figure 4.10 show the comparison between peak flows determined from the two studies and the current study. In comparison to the Curran et al. (2016) study, the current regionalization shows very similar results for the Interior Alaska and Alaska Range, which were covered in entirety by the study area of Curran et al. (2016). Peak flows for the Coast Mountains and the Yukon Boreal based on regressions from this study tend to be lower than values from Curran et al. (2016). Janowicz (1989) grouped gauges into two regions (Interior and Mountains) depending on the slope of the stream. Since stream slope was not calculated as part of this study, the Coast Mountain and Interior Mountains were assumed to fall into the “Mountains Region” and the Yukon Boreal was assumed to be similar to the “Interior Region”. There does not appear to be a

consistent bias when comparing results from the Yukon Boreal. Results from regressions from this study tend to provide higher flows for the Coast Mountains and slightly higher for the Interior Mountains in comparison to the 1989 study.

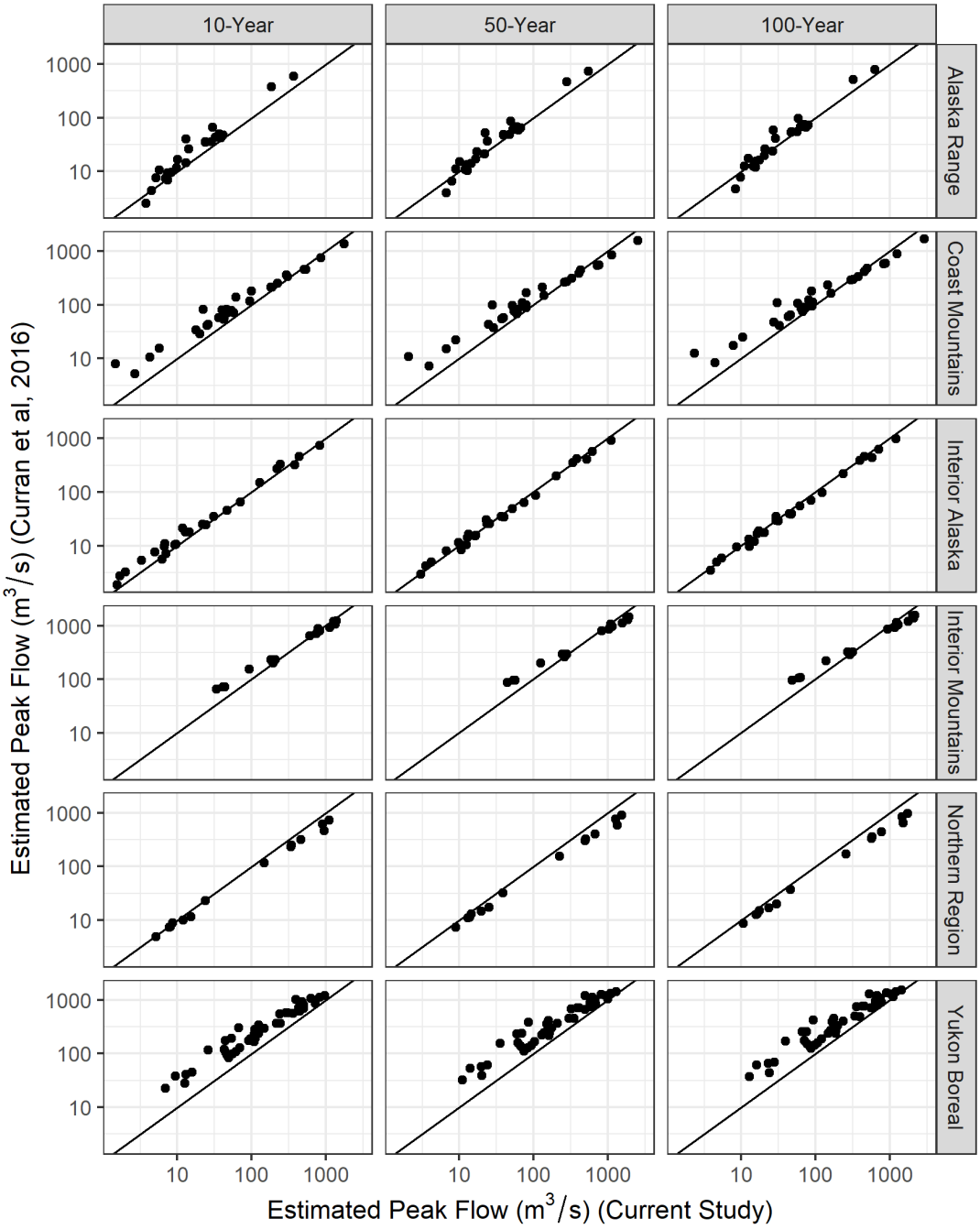

Figure 4.9 Comparison of peak flows calculated from Curran et al. (2016) regression equations to the current study. Black line indicates a 1:1 line.

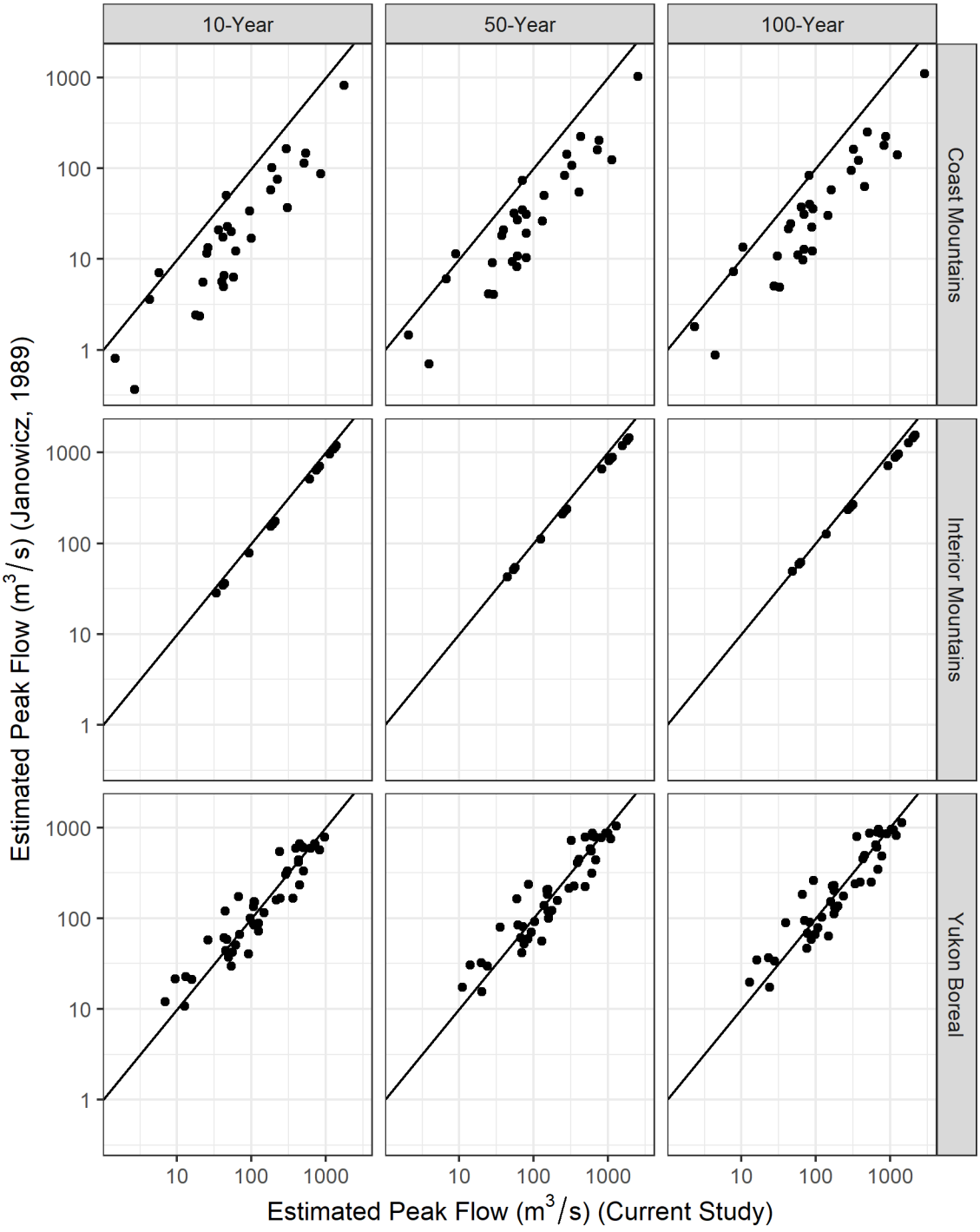

Figure 4.10 Comparison of peak flows calculated from Janowicz (1989) regression equations to the current study. Black line indicates a 1:1 line.

4.4.2 Prediction Intervals

Prediction intervals quantify uncertainty in the estimate of regression coefficients and the uncertainty associated with residuals. A prediction interval provides the expected range of peak flow when used in practice. The 90% prediction intervals for GLS (Tasker and Driver, 1988) can be calculated by:

$$\frac{Q_{pred|Xi}}{C} < Q_{pred|Xi} < Q_{pred|Xi}C$$

$$C = 10^{t_{(\frac{\alpha}{2},N-M-1)}\sigma_{Qpred|Xi}}$$

where Q_{pred} is the regression estimated peak flow for observation *i*, $t_{(\alpha/2,\ N\text{-}M\text{-}1)}$ is the critical value from the Student t-distribution with *N-M-1* degrees of freedom, $\sigma_{Qpred|Xi}$ is the standard error of prediction for observation *i* with X_i the vector of explanatory variables associated with observation *i*. The standard error of prediction can be calculated from the variance of prediction which is equal to:

$$\sigma_{Qpred|Xi}{}^2 = \sigma_\delta^2 + \sigma_{Q|X_i}^2 = \sigma_\delta^2 + X_i^T(X^T\Lambda^{-1}X)^{-1}X_i$$

where $\sigma^2_{Q|Xi}$ is the conditional variance of the estimated response variable, X_i is the row vector of explanatory variables associated with observation *i*, $(X^T\Lambda^{-1}X)^{-1}$ is the cross-correlation matrix of all explanatory variables adjusted by the weighting matrix for GLS.

An example of calculation of the prediction interval for an ungauged site is included in the example calculations (Appendix B). The cross-correlation matrices and model error variance for each of the peak flow regions, return periods, and duration are included in Appendix C and are embedded within the spreadsheet tool (Appendix D).

4.5 Skew Analysis

Skew describes the tail behaviour of the LP3 distribution and can have a large impact on high return period events. These high return period events are typically of interest in flood frequency analyses and hence particular attention has been paid to regional prediction of skew. The USGS has extensively studied patterns of skew in multiple iterations over the years. The most recent regional skew analysis for Alaska was completed in 2016 (Curran et al., 2016). The emulation of a USGS skew analysis is outside of the scope of this project; however, fitted skews were assessed by peak flow region and in space.

The skew analysis focused on gauges with at least 25 years of instantaneous data. This level of data is quite sparse within the study area, but the determination of skew is more reliable at records of this length. Table 4.12 summarizes the number of gauges within each peak flow region with this amount of data. Given the sparsity of the data, a regional skew adjustment was not considered for this study.

Table 4.12 Gauges with at least 25 years of instantaneous peak flow data used in skew analysis

Peak Flow Region	Number of Gauges with at least 25 years of data
Alaska Range	9
Coast Mountains	11
Interior Alaska	12
Interior Mountains	4
Northern Mountains	3
Yukon Boreal	31

Figure 4.11 shows the kernel density of the skew for the five peak flow regions. The Coast Mountains appear to have higher skew than the other regions but the limited number of gauges within each region does not allow to conclude this with certainty. In British Columbia, gauges with a higher proportion of winter peaks (rainfall driven peaks),which may be expected in the Coast Mountains where temperatures are warmer, have been shown to have higher skews (NHC, 2021). Figure 4.12 shows the spatial distribution of fitted skew values across the study area. Again, no discernible spatial pattern is obvious from the data.

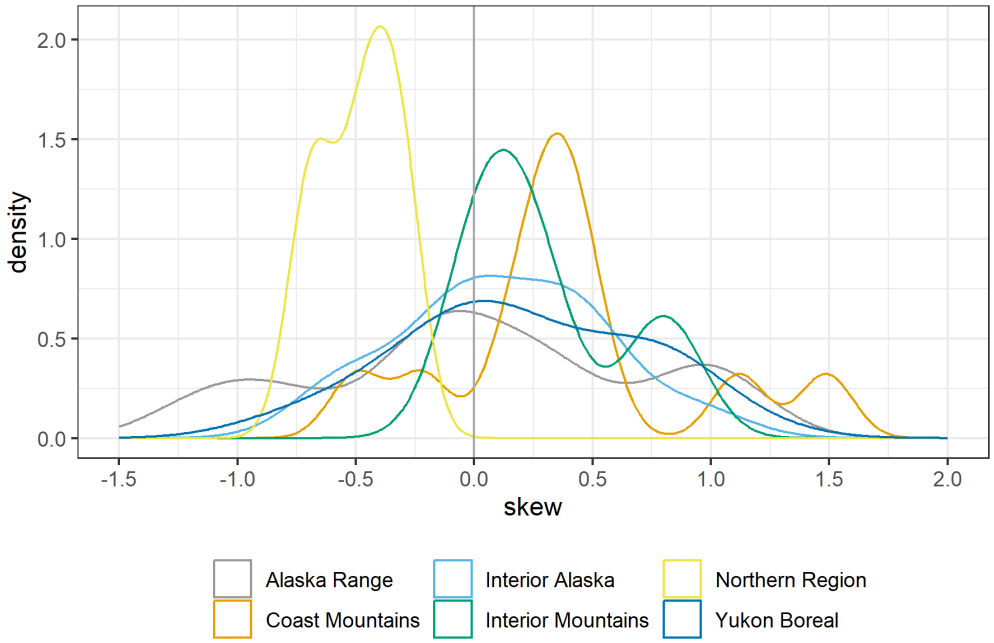

Figure 4.11 Kernel density of skew for each peak flow region

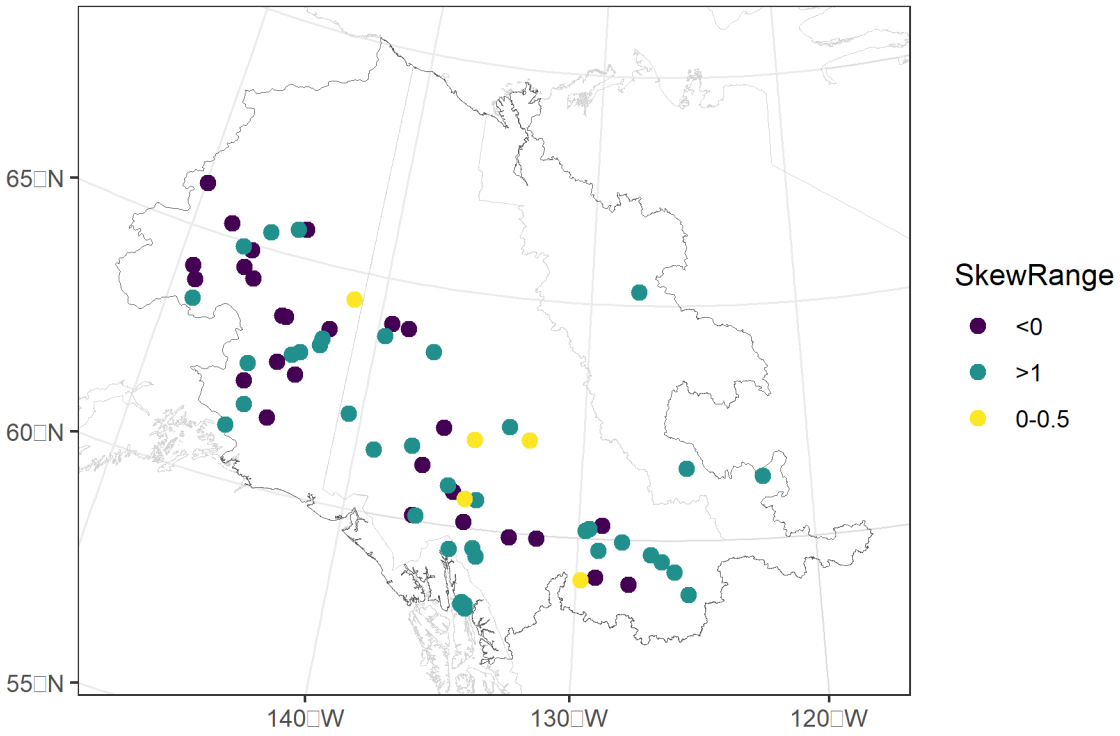

Figure 4.12 Spatial distribution of skew within the project study area for gauges with at least 25 years of instantaneous data

The distribution of skew based on key basin characteristics was also investigated. This included all of the significant variables from the regional regression analysis as well as an indicator of the seasonality of a gauge (described in Section 3.3).

As shown in Figure 4.13, there is no strong relationship between skew and the explanatory variables. A weak relationship between skew and basin area may be present in the Yukon Boreal region but given the sparsity of data it is difficult to discern.

Although no regional skew adjustment has been developed, when applying a single station frequency analysis from this study, a user may elect to adjust the skew for that station. For example, if a station has a negative skew (i.e., an upper bound), this may not be suitable for some design or engineering applications. In these cases, skew could be adjusted to 0 (LN distribution) or to a higher value based on the distribution of skews in Figure 4.11.

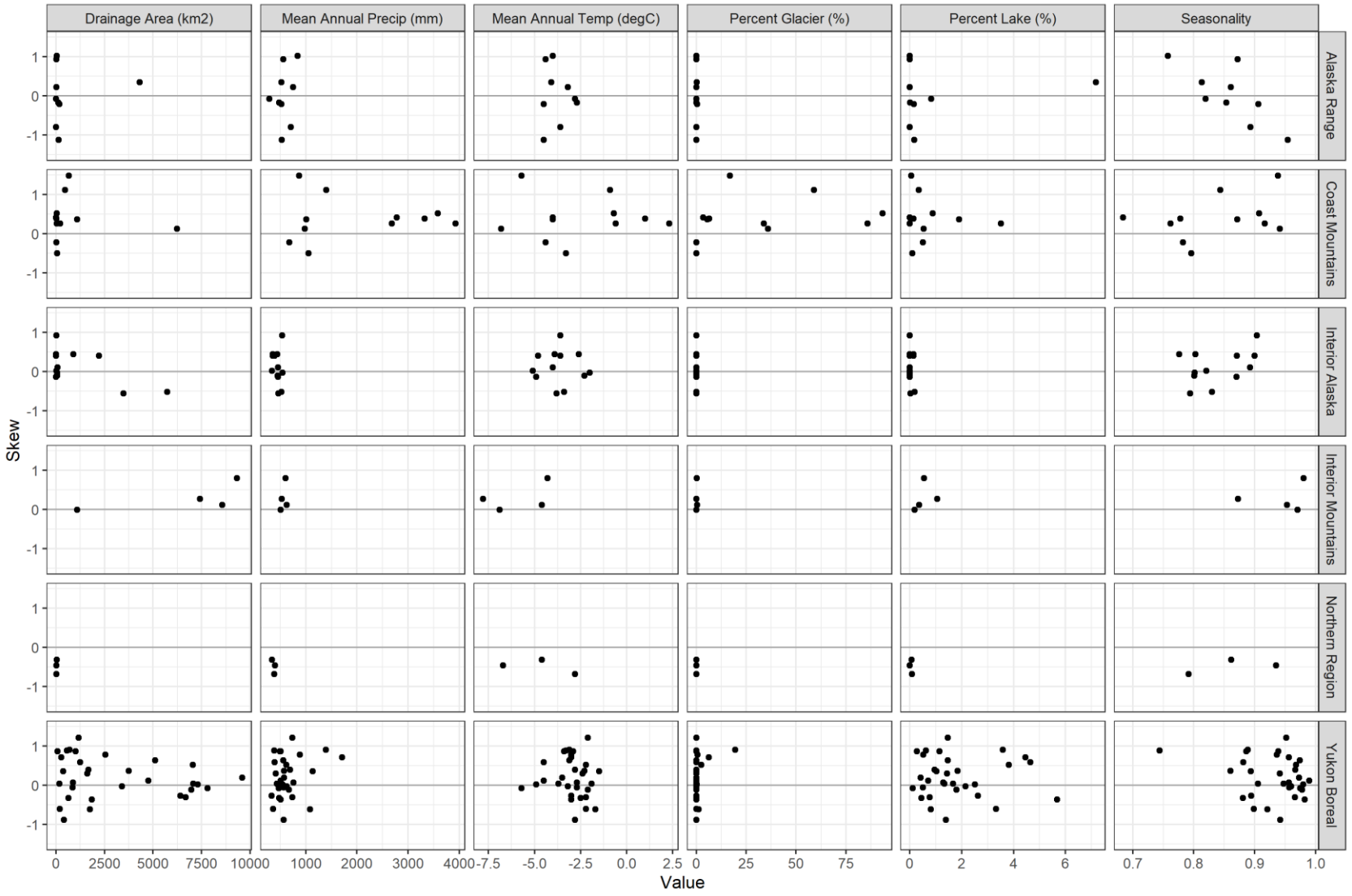

Figure 4.13 Relationship between skew and explanatory variables by peak flow region

4.6 Basin Drainage Area Scaling

Drainage area based scaling from one or more proxy gauges with similar characteristics can be used to estimate peak flows in an ungauged basin or for a location downstream or upstream of an existing gauge. Area based scaling follows the form:

$$Q_{ungauged} = Q_{gauged} \cdot \left(\frac{Area_{ungauged}}{Area_{gauged}} \right)^{b}$$

where Q_{gauged} is a peak flow of a gauged site, and $Area_{gauged}$ and $Area_{ungauged}$ are the basin drainage areas for the gauged and ungauged basins. The scaling exponent *b* is used as it is assumed that peak flows scale according to a power law form. A range of values for *b* have been suggested, with studies suggesting that this scaling exponent can vary regionally (Eaton et al., 2002; NHC, 2021; Sumioka et al., 1998; Thomas et al., 1994).

A power law model was fit to the 2-, 5-, 10, 25-, 50-, 100-, and 200-year return period flows for the instantaneous and daily peaks for each ecoregion. The power law took the form:

$$Q = C \cdot A^{b}$$

where *Q* is the flow, *C* is a constant, *A* is the drainage area of the basin, and *b* is the scaling exponent. As this equation is used only for scaling, the constant C was not used in any manner after the model fitting. A summary of the fitted exponent, *b*, by peak flow region is shown in Figure 4.14 and the model performance range shown in Figure 4.15.

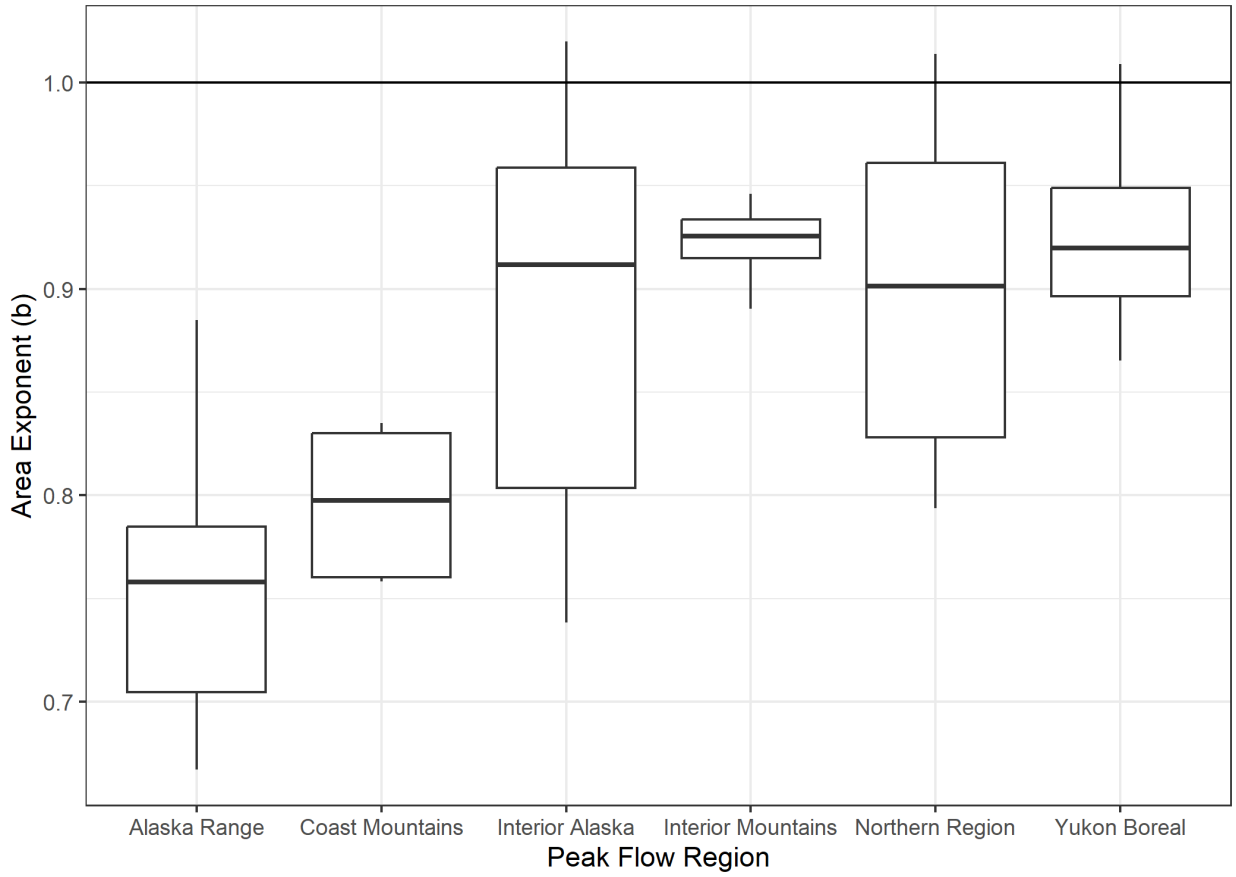

Figure 4.14 Boxplots displaying the range of drainage area scaling exponents (*b*) for the fitted models (all durations and all return periods) for each peak flow region. The center line of the box is the median, the ends of the box represent the 25th and 75th percentiles, and the vertical lines are the maximum and minimums.

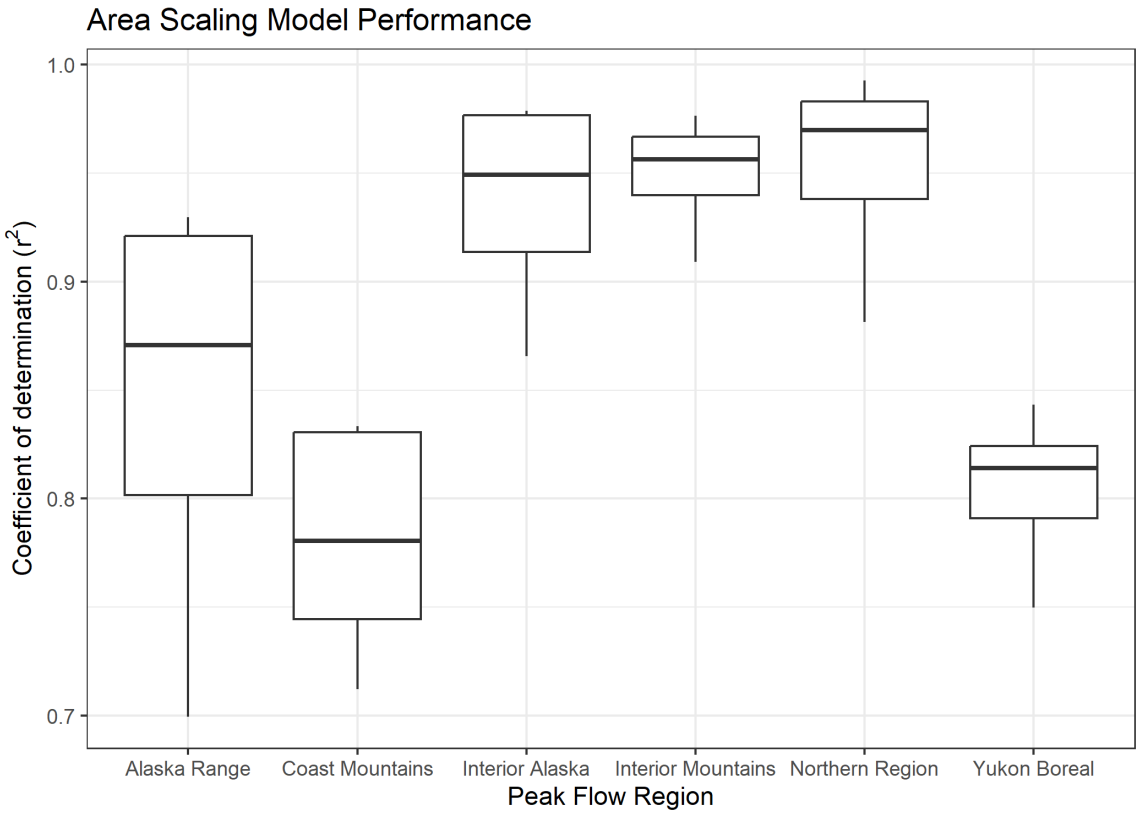

Figure 4.15 Boxplots showing the range of model performance (given as R^2) for all models (all durations and return periods fitted for each peak flow region. The center line of the box is the median, the ends of the box represent the 25th and 75th percentiles, and the vertical lines are the maximum and minimums.

Different aggregation methods for the models were explored, as separate models for each return period, duration, and peak flow region are not likely to be tenable to the end user. Other studies have computed an average exponent based on all return periods (Sumioka et al., 1998) and an average exponent based on all return periods and all durations (NHC, 2021). In general, fitted area scaling exponents in the present study are found to increase by duration (i.e., the daily models have higher b exponents than the instantaneous models) and decrease with return period (e.g., the 200-year return period has the lowest value). The average exponents that would result (points in Figure 4.16) are fairly similar when aggregating by duration or return period, despite there being some differences in the range (length of vertical lines in Figure 4.14).

Given that the average of the two variables are similar, and that it has previously been accepted to compute an average value both across all return periods (Sumioka et al., 1998) and return periods and duration (NHC, 2021), scaling exponents were averaged by both return period (2-, 5-, 10, 25-, 50-, 100-, and 200-year) and duration (instantaneous and daily). Table 4.13 summarizes the scaling exponents that could be used for a peak flow region along with minimum and maximum values that could be applied for a sensitivity analysis. Site specific knowledge should override these exponents when available. For

example, if it is known that the ungauged site is drier and a larger size than the gauged watershed, the user could determine that adjusting the scaling exponent downward is appropriate. In some cases, the fitted exponent b was slightly above 1, but it has been reported as 1 (i.e., linear scaling). There is no physical basis for a regional scaling exponent greater than 1 and results above 1 are most likely due to uncertainty in model fitting. Sumioka et al. (1998) note that the area based scaling is most applicable for basins within 50% of the same watershed area.

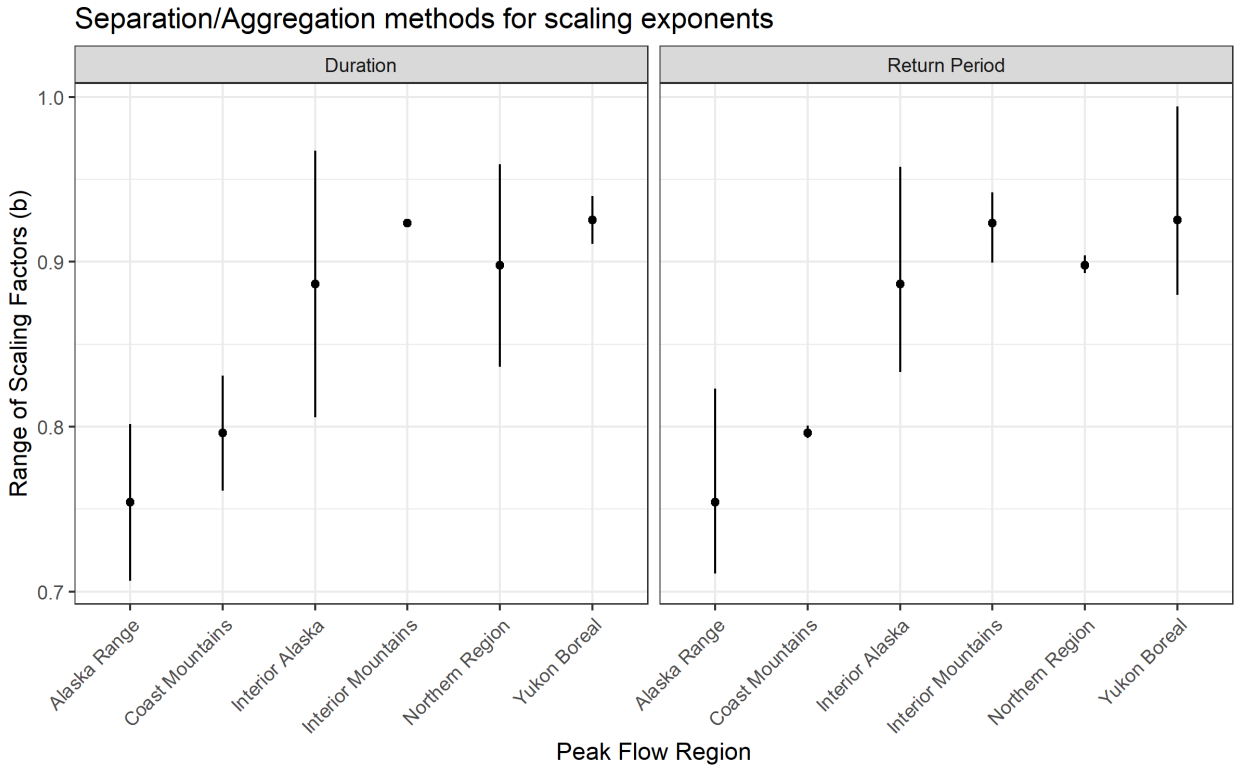

Figure 4.16 Comparison of separation of area scaling exponent (*b*) by duration (i.e., averaging over return period) and separation by return period (i.e., averaging over duration)

Table 4.13 Suggested scaling exponents for peak flow regions

Peak Flow Region	Scaling Exponent (b)		
	Average	Minimum	Maximum
Alaska Range	0.75	0.71	0.82
Coast Mountains	0.80	0.76	0.83
Interior Alaska	0.89	0.81	0.97
Interior Mountains	0.92	0.90	0.94
Northern Region	0.90	0.84	0.96
Yukon Boreal	0.93	0.88	0.99

4.7 Limitations

The determination of peak flows based on regional analysis is inherently difficult. The extent of the study area, variation in hydrologic responses, and sparse data coverage contribute to difficulties in estimation of peak flow. Key limitations and sources of uncertainty include:

- The regression analysis is an empirical analysis that relates peak flows to basin characteristics. The relationships must be interpreted within the limits of the data used to develop the peak flow relationships with an understanding that the results are based on fitted estimates. Multiple methods (comparison against other regional studies or site-specific studies) are recommended when applying the equations in practice.
- The regression equations are intended for use with basin characteristics obtained using the same datasets described in this report. Substituting basin characteristics obtained through alternate data sources may result in unreliable values.
- The regression equations are not applicable to sites which are regulated or where peak flow may be substantially affected by urbanization, sediment, debris, ice, or glacial outburst floods. The regression equations are only applicable to open clearwater peak flow values.
- Coverage of streamflow data is very limited across the study area, with the sparsest coverage in the northern parts of the study area. Equations should be applied with caution as they are based on limited sample size.
- Station records as short as 10 years were used in the development of regression equations, therefore higher uncertainty exists for the higher return period regression equations. A detailed review of all extreme, provisional, or estimated peak flow values was not undertaken and can add uncertainty to the regional analysis. Limitations and uncertainty from the single station analysis (Section 3.4) are applicable to the results from the regression analyses, with uncertainty further compounded in the regional analysis.
- The inclusion of mean annual precipitation and mean annual temperature as part of the regression analysis considers the historical conditions of these variables. These variables will change with a changing climate, and this must be considered in the application of these equations in the future. This is further discussed in Section 5. A review of the study results is recommended in 5 years, with an update to the study recommended within 10 years.

5 CLIMATE CHANGE

Climate change is an important factor when considering how peak flows may change when designing and assessing transportation infrastructure, water crossings, conveyance structures, and other water resource projects.

This section provides a summary of climate change projections available at the time of this study for the Yukon (Section 5.2), and guidance for applying the regional regressions developed in this report for the purpose of obtaining future projections of peak flow (Section 5.1). Supplementary information detailing permafrost change and current trends in long term Yukon climate data and snow data are contained within Appendix E.

5.1 Climate Change Projections for Yukon

Climatic projections over any region are subject to multiple sources of uncertainty. The principal sources of uncertainty for more proximal time horizons (e.g., 2021-2040 or 2041-2060) are the natural variability of climate (and the analogous stochastic variability that is present in any run of a global climate model), the differences in formulation between the models, the limitations of our knowledge and of any of our models, and the unknown future emissions of greenhouse gases. The latter factor – unknown future emissions – becomes the dominant source of projection uncertainty for more distal time horizons (e.g., 2081-2100). Given these different uncertainties, future projections for any climatic variable cover a wide range of values.

Figure 5.1 displays the range of projections (i.e., the range from the 25th and 75th percentile of the ensemble of global climate models) of mean annual temperature for different time horizons and the six principal emissions scenarios from CMIP6 (Shared Socio-economic Pathways, SSPs). Projections are expressed as a difference relative to the reference period 1995-2014.

Projected warming is large, even for the most optimistic scenarios (SSP1), and large enough in the higher scenarios (Figure 5.1, top panel) to transform the Yukon landscape. Projected temperature rise is not homogeneous across the Yukon, but increases with more northern latitude, a pattern that holds across Canada for all emissions scenarios – this is shown in Figure 5.2 for scenario SSP2-4.5. Projected increases in mean annual precipitation are also significant (Figure 5.1, bottom panel; and Figure 5.3 for SSP3-7.0). For all scenarios, projected precipitation increases are greatest in the fall (defined as September – November).

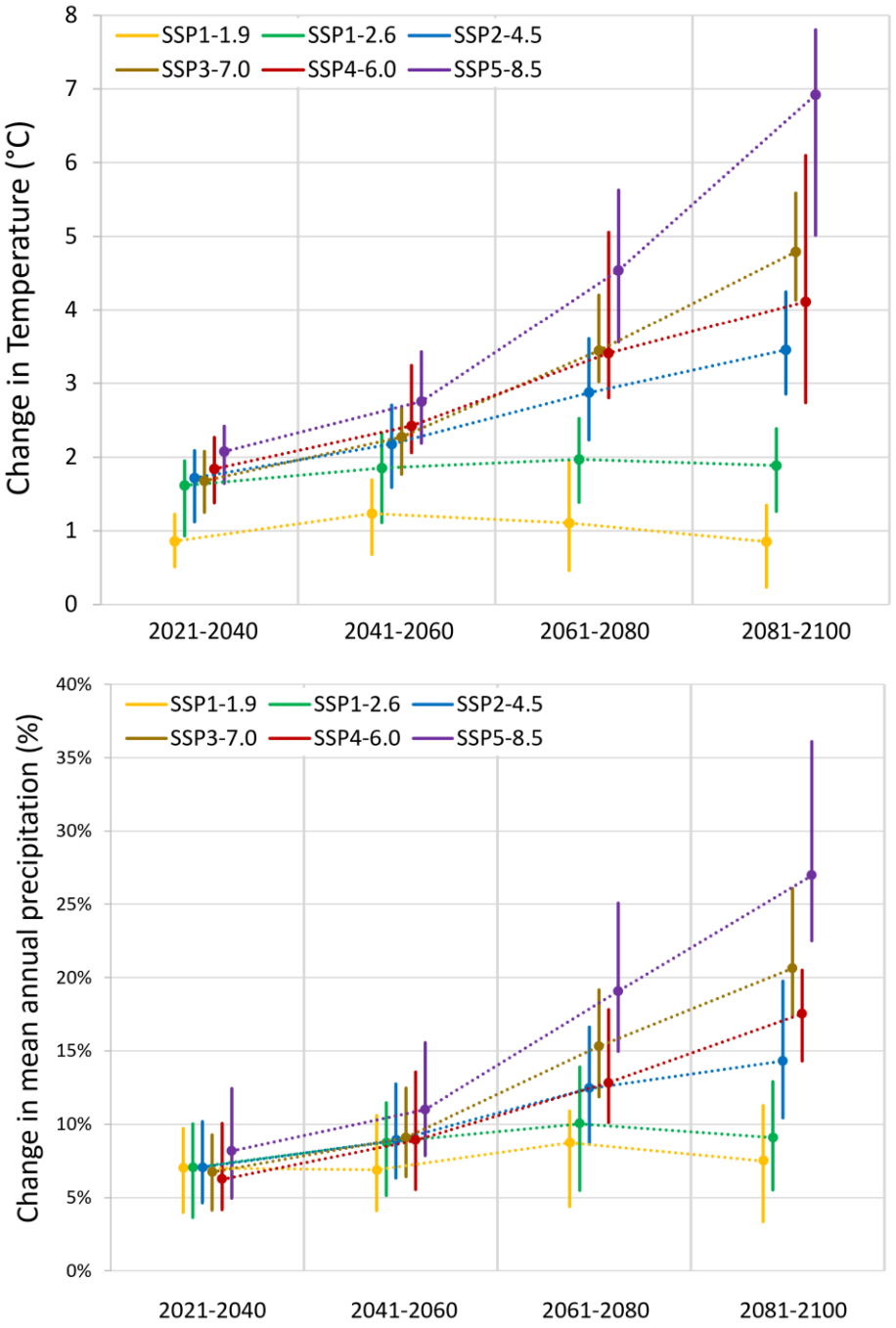

Figure 5.1 Projected changes in mean annual air temperature (top) and precipitation (bottom) averaged over Yukon for future time horizons and for the six SSPs. Changes are relative to the reference period 1995-2014. The vertical bars indicate the range from the 25th to the 75th percentile of projections in the multi-model ensemble. The points indicate the median of projections. Source of data: Canadian Climate Data and Scenarios[2].

[2] https://climate-scenarios.canada.ca/?page=cmip6-scenarios

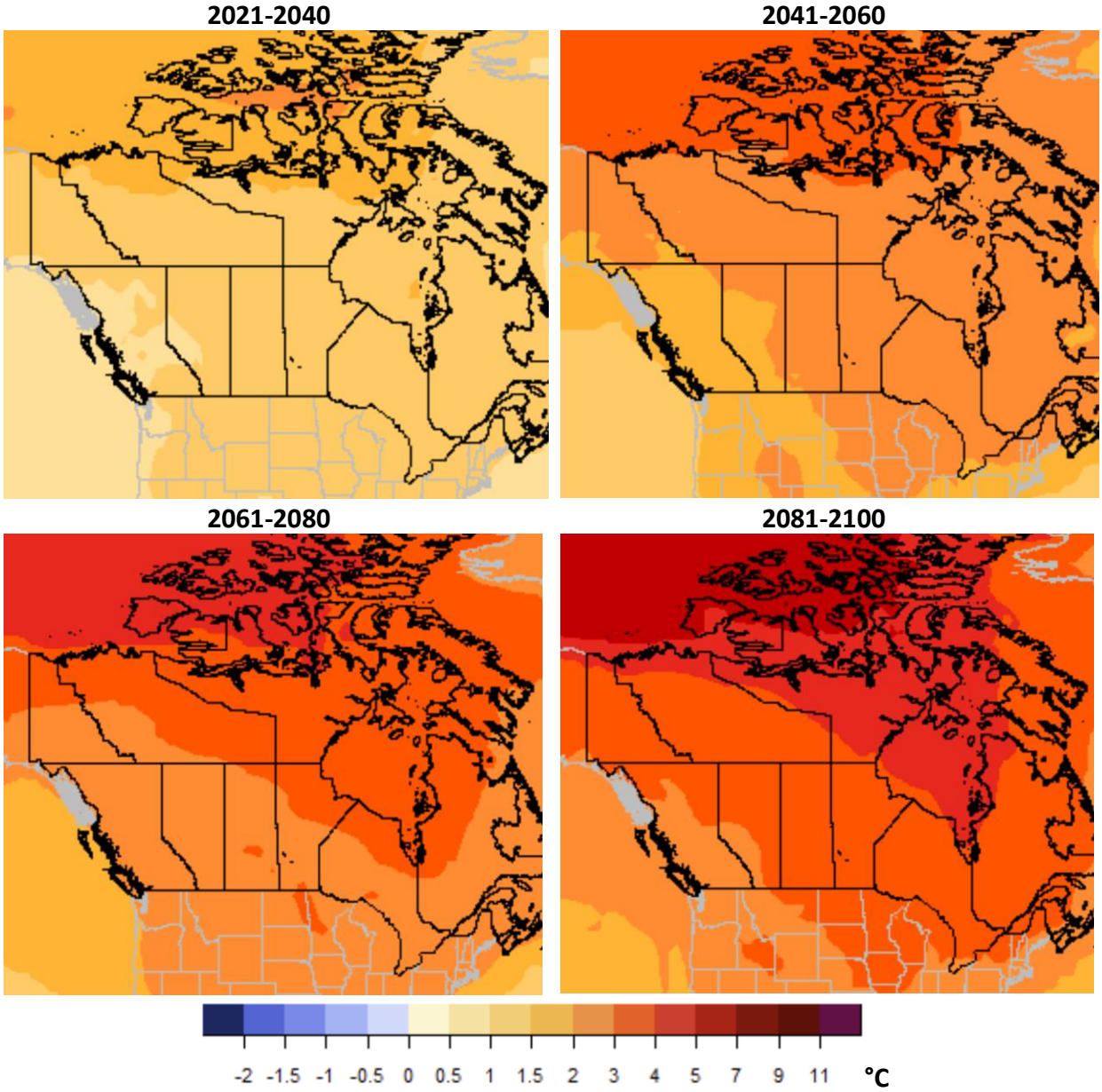

Figure 5.2 Spatial distribution of the median of projected changes in mean annual air temperature (°C) for future time horizons for SSP2-4.5. Source of data: Canadian Climate Data and Scenarios[2].

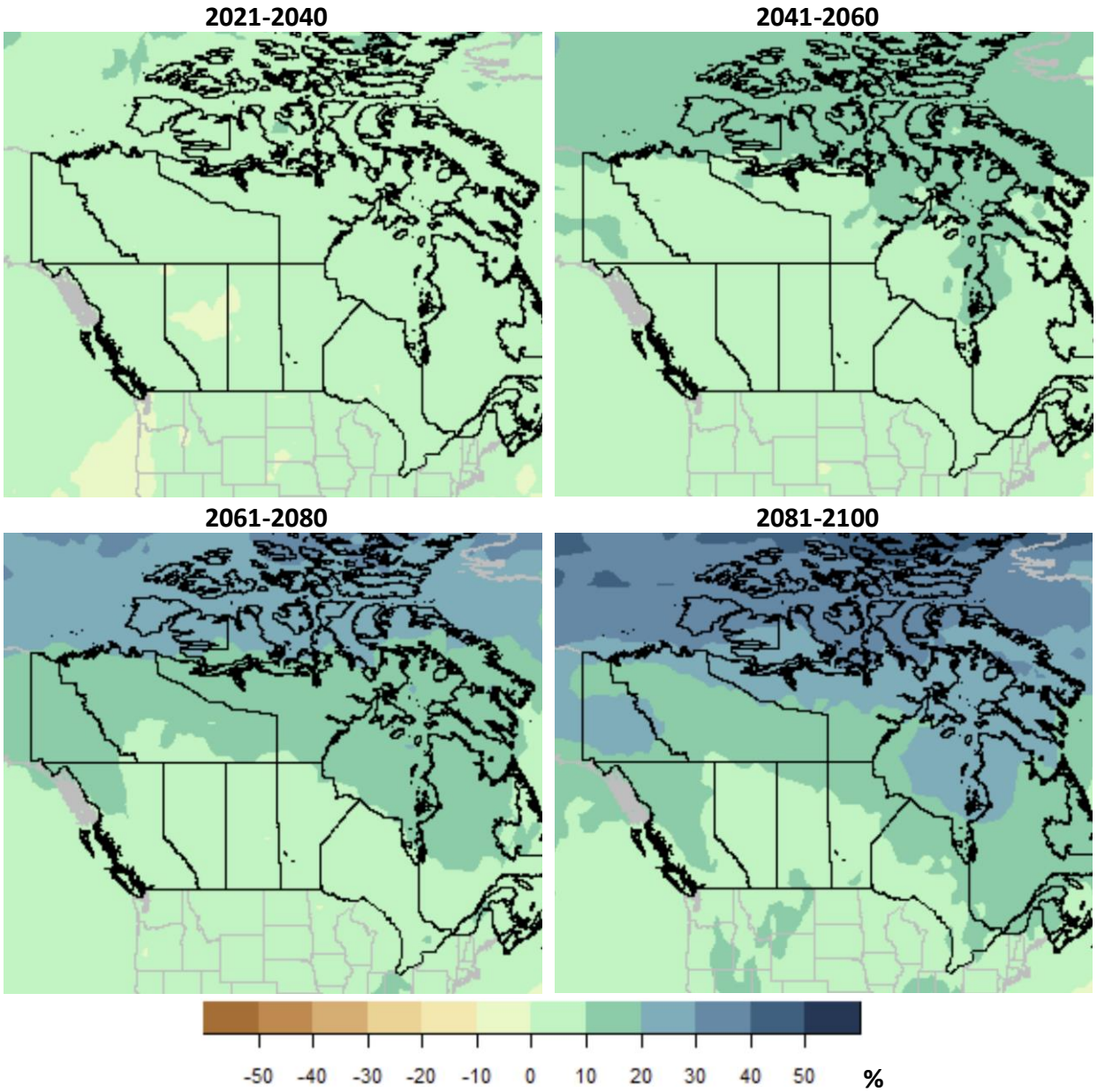

Figure 5.3 Spatial distribution of the median of projected changes (in percentage) in mean annual precipitation (mm a^{-1}) for future time horizons for SSP3-7.0. Source of data: Canadian Climate Data and Scenarios[2].

To support the understanding of climate change projections within the study area, NHC undertook a trend analysis of long-term precipitation and temperature observations from within the study area at Mayo Airport, Watson Lake Airport, Whitehorse Airport, and Dawson (Appendix E). The analysis identified a clear breakpoint in climate trends around 1976. Prior to 1976, temperatures were predominately below the long-term average whereas after 1976 temperatures were above the long-term average. For the most part, seasonal temperatures post 1976 have shown a warming trend among all quantiles although there are seasonal differences among stations. The explanation for the 1976 break

point is currently not known but may be a result of the shift in phase of the Pacific Decadal Oscillation that occurred in 1976 and the inhomogeneity in time series data reflected by smaller precision pre-1976.

For the period post-1976, the fall/winter experienced intense warming trends, especially in the fall season and especially affecting the lower quantiles of the distribution where trends lie between +1°C/decade and +2°C/decade. For the upper quantiles of the distribution, the post-1976 regression trend is more moderate and in some cases, it is negative (cooling). The overall slope for the entire temperature distribution in the post-1976 period is in most cases positive (warming), and especially high in the fall season.

Although warming has been observed, statistically significant trends in temperature were only found for the entire period of record for multiple stations based on the annual time series of minimum seasonal spring and summer temperatures. Statistically significant trends were not found for other seasons or other minimum temperature statistics.

An analysis of historical snow water equivalent (SWE) data across the Yukon was also undertaken to understand potential changes in precipitation. SWE measurements from three measurement periods (March 1, February 1, April 1) were analyzed for 51 stations across the territory. Of the 51 stations, 13 stations had a statistically significant positive trend for March 1 SWE measurements, 12 stations had a statistically significant positive trend for February 1 SWE measurements, and 14 stations had a statistically significant positive trend for April 1. There were no spatial trends in the stations with statistically significant trends. The increase in SWE values may indicate that the warming temperatures since 1976 have not resulted in a smaller snowpack.

The trend analysis for this study was limited to a small number of stations and analyses. Other analyses have also observed a noted increase in annual temperature of 2°C from 1972 to 2022 (Environment and Climate Change Canada, 2022). There is lower confidence in precipitation trends due to interannual variability as well as challenges with precipitation monitoring (Perrin and Jolkowski, 2022).

5.2 Potential Effects of Climate Change on Peak Flows

The projected changes in precipitation and temperature have the potential to alter hydrological processes and peak flows across the Yukon. For example, in some places warmer temperatures may result in a shorter winter period where snow accumulates, decreasing the snowpack and shifting freshet peaks to earlier and lower magnitudes. In other locations, the increased precipitation in October and November coupled with temperatures still below freezing, may lead to a larger snowpack and higher freshet peaks. The shift to warmer temperatures may also lead to increased rain-on-snow events in the fall and spring. Increased precipitation could result in more extreme rainfall events in the spring and summer, shifting flow regimes from freshet dominated to a more mixed regime.

Extensive disintegration of permafrost, which is likely to occur at different rates in different regions, is expected to deeply alter hydrologic response by adding groundwater pathways, potentially attenuating peak flows and limiting the applicability of the regional peak flow equations developed in this and other studies. Significant changes in baseflow have already been detected in the Yukon, the Northwest

Territories, and other arctic regions. Walvoord and Striegl (2007) studied the Yukon River Basin flows measured under ice between January 1 and March 31, a period with negligible surface runoff and mainly subsurface flow contributions. Using records longer than 30 years, they identified an increasing trend in the groundwater contribution to total annual streamflow (by an estimated 0.7–0.9% per year). They proposed this was predominantly a result of permafrost thawing which enhanced infiltration and supported deeper flow paths. Using methods similar to Walvoord and Striegl (2007), a study by St. Jacques and Sauchyn (2009) also reported increases in winter baseflow for 23 rivers in the Northwest Territories. Toohey et al. (2016) used a different methodology, studying the concentration of chemical species in flows of the Yukon River and its major tributary, the Tanana River, to estimate chemical flow rates and infer changes in flow paths over the preceding three decades. They noted notable rises in the annual flux (and especially in the fall/winter flux) of major ions and dissolved organic carbon and suggested that active layer expansion and increased weathering due to permafrost degradation and erosion were the cause. The presence of groundwater pathways may also accelerate permafrost degradation, as suggested by process modeling studies (e.g., McKenzie and Voss, 2013; Lamontagne-Hallé et al., 2018). Appendix E provides a review of projected permafrost changes within the study area. Slope stability following permafrost disintegration is greatly reduced, giving rise to landslides and debris flows, which may also trigger floods.

Menounos et al. (2018) documented the accelerated rate at which glacier mass has been lost in the Yukon and British Columbia, using spaceborne optical satellite imagery. Their analysis showed that glacier loss over the nine more recent years (2009-2018) was four times that of the preceding nine years (2000-2009), a rate increase they partly attributed to changes in atmospheric circulation. Further extensive loss of glacier mass (already greatly-reduced in recent decades; Shugar and Clague, 2018; Menounos, 2021), will create conditions more favorable to glacier outburst floods, and releasing large amounts of sediment. Such floods have occurred historically in the warmer regions of southwest Yukon, and neighbouring southeast Alaska and northwest BC (Moore et al., 2009), but may become more common. Another change which may impact peak flows is the significant reorganization of river networks in response to deglaciation, i.e., the capture of a tributary by a different river, such as occurred in 2011 near Llewellyn Glacier (in the Yukon River headwaters in B.C.) and with a portion of the Slims River watershed in 2016 (Shugar and Clague, 2018). Further glacial loss due to climate change will have dramatic effects on the regional hydrology. Peak flows are expected to initially increase due to warmer temperatures but ultimately will decrease as the glacier volume decreases. Greater inter-annual variability of streamflow may also occur with continued glacier loss, with a shift from predictable glacial melt driven peaks to less predictable rainfall or snowmelt peaks (Milner et al., 2017). Important hydrologic changes can be expected in the glaciated portions of the study area (e.g., for the White River in Yukon, which drains the largest icefields in North America).

How these different effects will combine together in time will influence compound floods, i.e., floods involving multiple drivers (e.g., Zscheischler et al., 2018). Additionally, changes in channel carrying capacity resulting from increasing rates of river bank erosion (Brown et al., 2020), more frequent landslides and debris flows (Huss et al., 2017; Coe et al., 2017), and more frequent wildfires in forested regions, will also influence flood frequency.

5.3 Guidance for Applying Regional Equations for Future Projections

Water resource projects typically have a projected life cycle that can extend out 50 to 100-years, which requires that potential changes to peak flow during that time period be considered. To help understand the potential effects of climate change when applying the results from this study, a qualitative assessment of the potential changes to temperature and precipitation within the basin and the potential effect those changes may have on mechanisms that generate peak flow should be undertaken for each location of interest. The qualitative assessment should include:

- An understanding of changes to seasonal precipitation and temperature (How could these changes potentially impact the snowpack and freshet? Is there the potential for rain-on-snow events or purely rainfall driven events? Is the basin glacierized? What potential impacts could occur due to the loss of glaciers within the basin?)
- An understanding of changes to short duration, high intensity rainfall events (How are extreme precipitation events expected to change? Could this potentially lead to larger rainfall driven events within this basin?)

Once a qualitative understanding is established, projected mean annual precipitation (MAP) and mean annual temperature (MAT) values can then be substituted into the equations, where applicable, to understand the relative change in peak flows. Given the high uncertainty in the quantitative approach, a qualitative understanding is required as it helps ensure that the quantitative results are in line with current understanding.

The most northern regions of the study area (Interior Mountains and Northern Region) do not have climatic variables as part of the regressions. In these cases, the qualitative understanding should be used to guide potential changes to peak flows. Additionally, other studies, including modelling studies such as the results in the 2017 study investigating the sensitivity of the Dempster Highway Hydrological Response to Climate Warning (Janowicz, 2017; Janowicz et al., 2016), may be used to support an understanding of appropriate changes to peak flow.

The regional flood frequency regression equations developed in this report are only valid within the range of climatic variables sampled in the historical period that served as a basis for development of the equations (Table 4.11). When applying the equations for obtaining future projected flood frequency, it is important to ensure that the climatic projections used in the equations are within the range sampled in the same peak flow region during equation development. If the projected mean annual temperature and precipitation exceed the range sampled, this represents an extrapolation of the equations which has high uncertainty and potential error. It is expected that in most cases, temperatures will exceed the historical range used in this analysis well before the end of century. Given the typical life cycle of water resource projects (50 to 100 years), the user of the regression equations must rely on professional judgement to the appropriate application and potential implication associated with extrapolation of the regression equations beyond their current climatic projections. Where the implications of the use of climate change flows are high, the user of the regression equations should elect to undertake additional climate change analysis, such as a modelling study. Appendix B provides climate change resources, at the time of this study, that can be used to determine projected changes to MAT and MAP.

Given the rapid changes underway across the Yukon Territory, the equations may be valid for different lengths of time before projected climatic variables will lie outside the range sampled during the development of the regional equations. The length of time will vary with location (i.e., depending on the local rate at which disintegration of permafrost, glacier mass loss, increasing ratio of rainfall to snowfall, morphological changes, and intensification of precipitation are projected to occur). Those watersheds which are expected to change more slowly, may remain for some time within the range of conditions sampled in the empirical regionalization of the equations. However, for those watersheds experiencing rapid and major changes, the equations' time horizon of applicability may be limited.

The regression equations and quantitative assessment of climate change are only applicable to open clearwater floods. They are solely dependent on changes to precipitation and temperature. They do not consider debris flows, debris floods, glacial outbursts, ice jam damming, or changes to the channel which may impact the magnitude and frequency of peak flows.

While there is a need to provide quantitative information for water resources planning and flood protection planning, the underlying projections of climate change and changes in extreme flows are subject to large and unquantifiable uncertainty (e.g., Kundewicz and Stakhiv, 2013). The main sources of uncertainty are unknown future emissions of greenhouse gases, uncertain response of the global climate system to increases in greenhouse gas concentrations, incomplete understanding of regional manifestations that will result from global changes, and uncertainty of the hydrological response and processes to climate change, with potential dampening or exponential effects (e.g., Hawkins and Sutton, 2010). Additionally, precipitation processes are particularly complex and difficult to simulate accurately in models.

5.4 Limitations

The projection of peak flows under climate change is inherently uncertain. Key limitations which should be considered when considering the guidance provided in this document include:

- The study provides guidance for a high level assessment of climate change impacted peak flows. Depending on the scope and application of the peak flows a more in-depth study may be required. It is up to the user to determine if a more detailed study is required for the application to their use.
- Knowledge and tools about climate change projections and tools are constantly evolving. The user should make use of the most recent sources of information and tools to help with the assessment of climate change.
- The guidance provided does not consider a wide range of climate change impacts to the landscape that have the potential to ultimately change the peak flow (e.g., permafrost thaw and disintegration, glacier mass loss, land slides, debris flow).

6 GUIDANCE AND EXAMPLES

This study provides several methods for determining peak flows for ungauged basins. For ungauged locations, the regression equations (Section 4.3) can be used to determine peak flows while the basin scaling factors (Section 4.6) can be used to determine peak flows for locations on the same river as a gauge or from nearby proxy gauges. For locations of interest that are gauged, the results from the gauge reports (Appendix A) can be used directly with adjustments to skew based on professional judgement.

Appendix B contains detailed examples of applying the regression equations and the basin scaling. A spreadsheet tool (Appendix D) has also been provided to support the calculation of peak flows using these methods.

When using the methods and tools developed by this study, the following is recommended:

- Rely on a qualified Registrant for the interpretation and application of the study results.
- Several means of peak flow estimation should be undertaken to assess the possible divergence or convergence of estimates. This may include using both drainage area scaling and regression equations, or comparison of results from this study to other studies that cover the study area.
- The prediction intervals and confidence intervals provided in the single station frequency analysis and the regression analysis should be reviewed by the user as part of their assessment of overall uncertainty.
- The regression analysis and drainage area scaling only apply to basins with similar characteristics as those used to develop these tools. Table 4.11 summarizes the limitations of these characteristics.
- The same spatial datasets used to develop the basin characteristics (Table 2.3) should be used when determining the characteristics of a new or ungauged location.
- Regressions for the Interior Mountains and Northern Region should be used with caution given the limited number of stations used to develop these equations.
- For basins which are near the border or cross multiple peak flow regions, equations from both regions should be considered.
- Results from gauges with a significant trend ($p < 0.05$) should be examined closely prior to use.
- When considering climate change, a qualitative assessment of climate change impacts should always be undertaken to help validate and understand the quantitative assessment. The qualitative assessment should include an understanding of seasonal changes to precipitation and temperature and how they could potentially impact peak flow processes (i.e., freshet, rain on snow, rainfall, glacier melt driven peaks). The assessment should also look at potential changes to short duration rainfall. The regression equations do not consider a wide range of climate change impacts to the landscape that have the potential to ultimately change the peak flow (e.g., permafrost thaw and disintegration, glacier mass loss, land slides, debris flow). This should be explicitly considered when qualitatively discussing potential changes to peak flows.

- To quantitatively estimate potential climate change impacts, projected mean annual precipitation and mean annual temperature can be used in regression equations with these variables. In these cases, the climatic conditions under which the regressions were developed should be considered (Table 4.11). When extrapolating beyond the original climatic conditions, the results are highly uncertain and potentially unreliable. The user of the equations should use their judgement on the application and implications of these extrapolated peak flows. In cases where climate change peak flows are of critical importance or have significant implications, a site-specific study should be undertaken.
- If the regression equations do not contain climatic variables, the quantitative climate change assessment could rely on the qualitative assessment. Other studies such as the work done by Janowicz (2017) may be used to support quantitative values for climate change.

7 SUMMARY AND CONCLUSIONS

This study provides an updated methodology for estimating the magnitude and frequency of peak flows across the Yukon. The study area included the Yukon, and portions of the Northwest Territories, British Columbia, and Alaska.

Peak flow data throughout the study area was compiled through to 2021 for both instantaneous and daily annual peak flows for all gauges with at least 10-years of data. Data infilling was performed for the instantaneous series based on the instantaneous to daily peak flow relationship at the gauge and from nested gauges on the same river.

Frequency analyses were performed for the instantaneous, daily, and infilled instantaneous annual peak series. A LP3 distribution was used for gauges with at least 20-years of data, whereas a LN distribution was used for gauges with 10 to 20 years of data. Basin characteristics were compiled for each gauge including drainage area, land cover / land use, climatic conditions, basin topography, dominant permafrost zone and ecoregion. Gauge reports (Appendix A) were generated for each gauge showing a summary of the basin characteristics and the results from the single station frequency analysis.

A regional analysis using regressions that relate peak flow to basin characteristics was performed. The regression analysis used five peak flow regions which were defined based on Level 3 Ecoregions. Variables which were found to be significant to define peak flow varied slightly by peak flow region and included drainage area, mean annual precipitation, mean annual temperature, and % lake. Regional regression equations and prediction intervals were developed using GLS for the 2-year to 200-year peak flows. A limited skew analysis was undertaken which did not find any trends in skew by peak flow region or in space. This analysis was limited to a small number of stations with at least 25-years of peak flow data. In general, a greater density of gauges with longer gauge records is required for a skew analysis. Factors for basin scaling by drainage area were also determined for the five peak flow regions. The suggested scaling exponents were averaged by both duration (instantaneous and daily) and return period.

When considering climate change, projected mean annual precipitation and mean annual temperatures can be used within the regression equation to help estimate the potential change in peak flow. A qualitative assessment of how projected changes in climate will impact peak flow processes can help support use of the regression equations. The regression equations do not consider a wide range of climate change impacts to the landscape that have the potential to ultimately change the peak flow (e.g., disintegration of permafrost, glacier mass loss, land slides, debris flow).

Several examples and a spreadsheet tool were developed to support the utility of this study in practice. Examples are included for developing estimates at a gauged location, an ungauged location using regression equations, and an ungauged location using drainage area based scaling.

It is recommended that users of the results of this study rely on a qualified Registrant for the interpretation and application of the study results. A review of the study results is recommended in 5 years, with an update in 10 years. Potentially significant flood risk changes associated with climate change suggest the need for future periodic updates of stream flow frequency analyses.

8 REFERENCES

Agriculture and Agri-Food Canada (2013). *National Ecological Framework for Canada*. [online] Available from: https://open.canada.ca/data/en/dataset/ade80d26-61f5-439e-8966-73b352811fe6.

Albers, S. (2017). tidyhydat: Extract and Tidy Canadian Hydrometric Data. *The Journal of Open Source Software*, 2(20), 511. doi:10.21105/joss.00511.

Asquith, W. (2011). *Univariate distributional analysis with L-moment statistics using R* (PhD thesis). Texas Tech University.

Brown, D. R. N. et al. (2020). Implications of climate variability and changing seasonal hydrology for subarctic riverbank erosion. *Climatic Change*, 162, 385–404. doi:10.1007/s10584-020-02748-9.

Burn, D. H. (1997). Catchment similarity for regional flood frequency analysis using seasonality measures. *Journal of Hydrology*, 202(1–4), 212–230. doi:10.1016/S0022-1694(97)00068-1.

Coe, J. A., Bessette-Kirton, E. K., and Geertsema, M. (2017). Increasing rock-avalanche size and mobility in Glacier Bay National Park and Preserve, Alaska detected from 1984 to 2016 Landsat imagery. *Landslides*, 15(3), 393–407. doi:10.1007/s10346-017-0879-7.

Cohn, T. A., England, J. F., Berenbrock, C. E., Mason, R. R., Stedinger, J. R., and Lamontagne, J. R. (2013). A generalized Grubbs-Beck test statistic for detecting multiple potentially influential low outliers in flood series. *Water Resources Research*, 49(8), 12. doi:10.1002/wrcr.20392.

Cohn, T. A., Lane, W. L., and Baier, W. G. (1997). An algorithm for computing moments-based flood quantile estimates when historical flood information is available. *Water Resources Research*, 33(9), 2089–2096.

Commission for Environmental Cooperation (1997). *Ecological regions of North America: toward a common perspective*. [online] Available from: https://www.epa.gov/eco-research/ecoregions-north-america.

Curran, J. H., Barth, N. A., Veilleux, A. G., and Ourso, R. T. (2016). *Estimating flood magnitude and frequency at gaged and ungaged sites on streams in Alaska and conterminous basins in Canada, based on data through water year 2012* (2016–5024). Report. Reston, VA. 58 pp. [online] Available from: http://pubs.er.usgs.gov/publication/sir20165024.

Curran, J. H., Meyer, D. F., and Tasker, G. D. (2003). *Estimating the magnitude and frequency of peak streamflows for ungaged sites on streams in Alaska and conterminous basins in Canada* (03–4188). Report. 101 pp.

Dalrymple, T. (1960). *Flood-frequency analyses, Manual of Hydrology: Part 3* (1543A). Report. [online] Available from: http://pubs.er.usgs.gov/publication/wsp1543A.

De Cicco, L. A., Hirsch, R. M., Lorenz, D., and Watkins, D. (2018). *dataRetrieval*. doi:10.5066/P9X4L3GE. [online] Available from: https://code.usgs.gov/water/dataRetrieval/-/tree/v2.7.11 (Accessed 30 August 2022).

Eaton, B., Church, M., and Ham, D. (2002). Scaling and regionalization of flood flows in British Columbia, Canada. *Hydrological Processes*, 16(16), 3245–3263. doi:10.1002/hyp.1100.

England Jr., J. F., Cohn, T. A., Faber, B. A., Stedinger, J. R., Thomas Jr., W. O., Veilleux, A. G., Kiang, J. E., and Mason, Jr., R. R. (2019). *Guidelines for determining flood flow frequency — Bulletin 17C* (4-B5). USGS Numbered Series. U.S. Geological Survey, Reston, VA. 168 pp. [online] Available from: http://pubs.er.usgs.gov/publication/tm4B5 (Accessed 23 July 2022).

Environment and Climate Change Canada (2020). *National hydrometric network basin polygons*. [online] Available from: https://open.canada.ca/data/en/dataset/0c121878-ac23-46f5-95df-eb9960753375 (Accessed 25 May 2022).

Environment and Climate Change Canada (2022). *Climate Trends and Variations Bulletin*. [online] Available from: https://www.canada.ca/en/environment-climate-change/services/climate-change/science-research-data/climate-trends-variability/trends-variations/annual-2022-bulletin.html.

Falcone, J. (2011). *GAGES-II: Geospatial Attributes of Gages for Evaluating Streamflow*. [online] Available from: https://water.usgs.gov/GIS/metadata/usgswrd/XML/gagesII_Sept2011.xml (Accessed 25 May 2022).

Farmer, W. H. (2021). *WREG: Weighted Least Squares Regression for Streamflow Frequency Statistics*. doi:10.5066/P9ZCGLI1. [online] Available from: https://code.usgs.gov/water/wreg (Accessed 18 February 2023).

Farmer, W. H., Kiang, J. E., Feaster, T. D., and Eng, K. (2021). Regionalization of surface water statistics using multiple linear regression. *U.S. Geological Survey Techniques and Methods, Book 4 Hydrologic Analysis and Interpretation*. U.S Geological Survey.

Fill, H. D., and Stedinger, J. R. (1995). Homogeneity tests based upon Gumbel distribution and a critical appraisal of Dalrymple's test. *Journal of Hydrology*, 166(1–2), 81–105. doi:10.1016/0022-1694(94)02599-7.

Gallant, A. L., Binnian, E. F., Omernik, J. M., and Shasby, M. J. (1995). *Ecoregions of Alaska* (1567). U.S. Geologicaly Survey Professional Paper. United States Government Printing Office, Washington.

Government of Canada (2022). Canadian Digital Elevation Model (CDEM). Canadian Digital Elevation Model. [online] Available from: https://open.canada.ca/data/en/dataset/7f245e4d-76c2-4caa-951a-45d1d2051333.

Graf, W. L. (1999). Dam nation: A geographic census of American dams and their large-scale hydrologic impacts. *Water Resources Research*, 35(4), 1305–1311. doi:10.1029/1999WR900016.

Griffis, V. W., and Stedinger, J. R. (2007). The use of GLS regression in regional hydrologic analyses. *Journal of Hydrology*, 344(1–2), 82–95. doi:10.1016/j.jhydrol.2007.06.023.

Grover, P. L., Burn, D. H., and Cunderlik, J. M. (2002). A comparison of index flood estimation procedures for ungauged catchments. *Canadian Journal of Civil Engineering*, 29(5), 734–741. doi:10.1139/l02-065.

Grubbs, F., and Beck, G. (1972). Extension of Sample Sizes and Percentage Points for Significance Tests of Outlying Observations. *Technometrics*, 14(4), 847–854.

Hawkins, E., and Sutton, R. (2010). The potential to narrow uncertainty in projections of regional precipitation change. *Climate Dynamics*, 37, 407–418. doi:10.1007/s00382-010-0810-6.

Hinzman, L. D., Kane, D. L., Yoshikawa, K., Carr, A., Bolton, W. R., and Fraver, M. (2003). Hydrological variations among watersheds with varying degrees of permafrost. *Proceedings of the Eighth International Conference on Permafrost - ICOP 2003*.

Hosking, J. R. M., and Wallis, J. R. (1997). *Regional Frequency Analysis: An approach based on L-Moments*. Cambridge University Press.

Huss, Bookhagen, B., Huggel, C., Jacobsen, D., Bradley, R. S., Clague, J. J., and et al. (2017). Toward mountains without permanent snow and ice. *Earth's Future*, 5, 418–435. doi:10.1002/eft2.207.

Janowicz, J. R. (1986). A methodology for estimating design peak flows for Yukon Territory. *Cold Regions Hydrology Symposium. American Water Resources Association.*

Janowicz, J. R. (1989). *Design flood estimating guidelines for the Yukon Territory*. Whitehorse, YT.

Janowicz, J. R. (2008). Apparent recent trends in hydrologic response in permafrost regions of northwest Canada. *Hydrology Research*, 39(4), 267–275. doi:10.2166/nh.2008.103.

Janowicz, J. R. (2017). *Sensitivity of Dempster Highway Hydrological Response to Climate Warming Addendum*. Yukon Water Ressources Branch.

Janowicz, J. R., Krogh, S., Pomeroy, J. W., Carey, S., and Agnew, C. and A. (2016). *Sensitivity of Dempster Highway Hydrological Response to Climate Warming*.

Jones, S. H., and Fahl, C. B. (1994). *Magnitude and frequency of floods in Alaksa and conterminous basins of Canada* (93–4179). Water Resources Investigation Report. U.S. Geological Survey.

Kane, D. L., and Yang, D. (2004). Overview of water balance determinations for high latitude watersheds. *Northern Research Basins Water Balance*, IAHS Publ 290.

Kendall, M. G. (1975). *Rank correlation methods*. Griffin, London.

Kundewicz, Z. W., and Stakhiv, E. Z. (2013). Are climate models "ready for prime time" in water resources management applications, or is more research needed? *Hydrological Sciences Journal*, 55(7). doi:10.1080/02626667.2010.513211.

Lamontagne-Hallé, P., McKenzie, J. M., Kurylyk, B. L., and Zipper, S. C. (2018). Changing groundwater discharge dynamics in permafrost regions. *Environmental Research Letters*, 13. doi:10.1088/1748-9326/aad404.

Loukili, Y., and Pomeroy, J. W. (2018). *The Changing Hydrology of Lhù'ààn Mãn - Kluane Lake - under Past and Future Climates and Glacial Retreat* (Centre for Hydrology Reoprt No 15.). University of Saskatchewan, Saskatoon, Saskatchewan.

McKenzie, J. M., and Voss, C. I. (2013). Permafrost thaw in a nested groundwater-flow system. *Hydrogeology Journal*, 21. doi:10.1007/s10040-012-0942-3.

McNamara, J. P., Kane, D. L., and Hinzman, L. D. (1998). An analysis of streamflow hydrology in the Kuparuk River Basin, Arctic Alaska: a nested watershed approach. *Journal of Hydrology*, 206, 39–57.

Menounos, B. (2021). *Remote Sensing Strategies to Monitor British Columbia's Glaciers, in State of the Mountains Report of the Alpine Club of Canada*. Edited by Parrotte L. et al. [online] Available from: https://static1.squarespace.com/static/5e7568e0698dd75764fc4247/t/6144c01fefbcdc7e008d6b03/1631895594759/ACC+SotMR+2021+WEB+DL.pdf.

Menounos, B., Hugonnet, R., Shean, D., Gardner, A., Howat, I., Berthier, E., Pelto, B., Tennant, C., Shea, J., Myoung-Jong, N., Brun, F., and Dehecq, A. (2018). Heterogeneous Changes in Western North American Glaciers Linked to Decadal Variability in Zonal Wind Strength. *Geophysical Research Letters*, 46, 200–209. doi:10.1029/ 2018GL080942.

Milner, A. M., Khamis, K., Battin, T. J., Brittain, J. E., Barrand, N. E., Füreder, L., Cauvy-Fraunié, S., Gíslason, G. M., Jacobsen, D., Hannah, D. M., Hodson, A. J., Hood, E., Lencioni, V., Ólafsson, J. S., Robinson, C. T., Tranter, M., and Brown, L. E. (2017). Glacier shrinkage driving global changes in downstream systems. *Proceedings of the National Academy of Sciences*, 114(37), 9770–9778. doi:10.1073/pnas.1619807114.

Moore, R. D., Fleming, S. W., Menounos, B., Wheate, R., Fountain, A., Stahl, K., Holm, K., and Jakob, M. (2009). Glacier change in western North America: influences on hydrology, geomorphic hazards and water quality. *Hydrological Processes*, 23(1), 42–61. doi:10.1002/hyp.7162.

NHC (2021). *British Columbia Extreme Flood Project*. Final Report Prepared for The Ministry of Forests, Lands, Natural Resource Operations and Rural Development by Northwest Hydraulic Consultants Ltd. 170 pp.

Obu, J., Westermann, S., Bartsch, A., Berdnikov, N., Christiansen, H. H., Dashtseren, A., Delaloye, R., Elberling, B., Etzelmüller, B., Kholodov, A., Khomutov, A., Kääb, A., Leibman, M. O., Lewkowicz, A. G., Panda, S. K., Romanovsky, V., Way, R. G., Westergaard-Nielsen, A., Wu, T., Yamkhin, J., and Zou, D. (2019). Northern Hemisphere permafrost map based on TTOP modelling for 2000–2016 at 1 km2 scale. *Earth-Science Reviews*, 193, 299–316. doi:10.1016/j.earscirev.2019.04.023.

Obu, Jaroslav, Westermann, Sebastian, Kääb, Andreas, and Bartsch, Annett (2018). *Ground Temperature Map, 2000-2016, Northern Hemisphere Permafrost*. pp. 40 data points. doi:10.1594/PANGAEA.888600. [online] Available from: https://doi.pangaea.de/10.1594/PANGAEA.888600 (Accessed 24 March 2023).

Perrin, A., and Jolkowski, D. (2022). *Yukon climate change indicators and key findings*. YukonU Research Centre, Yukon University. 126 pp.

Shugar, D. J., and Clague, J. J. (2018). *Changing glaciers, changing rivers, in State of the Mountains Report of the Alpine Club of Canada*. Edited by Parrotte L. et al. [online] Available from: https://static1.squarespace.com/static/5e7568e0698dd75764fc4247/t/5e7a47ccd3ba3b15f0ae3ab8/1585072097291/ACC+SMR+2018+FINAL+180704.pdf.

Smith, C. A. S., Meikle, J. C., and Roots, C. F. (2004). *Ecoregions of the Yukon Territory Biophysical Properties of Yukon Landscapes*. Agriculture and Agri-Food Canada, PARC Technical Bulletin No. 04-01, Summerland, British Columbia. 313 pp.

St. Jacques, J.-M., and Sauchyn, D. J. (2009). Increasing winter baseflow andmean annual streamflow from possible permafrost thawing in the North-west Territories, Canada. *Geophysical Research Letters*, 36(L01401). doi:10.1029/2008GL035822.

Statistics Canada (2017). Ecological Land Classification. [online] Available from: https://www23.statcan.gc.ca/imdb/p3VD.pl?Function=getVD&TVD=426171.

Sumioka, S. S., Kresch, D. L., and Kasnick, K. D. (1998). *Magnitude and Frequency of Floods in Washington* (97–4277). US Geological Survey. 91 pp.

Tasker, G. D., and Driver, N. E. (1988). Nationwide regression models for predicting urban runoff water quality at unmonitored sites. *Journal of the American Water Resources Association*, 24(5), 1091–1101.

Thomas, B. E., Hjalmarson, H., and Waltemeyer, S. D. (1994). *Methods for estimating magnitude and frequency of floods in the southwestern United States*. US Government Printing Office.

Toohey, R. C., Herman-Mercer, N. M., Schuster, P. F., Mutter, E. A., and Koch, J. C. (2016). Multidecadal increases in the Yukon River Basin of chemical fluxes as indicators of changing flowpaths, groundwater, and permafrost. *Geophysical Research Letters*, 43. doi:10.1002/2016GL070817.

U.S. Geological Survey (2020). *Alaska Digital Elevation Model*. [online] Available from: https://data.usgs.gov/datacatalog/data/USGS:e250fffe-ed32-4627-a3e6-9474b6dc6f0b.

USGS (1982). *Guidelines for Determining Flood Flow Frequency, Bulletin #17B of the Hydrology Subcommittee*. Interagency Advisory Committee on Water Data, U.S. Department of the Interior, Geological Survey. 28 pp.

Veilleux, A. G., Cohn, T. A., Flynn, K. M., Mason Jr., R. R., and Hummel, P. R. (2014). *Estimating magnitude and frequency of floods using the PeakFQ 7.0 program*. U.S. Geological Survey Fact Sheet 2013-3108. [online] Available from: http://dx.doi.org/10.3133/fs20133108.

Walvoord, M. A., and Striegl, R. G. (2007). Increased groundwater to stream discharge from permafrost thawing in the Yukon River basin: Potential impacts on lateral export of carbon and nitrogen. *Geophysical Research Letters*, 34(L12402). doi:10.1029/2007GL030216.

Wang, T., Hamann, A., Spittlehouse, D., and Carroll, C. (2016). Locally Downscaled and Spatially Customizable Climate Data for Historical and Future Periods for North America. *PLOS ONE*, 11(6), 1–17. doi:10.1371/journal.pone.0156720.

Wang, T., Hamann, A., Spittlehouse, D. L., and Murdock, T. Q. (2012). ClimateWNA—High-Resolution Spatial Climate Data for Western North America. *Journal of Applied Meteorology and Climatology*, 51(1), 16–29. doi:http://dx.doi.org/10.1175/JAMC-D-11-043.1.

Wang, Y. (2000). *Development of methods for regional flood estimates in the province of British Columbia, Canada* (Text thesis). [online] Available from: https://open.library.ubc.ca/collections/831/items/1.0099688.

WSC (2022). National Water Data Archive HYDAT. Water Survey of Canada (WSC) National Water Data Archive. [online] Available from: https://www.canada.ca/en/environment-climate-change/services/water-overview/quantity/monitoring/survey/data-products-services/national-archive-hydat.html.

Zscheischler, J. et al. (2018). Future climate risk from compound events. *Nature Climate Change*, 8(6), 469–477. doi:10.1038/s41558-018-0156-3.

APPENDIX A

GAUGE REPORTS

APPENDIX B

EXAMPLES AND DESIGN TOOL GUIDANCE

Yukon Regional Flow Frequency Analysis and Empirical Equation Development
Appendix B – Examples and Design Tool Guidance

May 9, 2023
Final Report, Rev. 0

NHC Reference 3007020

DISCLAIMER

This report has been prepared by **Northwest Hydraulic Consultants Ltd.** for the benefit of **Government of Yukon** for specific application to the **Yukon Regional Flow Frequency Analysis Project**. The information and data contained herein represent **Northwest Hydraulic Consultants Ltd.** best professional judgment in light of the knowledge and information available to **Northwest Hydraulic Consultants Ltd.** at the time of preparation, and was prepared in accordance with generally accepted engineering and geoscience practices.

Except as required by law, this report and the information and data contained herein are to be treated as confidential and may be used and relied upon only by **Government of Yukon**, its officers and employees. **Northwest Hydraulic Consultants Ltd.** denies any liability whatsoever to other parties who may obtain access to this report for any injury, loss or damage suffered by such parties arising from their use of, or reliance upon, this report or any of its contents.

Note:
This appendix should only be used in conjunction with a review of the associated project report: Northwest Hydraulic Consultants Ltd. (NHC). 2023. Yukon Regional Flow Frequency Analysis and Empirical Equation Development – Final Report. Prepared for the Government of Yukon.

TABLE OF CONTENTS

LIST OF TABLES IN TEXT

LIST OF FIGURES IN TEXT

1 INTRODUCTION

A regional flow frequency analysis was completed to support the design and assessment of water resource-based infrastructure in the Yukon Territory (NHC, 2023). A spreadsheet tool was developed to provide users with a means of applying the analysis completed as part of the study (Appendix D of NHC, 2023). This tool can be used in conjunction with the gauge reports (Appendix A of NHC, 2023) to support peak flow estimation. This document provides guidance and instruction for use of the spreadsheet tool with example applications for:

- Estimating peak flow for a gauged site (Drury Creek)
    - Analysis includes using a gauge report, adjusting negative skew, application of the regional regression equations, and considering climate change.
- Estimating peak flows for an ungauged site (Bonanza Creek)
    - Analysis includes application of the regional regression equation, calculating the prediction intervals, comparison to other methodologies and considering climate change.
- Estimating peak flows for an ungauged site using a proxy gauge (McLean Creek)
    - Analysis includes application of drainage area based scaling, regional regression equation, and considering climate change.

It is recommended that users of this document and spreadsheet tool rely on a qualified Registrant for the interpretation and application of the results.

2 DESIGN TOOL GUIDANCE AND INSTRUCTIONS

The spreadsheet tool (Appendix D in NHC, 2023) facilitates application of the methodologies developed in the overall study. This section provides instruction and general guidance on the use of the spreadsheet tool. Documentation in NHC (2023) should be referred to when considering the application, limitations, and uncertainty associated with these methodologies.

2.1 Spreadsheet Tool Introduction

The tool "YG_RFFA_Tool_R3.xlsm" is a macro enabled Microsoft® Excel® workbook that uses custom user defined functions for the regional regression equations and calculation of prediction intervals. In order to use the spreadsheet, macros must be enabled within Microsoft® Excel®. When first opened, a security warning (Figure 2.1) will indicate that macros have been disabled. "Enable Content" must be clicked to enable the custom functions within the tool.

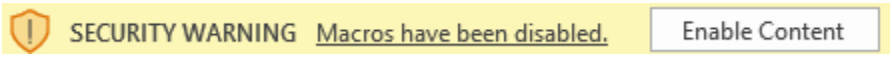

Figure 2.1 Microsoft® Excel® security warning upon opening tool. "Enable Content" must be clicked to use the tool.

The tool contains six sheets which are briefly described in Table 2.1. Additional detail and instructions for each sheet are described in the following sections.

Table 2.1 Summary of Microsoft® Excel® tool sheets

Sheet Name	Description	Additional Information
Description	Provides a description and basic instructions for using the tool	Section 2.1(This report)
PeakFlowRegionsMap	Map with the peak flow regions from the regionalization	Section 2.1(This report)
Regression_Eq	Calculation of instantaneous and daily peak flows under current and future conditions based on regional regression equations	Section 2.2(This report)
RegressionCharts	Displays results from "Regression_EQ" in chart format	Section 2.2(This report)
Area_Based_Scaling	Calculates instantaneous or daily peak flows based on drainage area-based scaling	Section 2.3 (This report)
AreaScalingCharts	Displays results from "Area_Based_Scaling" sheet in chart format	Section 2.3(This report)

The first sheet within the spreadsheet tool is named "Description". This sheet provides an overview of the tool with basic guidance. The user is referenced to this manual for further detail on the use of the tool.

The second sheet is named "PeakFlowRegionsMap." This sheet contains a map showing the peak flow regions developed as part of the study. The map can be used to reference which peak flow region is of interest to a user. A shapefile with the peak flow regions has also been provided which can be imported into a GIS program.

2.2 Regression Equations

The sheet "Regresssion_Eq" is the primary worksheet for calculating peak flows based on the regional regression equations. Users are required to input relevant values into Table 1 (basin characteristics). The peak flow region is selected from a drop down and all values shaded in blue must be input by the user. If a cell turns red, it indicates that the range of the basin characteristic is outside that used to develop the regional regression. If the cell is shaded grey, it indicates that the basin characteristic was not used in the regression equation. Figure 2.2 shows an example input for the Yukon Boreal.

INPUT		
Table 1: BASIN CHARACTERISTICS		
Basin Characteristic	**User Input**	**Range of values applicable to the regional regression equation**
Drainage Area (km^2)	*125*	73 - 9593
Percent Lake (%)	*0%*	0% - 6%
Mean Annual Precipitation (mm)	*350*	331 - 1708
Future Climate Mean Annual Precipitation (mm)	*400*	331 - 1708
Mean Annual Temperature (°C)	*-5*	(-5.7) - (-1.5)
Future Climate Mean Annual Temperature (°C)	*-2*	(-5.7) - (-1.5)
Peak Flow Region	*Yukon Boreal*	

Figure 2.2 Example of required input for regression equations

The basin characteristics inputs are summarized in Table 2.2. Where specific spatial files were used to calculate the values for the regressions, they have been indicated in Table 2.2. Use of other sources may produce unpredictable results.

Table 2.2 Basin characteristic description and data sources

Basin Characteristic	Description	Source
Drainage Area (km^2)	Area of watershed of interest.	Delineated externally in a GIS program.
Percent Lake (%)	Percent of the basin that is covered by lakes.	Calculated externally from combined NHN and USGS datasets
Mean Annual Precipitation (mm)	Mean annual precipitation of the basin	Calculated externally from raster data from Wang et al. (2016)
Mean Annual Temperature (°C)	Mean annual temperature of the basin	Calculated externally from raster data from Wang et al. (2016)
Future Climate Mean Annual Precipitation (mm)	Mean annual precipitation under climate change condition	See Section 3.4
Future Climate Mean Annual Temperature (°C)	Mean annual temperature under climate change condition	See Section 3.4

Four output tables are provided on the "Regression_Eq" sheet. They include:

- Table 2A: Estimated Instantaneous Peak Flows (including 90% prediction intervals)
- Table 2B: Estimated Daily Peak Flows (including 90% prediction intervals)
- Table 3A: Future Climate Estimated Instantaneous Peak Flows (including 90% prediction intervals)
- Table 3B: Future Climate Estimated Daily Peak Flows (including 90% prediction intervals)

The four output tables (Figure 2.3) contain peaks flows for the 2-, 5-, 10-, 25-, 50-, 100-, and 200-year return period. No results are provided in Table 2B and 3B for daily peak flows for the Alaska Range, Interior Alaska, or Northern Mountains regions. If a climatic variable is not an input to the regression equation (greyed out in the basin characteristics in Table 1), the results for Table 3A and 3B (results under climate change) will match those from Table 2 (historic conditions). In these situations, the user is referred to the primary report for climate change considerations. As recommended in NHC (2023), all climate change analyses should be preceded with a qualitative understanding of climate change impacts and their potential to change the basin hydrology and peak flows.

The sheet "RegressionCharts" contains four charts with results from the four output tables on the "Regression_Eq" sheet.

OUTPUT				
Table 2A: ESTIMATED INSTANTANEOUS PEAK FLOWS				
Return Period (Year)	**Annual Exceedance Probability**	**Estimated Peak Flow (m^3/s)**	**90% Prediction Interval (m^3/s)**	
			Lower	**Upper**
2	50.0%	5.8	3	11
5	20.0%	9.8	5.2	19
10	10.0%	13	6.7	25
25	4.0%	17	8.8	35
50	2.0%	21	10	44
100	1.0%	25	12	55
200	0.5%	30	13	68

OUTPUT				
Table 3A: FUTURE CLIMATE ESTIMATED INSTANTANEOUS PEAK FLOWS				
Return Period (Year)	**Annual Exceedance Probability**	**Estimated Peak Flow (m^3/s)**	**90% Prediction Interval (m^3/s)**	
			Lower	**Upper**
2	50.0%	6.4	2.3	18
5	20.0%	11	4.1	28
10	10.0%	14	5.3	38
25	4.0%	19	6.9	52
50	2.0%	23	7.9	67
100	1.0%	27	8.7	87
200	0.5%	32	9.2	112

OUTPUT				
Table 2B: ESTIMATED DAILY PEAK FLOWS				
Return Period (Year)	**Annual Exceedance Probability**	**Estimated Peak Flow (m^3/s)**	**90% Prediction Interval (m^3/s)**	
			Lower	**Upper**
2	50.0%	4.8	2.4	9.4
5	20.0%	7.9	4	15
10	10.0%	10	5.2	20
25	4.0%	14	6.6	28
50	2.0%	16	7.5	35
100	1.0%	19	8.5	43
200	0.5%	22	9.4	53

OUTPUT				
Table 3B: FUTURE CLIMATE ESTIMATED DAILY PEAK FLOWS				
Return Period (Year)	**Annual Exceedance Probability**	**Estimated Peak Flow (m^3/s)**	**90% Prediction Interval (m^3/s)**	
			Lower	**Upper**
2	50.0%	5.3	2.7	10
5	20.0%	8.6	4.4	17
10	10.0%	11	5.6	22
25	4.0%	15	7.1	31
50	2.0%	18	8.2	38
100	1.0%	21	9.3	47
200	0.5%	24	10	58

Figure 2.3 Example of output tables for regression equations

When using the regression equations, the following should be considered:

- For basins which are near the border or cross multiple peak flow regions, equations from both regions should be considered.
- The prediction intervals should be used to understand the associated uncertainty related to the application of the regression equations.
- The regression analyses only apply to basins with similar characteristics as those used to develop these tools. The primary report (NHC, 2023) summarizes the limitations of these characteristics.
- The same spatial datasets used to develop the basin characteristics should be used when determining the characteristics of a new or ungauged location.
- Several means of peak flow estimation should be undertaken to assess the possible divergence or convergence of estimates. This may include using both area scaling and regression equations, or comparison of results from this study to other studies which cover the study area.
- The user should refer to the primary report (NHC, 2023) for specific guidance on the application of climate change.

2.3 Area Based Scaling

The sheet "Area_Based_Scaling" is the primary sheet for calculating peak flows based on area scaling. This method is appropriate when estimating peak flows on a stream or river that is gauged at a different location or using a proxy basin to scale peak flows from. The input required for the calculations are located in Table 1A. The user must enter the values in the blue shaded cells. An example of the input is shown in Figure 2.4.

INPUT	
Table 1A: Basin Characteristics	
Ungauged Site	
Drainage Area (km^2)	*20*
Gauged Site	
Gauge ID	*29AB002*
Gauged Drainage Area (km^2)	184
Region	Yukon Boreal
b	*0.94*

Figure 2.4 Example of input required for area-based scaling

The drainage area of the ungauged site must be calculated by the user. The Gauge ID refers to the gauge which flows will be scaled from. The gauged drainage area and region automatically populate within the input table. The user must enter a scaling exponent (b). Table 1B within the worksheet provides

recommended scaling exponents (b values) based on the analysis from NHC (2023). Table 3 at the bottom of the sheet (Row 75) contains all available gauge IDs which can be used for scaling and their associated drainage area and region. The table can be filtered to constrain the gauge IDs by drainage area or region (Figure 2.5).

Table 3: Gauged Drainage Area by Peak Flow Region			
Gauge ID	**Gauge Name**	**Drainage Area (km^2)**	**Region**
15200000	GAKONA R AT GAKONA AK	1616	Alaska Range
15200280	GULKANA R AT SOURDOUGH AK	4314	Alaska Range
15202000	TAZLINA R NR GLENNALLEN AK	6840	Alaska Range
15478040	PHELAN C NR PAXSON AK	30	Alaska Range
15516000	NENANA R NR WINDY AK	1875	Alaska Range
15518000	NENANA R NR HEALY AK	4904	Alaska Range
15515060	MARGUERITE C AB EMMA C NR HEALY AK	40	Alaska Range

Figure 2.5 Example of Table 3 within the area-based scaling sheet. Table 3 can be filtered by drainage area and region to help identify gauge IDs for basin scaling.

Three output tables (Figure 2.6) are provided on the area-based scaling sheet. The three tables include:

- Table 2A: Estimated Instantaneous Peak Flows (with 90% confidence intervals)
- Table 2B: Estimated Daily Peak Flows (with 90% confidence intervals)
- Table 2C: Estimated Instantaneous Peak Flows with Data Infilling (with 90% confidence intervals).

If results are not available for a certain duration (daily, instantaneous, or infilled), the table will not output a solution. Table 2C (Estimated Instantaneous Peak Flows with Data Infilling) refers to the frequency analysis performed on the instantaneous series which included data infilling.

OUTPUT					
Table 2A: ESTIMATED INSTANTANEOUS PEAK FLOWS					
Return Period (Year)	**Annual Exceedance Probability**	**Q_{gauged} (m^3/s)**	**$Q_{ungauged}$ (m^3/s)**	**90% Confidence Intervals (m^3/s)**	
				Lower	**Upper**
2	50.0%	5.2	0.6	0.5	0.8
5	20.0%	7.4	0.9	0.8	1.2
10	10.0%	9	1.1	0.9	1.5
25	4.0%	11	1.4	1	2
50	2.0%	13	1.6	1.1	2.5
100	1.0%	14	1.8	1.2	3.1
200	0.5%	16	2	1.2	3.8

OUTPUT					
Table 2B: ESTIMATED DAILY PEAK FLOWS					
Return Period (Year)	**Annual Exceedance Probability**	**Q_{gauged} (m^3/s)**	**$Q_{ungauged}$ (m^3/s)**	**90% Confidence Intervals (m^3/s)**	
				Lower	**Upper**
2	50.0%	4.4	0.6	0.5	0.7
5	20.0%	6.3	0.8	0.7	1
10	10.0%	7.6	1	0.8	1.2
25	4.0%	9.3	1.2	0.9	1.6
50	2.0%	11	1.3	0.9	2
100	1.0%	12	1.5	1	2.4
200	0.5%	13	1.7	1	3

Table 2C: ESTIMATED INSTANTANEOUS PEAK FLOWS WITH DATA INFILLING					
Return Period (Year)	**Annual Exceedance Probability**	**Q_{gauged} (m^3/s)**	**$Q_{ungauged}$ (m^3/s)**	**90% Confidence Intervals (m^3/s)**	
				Lower	**Upper**
2	50.0%	5.1	0.6	0.5	0.8
5	20.0%	7.3	0.9	0.8	1.1
10	10.0%	8.9	1.1	0.9	1.4
25	4.0%	11	1.4	1	1.9
50	2.0%	13	1.6	1.1	2.4
100	1.0%	14	1.8	1.1	3
200	0.5%	16	2	1.2	3.7

Figure 2.6 Example of output tables for area-based scaling sheet.

The sheet “AreaScalingCharts” contains two charts which display the results from the area based scaling. One chart is for instantaneous results (both with and without data infilling) and the other for daily results.

The user should consider the following guidance when using the area-based scaling sheet:

- The gauge report and individual frequency analysis of the gauge which is being scaled from should be examined by the user.

- Results from gauges with a positive trend ($p < 0.05$) should be examined closely when using these gauges for area based scaling.
- A range of b values should be considered based on project understanding and uncertainty. Recommended values are provided based on a regional analysis of peak flows.
- Several means of peak flow estimation should be undertaken to assess the possible divergence or convergence of estimates. This may include using both area scaling and regression equations, or comparison of results from this study to other studies which cover the study area.
- Area-based scaling should be limited to ungauged locations within 50% of the gauged watershed area.
- The user should refer to the primary report (NHC, 2023) for specific guidance on the application of climate change. The regression equations can be used in conjunction with the area based scaling to determine appropriate relative changes to peak flows.

2.4 Climate Change Data Sources

Climate change projections for Yukon and all of Canada are available online from websites set up by the Canadian government to support climate adaptation efforts. In this section the websites and online data sources currently available that are most pertinent to this project are reviewed and a recommended website is indicated for this project (Section 2.4.1).

Websites are expected to keep evolving in the future as newer projections are released or are processed in new ways. The current websites reviewed here are able to support users who wish to apply the Yukon flood frequency regression equations developed in this report to project future flood frequency at a specific watershed of interest. The limitations of using the equations for future projections are reviewed in the main report (NHC, 2023).

Other climate change data sources which the user may find useful for their analysis include:

- PCIC Climate Explorer (as of February 2023, provides limited CMIP6 projections) – https://www.pacificclimate.org/analysis-tools/pcic-climate-explorer
- Climate adjusted IDF curves from:
    - IDF CC tool - https://www.idf-cc-uwo.ca/
    - Climatedata.ca - https://climatedata.ca/download/#idf-download

2.4.1 Recommended climate projections website for this project: *ClimateData.ca*

The Canadian government's website "Climate Data for a Resilient Canada[1]" (henceforth referred to as "ClimateData.ca") represents a valuable resource that can be readily used for the purposes of this

[1] https://climatedata.ca or https://donneesclimatiques.ca/

project. ClimateData.ca can be used to retrieve and visualize detailed projections specific to regional watersheds.

In addition to watershed area, one or both of the following climatic variables (depending on the region) are necessary for entry into the Yukon flood frequency regression equations developed in this project:

- Mean annual temperature (MAT)
- Mean annual precipitation (MAP)

Values of MAT and MAP projected for a specific future time horizon can be readily obtained from ClimateData.ca for any watershed or location of choice. In ClimateData.ca choose “Variable” from the menu at the top. A new menu will appear. The user should choose “Mean Temperature” (MAT) or “Total Precipitation”(MAP) from this menu. The user will now be prompted to choose one of these three scenarios:

(a) SSP1-2.6 (marked as “low emissions”)

(b) SSP2-4.5 (marked as “moderate emissions”)

(c) SSP5-8.5 (marked as “high emissions”)

The user must make a choice from the above three future scenarios. They refer to future global emissions of anthropogenic greenhouse gases, of which the principal ones are carbon dioxide, methane and nitrous oxide. It is unknown what the future course of emissions of these gases into the earth’s atmosphere will be from worldwide sources. Predicting future emissions carries great uncertainty, because emissions will depend on future political decisions, technological advances, economic development, and global markets, among other factors.

ClimateData.ca offers a tutorial on the SSP scenarios, and guidance on criteria for scenario selection depending on the purpose of use.

Once the user has chosen one of the above three scenarios, a map of Canada will appear on the screen. A pull-down menu near the top offers the choice of viewing the map with grid cells, census subdivisions, health regions, or watersheds. The choice “watersheds” offers the opportunity to download the projected Mean Annual Temperature and Mean Annual Precipitation calculated over the area of each specific watershed. The example of the Upper Porcupine-Bell watershed is shown in Figure 2.7. Since each global climate model that is run for a fixed scenario produces different projections, this website provides the median (50th percentile) of the projections ensemble, as well as a range defined by the 10th and 90th percentiles.

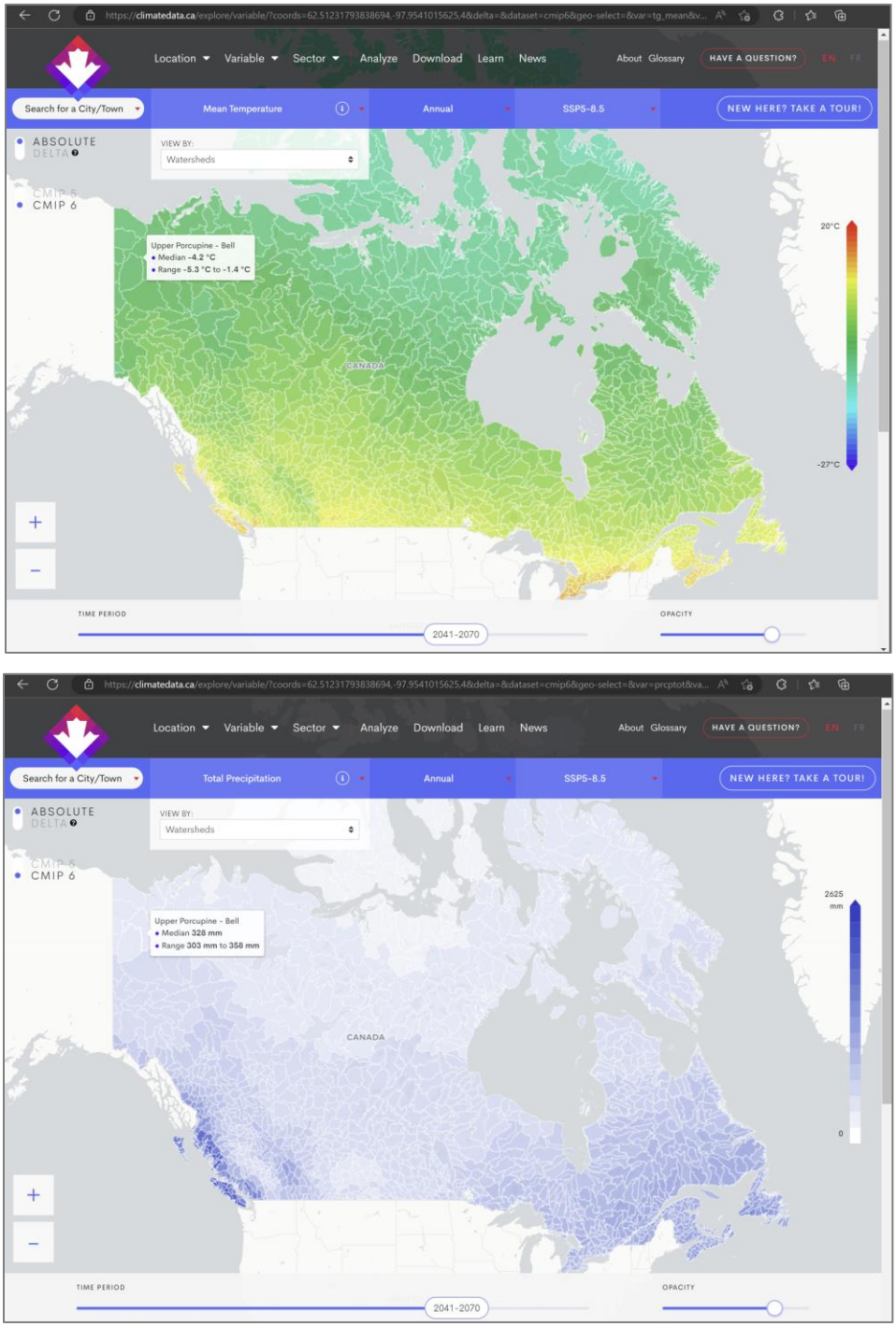

Figure 2.7 Map view in website ClimateData.ca. Hovering the mouse cursor over a watershed of interest gives the projected temperature (top panel) and precipitation (bottom panel) in the form of the median and a range of model projections for the time horizon chosen with the sliding bar at the bottom and the chosen scenario. The screen images captured in this figure show the Upper Porcupine-Bell watershed. These values can be used directly into the flood frequency regression equations.

2.4.2 Alternative recommended climate projections website: *Climate-Scenarios.Canada.ca*

Compared to ClimateData.ca (Section 2.4.1), the Climate-Scenarios.Canada.ca[2] website offers a larger number of future emissions scenarios (six scenarios instead of three) but does not offer the option of downloading results by watershed. Instead, projections are downloaded for a rectangular region specified by the user, or over the regular grid that covers Canada, in the NetCDF file format (which is a specialized file format used for large, spatially distributed climate datasets).

A solution for users not familiar with the NedCDF file format is to visualize the projected changes in temperature or precipitation over a map of North America generated on this website, and these changes can then be used to modify the historical climatic means of the watershed of interest before inputing the results into the flood-frequency regression equations.

Figure 2.8 and Figure 2.9 show maps of projected changes in MAT and MAP for a specific emissions scenario chosen by the user (SSP3-7.0, in this example) and for different future time horizons. To access similar maps, the user goes to the following website and clicks on the tab “Maps”: https://climate-scenarios.canada.ca/?page=cmip6-scenarios

This website offers all six emissions scenarios for which a large number of global climate models results have been produced, and provides a detailed explanation of each scenario[3].

The scenarios are the following:

(a) SSP1-1.9
(b) SSP1-2.6
(c) SSP2-4.5
(d) SSP3-7.0
(e) SSP4-6.0
(f) SSP5-8.5

Since each global climate model that is run for a fixed scenario produces different projections, this website offers the user the option of visualizing (or downloading) the 5th, 25th, 50th (median), 75th or 95th percentile of the projections ensemble.

2 https://Climate-Scenarios.Canada.ca

3 https://climate-scenarios.canada.ca/?page=cmip6-overview-notes

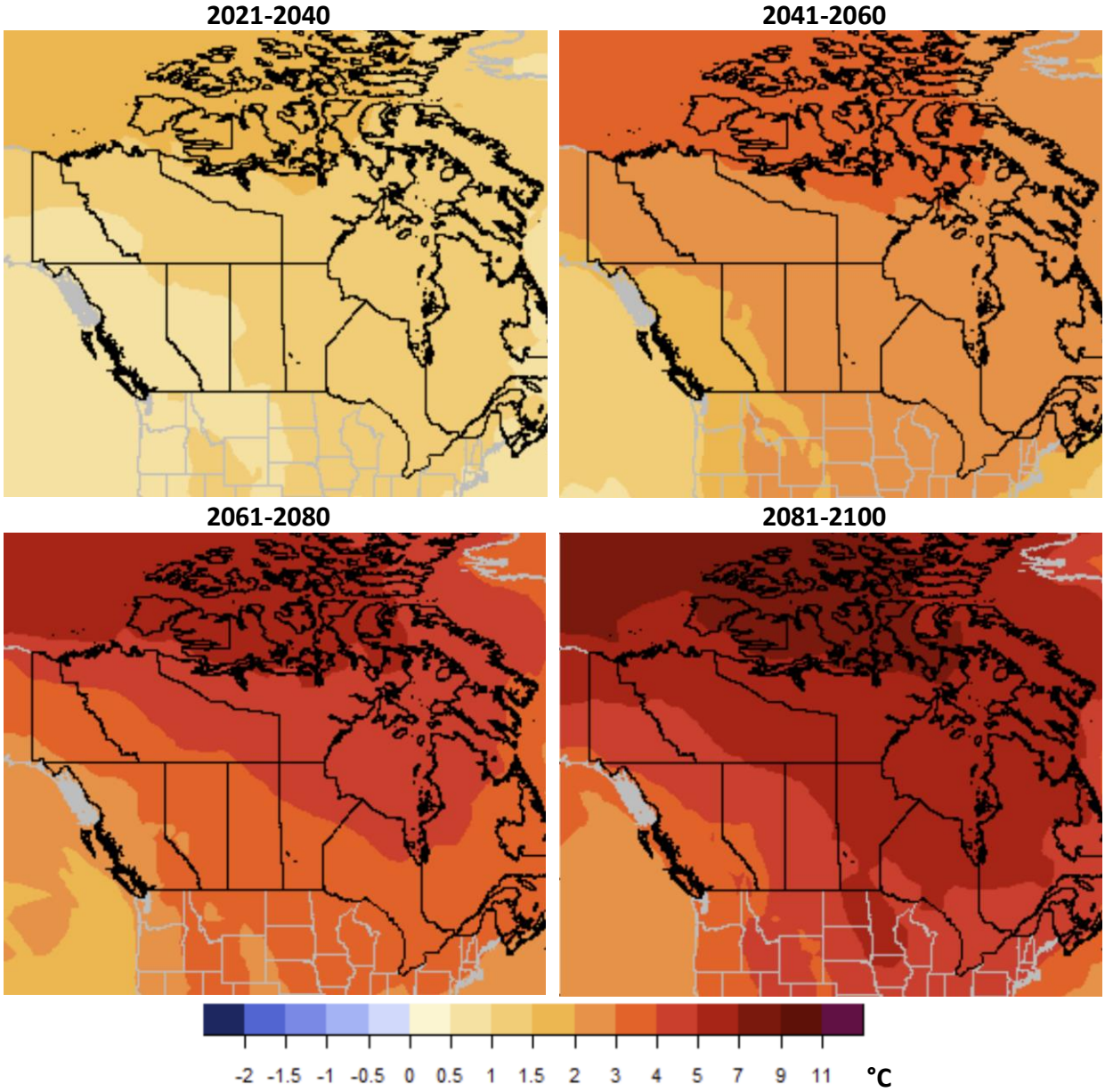

Figure 2.8 Spatial distribution of the median of projected changes in mean annual air temperature (°C) for future time horizons for SSP3-7.0 Source of data: Canadian Climate Data and Scenarios[4].

[4] https://climate-scenarios.canada.ca/?page=cmip6-scenarios

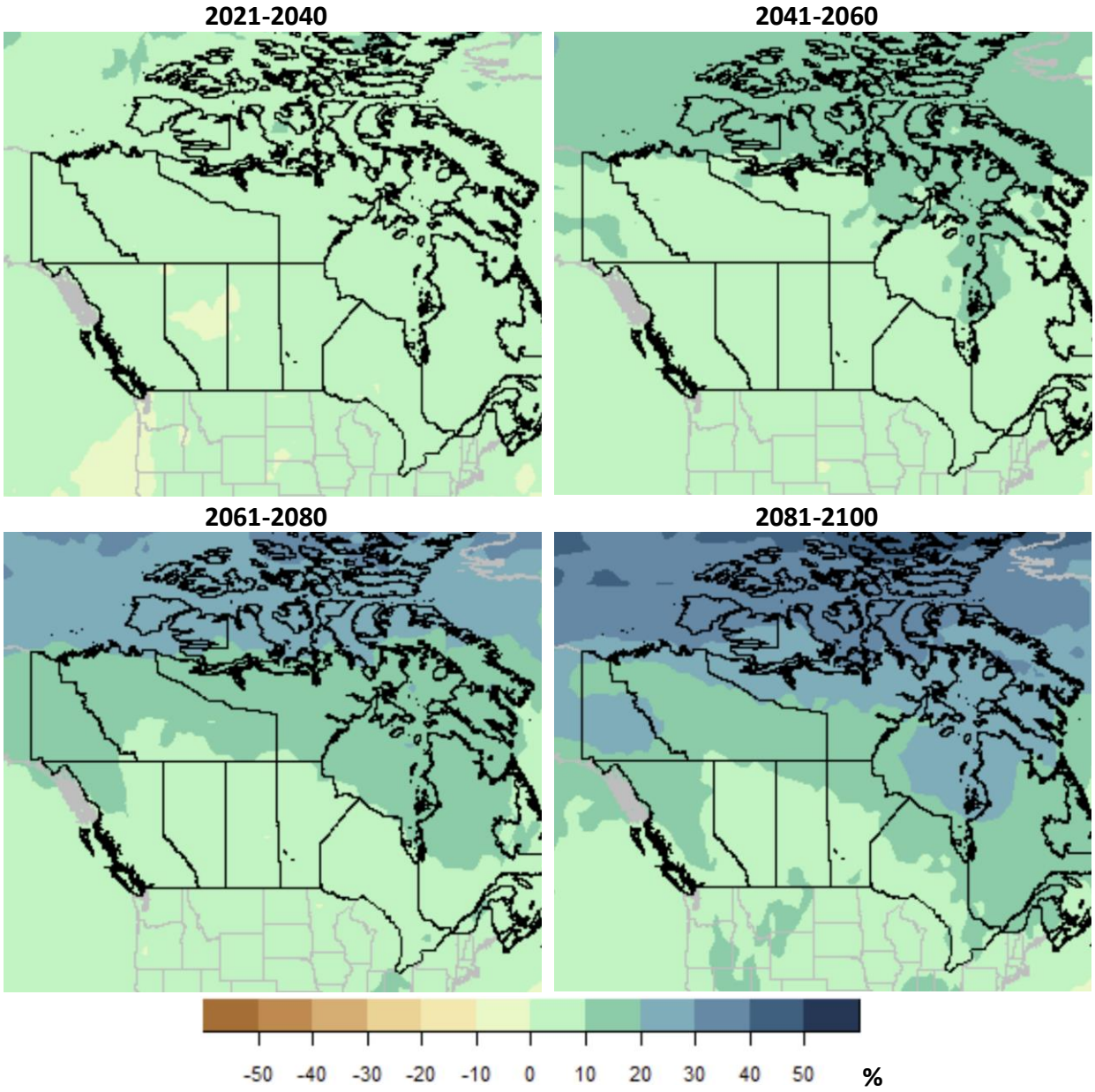

Figure 2.9 Spatial distribution of the median of projected changes (in percentage) in mean annual precipitation (mm a^{-1}) for future time horizons for SSP3-7.0 Source of data: Canadian Climate Data and Scenarios[5].

[5] https://climate-scenarios.canada.ca/?page=cmip6-scenarios

3 EXAMPLES

3.1 Estimate for a gauged site (Drury Creek)

For sites with a gauge, information from the gauge reports can be used directly to determine the peak flows. For example, Drury Creek is a gauged watershed located in the Yukon Boreal peak flow region. WSC operates a gauge at the outlet of Drury Creek (09AH005 – Drury Creek at Km 469 Robert Campbell Highway) with data from 1995 to 2021. The gauge has a drainage area of 550 km^2, mean annual precipitation of 507 mm, and a mean annual temperature of -3.9°C. The gauged watershed includes Drury Lake which has a surface area of approximately 27 km^2, equating to 5% of the overall basin area.

The gauge report for 09AH005 was selected from the pdf gauge reports (Appendix A). Basin characteristics were reviewed, along with the instantaneous and daily frequency analyses. It was noted that the station does not have a significant trend (MK $p > 0.05$) and provisional data from 2020 and 2021 is being used in the frequency analysis. Given that provisional data was used in the analysis, the Water Survey of Canada data was checked to ensure that approved data for these years has not been released since the original analysis. The gauge also has a negative skew (-0.11) meaning that the upper end of the distribution appears to have an upper bound.

Depending on the application of the analysis, the user may choose to force the station skew to 0 (log-normal distribution) to avoid the higher return periods having an upper bound. This can be completed using the mean and standard deviation from the gauge reports to recalculate the frequency analysis results. For the 100-year peak flow this can be calculated as:

$$Q_{100} = 10^{log10(mean)+log10(st\ dev)*K_{100}}$$

$$Q_{100} = 10^{log10(18.37)+log10(1.44)*2.326} = 42.9\ cms$$

where K is dependent on the return period and skew. Values of K can be obtained from Appendix 3 of USGS (USGS, 1982). Table 3.1 summarizes the K values for a skew equal to 0.

Table 3.1 K values for a skew of 0

Return Period	K
2	0
5	0.842
10	1.282
25	1.751
50	2.054
100	2.326
200	2.576

Given the relatively short record of the basin (21 years), the frequency analysis can also be checked against the regional regression estimates. Using the equations for the Yukon Boreal, peak flow for the 100-year can be calculated as:

$$Q_{100} = Area^{0.851} MAP^{0.965} (MAT + 100)^{-1.435} (\%\ Lake + 1)^{-23.785}$$

$$Q_{100} = 550^{0.851} 507^{0.965} (-3.9 + 100)^{-1.435} (0.05 + 1)^{-23.785} = 39\ cms$$

The spreadsheet tool ("Regression_Eq" sheet) can be used to calculate the regression results. The input for the basin and resulting output for instantaneous peak flows are shown in Figure 3.1.

INPUT		
Table 1: BASIN CHARACTERISTICS		
Basin Characteristic	**User Input**	**Range of values applicable to the regional regression equation**
Drainage Area (km^2)	*550*	73 - 9593
Percent Lake (%)	*5%*	0% - 6%
Mean Annual Precipitation (mm)	*507*	331 - 1708
Future Climate Mean Annual Precipitation (mm)		331 - 1708
Mean Annual Temperature (°C)	*-3.9*	(-5.7) - (-1.5)
Future Climate Mean Annual Temperature (°C)		(-5.7) - (-1.5)
Peak Flow Region	*Yukon Boreal*	

OUTPUT				
Table 2A: ESTIMATED INSTANTANEOUS PEAK FLOWS				
Return Period (Year)	**Annual Exceedance Probability**	**Estimated Peak Flow (m^3/s)**	**90% Prediction Interval (m^3/s)**	
			Lower	**Upper**
2	50.0%	16	8.5	30
5	20.0%	22	12	41
10	10.0%	26	14	49
25	4.0%	31	16	61
50	2.0%	35	18	71
100	1.0%	39	19	83
200	0.5%	43	19	97

Figure 3.1 Input (top) and output (bottom) for regression equations for Drury Creek from the spreadsheet tool

Table 3.2 summarizes the results from the three different application methods. The three methods all provide similar values, indicating that the frequency analysis directly from the gauge data can likely be used for peak flow values.

Table 3.2 Summary of peak flows from different methodologies for Drury Creek

Return Period	Gauge Peak Flow (m^3/s)	Lower Confidence Interval (m^3/s)	Upper Confidence Interval(m^3/s)	Peak Flow – Skew Forced to 0 (m^3/s)	Peak Flow – Regional Regression (m^3/s)
2	18	15	22	18	16
5	25	21	30	25	22
10	29	24	36	29	26
25	34	26	46	35	31
50	38	28	55	39	35
100	41	28	66	43	39
200	45	29	78	47	43

Climate change impacts were also explored for Drury Creek. CMIP6 projections for mean temperature and precipitation changes for SSP5-8.5 for the Headwaters Yukon – Nordenskiold watershed are summarized in Table 3.3 (climatedata.ca, 2023). Overall, the projections show a significant increase in both temperature and precipitation, with mean temperatures increasing by over 6°C by the end-of-century and precipitation increasing by 45%. The seasonality of these changes was explored to better understand the impact of the relative changes on peak flow processes. Currently, the Drury Creek watershed appears to be freshet dominated with peak flows typically occurring in June. Monthly temperatures are expected to stay below freezing from November through March through to the end of century with the largest changes in precipitation occurring in the summer months and in November and December. The projected changes in temperature and precipitation may result in a larger snowpack accumulating through the winter, resulting in higher peak flows. Warmer temperatures in the spring may also result in lower snow accumulation during this period and an earlier freshet, potentially decreasing the overall peak flow. Increased precipitation in the summer months, may result in rainfall generated peak flows, shifting the watershed to a more mixed regime. Climate change scaled intensity duration frequency curve for Carmacks (80 km west of Drury Creek) indicate a 33% increase in the 12-hour 100-year event and a 76% increase in the 24-hour 100-year event (climatedata.ca, 2023).

Table 3.3 Summary of relative changes in temperature and precipitation for CMIP6 SSP5-8.5 for Drury Creek

Time Horizon	Variable	SSP5-8.5 10th Percentile	SSP5-8.5 50th Percentile	SSP5-8.5 90th Percentile
Mid-Century (2041-2070)	Mean Temperature *(Delta °C)*	2.5	3.5	5.4
	Mean Precipitation *(% Increase)*	21%	27%	40%
End-Century (2071-2100)	Mean Temperature *(Delta °C)*	4.4	6.3	8.6
	Mean Precipitation *(% Increase)*	32%	45%	60%

To help quantify the potential changes to peak flows, the projected mid- and end-of-century precipitation and temperature changes were used in the regional regression equation for the Yukon Boreal. The resulting precipitation for both time periods is still within the range used to generate the regional frequency analysis, but the temperature values are outside of the range used to develop the regional regression equations, adding uncertainty to this method. This is indicated in the spreadsheet tool in red in the input table (Figure 3.1) Temperature only stays within the range used for the regression equations for SSP2-4.5 for the time range of 2031-2060. The resulting relative changes compared to the historical regional regression are summarized in Table 3.4.

Table 3.4 Summary of relative changes in instantaneous peak flow for CMIP6 SSP5-8.5 for Drury Creek

Return Period	Mid-Century (2041-2070)			End-Century (2071-2100)		
	10th Percentile	50th Percentile	90th Percentile	10th Percentile	50th Percentile	90th Percentile
2	19%	25%	31%	25%	38%	44%
5	18%	23%	32%	27%	36%	45%
10	19%	23%	31%	23%	35%	42%
25	16%	23%	29%	26%	32%	42%
50	17%	20%	29%	23%	31%	40%
100	15%	21%	28%	23%	31%	38%
200	16%	21%	28%	23%	30%	40%

Depending on the application of the frequency analysis, different SSPs and timelines can be explored, specific to the project needs. The limitations of this study with respect to climate change are further discussed within the main report (NHC, 2023).

3.2 Estimate for an ungauged site (Bonanza Creek)

For sites without a gauge, the regional regression equations can be used to estimate peak flows and the corresponding prediction intervals. Bonanza Creek is an ungauged creek located near Dawson, YK. The basin is located within the Interior Alaska peak flow region but is very close to the border of both the Yukon Boreal and Interior Mountains peak flow regions. The basin is 190 km^2 with a mean annual precipitation of 409 mm, and a mean annual temperature of -4.9°C. The basin contains no significant lakes.

Given the proximity of the gauge to the Yukon Boreal and Interior Mountains peak flow regions, equations from all three regions were used to develop peak flows for this gauge. For Interior Alaska, the 100-year peak flow is calculated as:

$$Q_{100} = Area^{0.735} MAP^{1.444} MAT^{-1.816}$$

$$Q_{100} = 190^{0.735} 409^{1.444} (-4.9 + 100)^{-1.816} = 71.4\ cms$$

The prediction intervals for the 100-year peak flow can be calculated first by determining the standard error of prediction:

$$\sigma_{Qpred|Xi} = \sqrt{\sigma_\delta^2 + \sigma_{Q|X_i}^2} = \sqrt{\sigma_\delta^2 + X_i^T (X^T \Lambda^{-1} X)^{-1} X_i}$$

$$\sigma_{Qpred|Xi} = \sqrt{\sigma_\delta^2 + \sigma_{Q|X_i}^2} = \sqrt{0.0703 + 0.0034} = 0.2715$$

This is then used in conjunction with the critical value from the Student's t-distribution to determine the prediction intervals:

$$C = 10^{t_{(\frac{0.1}{2},24)} \sigma_{QPred|Xi}} = 10^{1.7109 * 0.2714} = 2.913$$

$$Q_{lower} = \frac{71.4\ cms}{2.913} = 24\ cms$$

$$Q_{upper} = 71.4\ cms * 2.913 = 208\ cms$$

The spreadsheet tool ("Regression_Eq" sheet) can be used to calculate the regression results. The input for the basin and resulting output for instantaneous peak flows for the Interior Alaska peak flow region are shown in Figure 3.1.

INPUT		
Table 1: BASIN CHARACTERISTICS		
Basin Characteristic	**User Input**	**Range of values applicable to the regional regression equation**
Drainage Area (km^2)	*190*	3 - 5737
Percent Lake (%)	*0%*	0% - 0%
Mean Annual Precipitation (mm)	*409*	302 - 571
Future Climate Mean Annual Precipitation (mm)		302 - 571
Mean Annual Temperature (°C)	*-4.9*	(-7.1) - (-1.6)
Future Climate Mean Annual Temperature (°C)		(-7.1) - (-1.6)
Peak Flow Region	*Interior Alaska*	

OUTPUT				
Table 2A: ESTIMATED INSTANTANEOUS PEAK FLOWS				
Return Period (Year)	**Annual Exceedance Probability**	**Estimated Peak Flow (m^3/s)**	**90% Prediction Interval (m^3/s)**	
			Lower	**Upper**
2	50.0%	15	5.6	41
5	20.0%	26	10	65
10	10.0%	35	14	87
25	4.0%	48	18	124
50	2.0%	59	21	163
100	1.0%	71	24	208
200	0.5%	85	27	269

Figure 3.2 Input (top) and output (bottom) for regression equations for Bonanza Creek from the spreadsheet tool

Table 3.5 summarizes the peak flow and prediction intervals based on the Interior Alaska, Yukon Boreal, and Interior Mountains peak flow regions. The Yukon Boreal equations indicate a much lower peak flow than the other two regions, with the Interior Mountains estimating a middle range between the two other equations. It was noted that the watershed of interest contains a mean annual precipitation lower than those used to develop the Interior Mountain equations.

Table 3.5 Summary of peak flows for Bonanza Creek using the Interior Alaska, Yukon Boreal, and Interior Mountains regression equations. Prediction intervals (PI) represent the 90th percentile.

Return Period (Years)	Interior Alaska			Yukon Boreal			Interior Mountains		
	Peak Flow (m^3/s)	Lower PI (m^3/s)	Upper PI (m^3/s)	Peak Flow (m^3/s)	Lower PI (m^3/s)	Upper PI (m^3/s)	Peak Flow (m^3/s)	Lower PI (m^3/s)	Upper PI (m^3/s)
2	15	5.6	41	10	5.6	20	26	16	41
5	26	10	65	17	9.2	32	34	20	57
10	35	14	87	22	12	42	39	22	70
25	48	19	123	29	15	57	46	24	88
50	59	21	163	35	18	71	51	25	106
100	71	24	208	42	20	88	57	26	125
200	85	27	269	49	22	109	62	26	148

Given the range of potential peak flows, other methodologies should also be explored to help find convergence (or divergence) of peak flows. For this example, the regional equations from Curran et al. (2016) were also used to calculate peak flows for the basin (Table 3.6). At the upper return periods (10 to 200-year), these peak flows show a closer convergence with the Interior Mountain results. Depending on the application of the peak flows, the user may choose to use the Interior Mountain results or the Interior Alaska peak flows may also be justified based on a more conservative approach. A sensitivity assessment could also be performed, examining how the range in 200-year peak flows (49 m^3/s up to 85 m^3/s) impacts the outcome of their application (e.g., sizing riprap); however, the user should also consider how the wide range of uncertainty in the prediction limits (27 m^3/s to 269 m^3/s based on the Interior Alaska region) factors into their sensitivity assessment.

Table 3.6 Summary of peak flows for Bonanza Creek using the regression analysis from Curran et al. (2016)

Return Period	Peak Flow Estimate from Curran et al. (2016) (m^3/s)
2	17
5	27
10	35
25	50
50	54
100	63
200	72

Climate change impacts were also explored at this site. CMIP6 projections for mean temperature and precipitation changes for SSP5-8.5 for the Klondike watershed are summarized in Table 3.7 (climatedata.ca, 2023). Overall, the projections show a significant increase in both temperature and precipitation, with mean temperatures increasing by over 5°C by the end-of-century and precipitation increasing by 46%. Mid-century changes are more moderate in comparison, with temperatures increasing by over 2°C and precipitation increasing by 27%. Monthly temperatures are expected to stay below freezing from November through March through to the end of century. Historically April and October temperatures, which have been below 0°C are expected to increase above freezing by the end-of-century. The greatest change in precipitation is expected to occur in the summer and fall months.

Table 3.7 Summary of relative changes in temperature and precipitation for CMIP6 SSP5-8.5 for Bonanza Creek

Time Horizon	Variable	SSP5-8.5 10th Percentile	SSP5-8.5 50th Percentile	SSP5-8.5 90th Percentile
Mid-Century (2041-2070)	Mean Temperature *(Delta °C)*	1.2	2.2	4.3
	Mean Precipitation *(% Increase)*	22%	27%	35%
End-Century (2071-2100)	Mean Temperature *(Delta °C)*	3.1	5.2	7.8
	Mean Precipitation *(% Increase)*	30%	46%	56%

Based on the current climate and other regional gauges, Bonanza Creek is expected to be a freshet dominated watershed although peak flows may also occur as a result of rainfall events in the summer. The projected changes in temperature and precipitation may result in a larger snowpack accumulating through the winter, resulting in higher peak flows. However, the shortened freezing period in the fall and spring may result in lower snow accumulation and an earlier freshet, potentially decreasing peak flows associated with the freshet. Increases in precipitation in the summer and fall may result in larger rainfall generated peak flows. Climate change scaled intensity duration frequency curve for Dawson indicate a 50% increase in the 12-hour 100-year event (climatedata.ca, 2023).

To help quantify the potential changes to peak flows, the projected mid- and end-of-century precipitation and temperature were used in the regional regression equation for Interior Alaska. The resulting relative changes compared to the historical regional regression are summarized in Table 3.8. End of century precipitation and temperature at the 50th and 90th percentile is outside of the range of values used to develop the equations, and temperature is outside of the range of values used to develop the equations for mid-century 90th percentile. As a result, these changes have increased uncertainty. Depending on the application of the frequency analysis, different SSPs and timelines can be explored, specific to the project needs. The limitations of this study with respect to climate change are further discussed within the main report (NHC, 2023).

Table 3.8 Summary of relative changes in peak flow for CMIP6 SS5-8.5 for Bonanza Creek based on the regional regression equation for Interior Alaska

Return Period	Mid-Century (2041-2070)			End-Century (2071-2100)		
	10th Percentile	50th Percentile	90th Percentile	10th Percentile	50th Percentile	90th Percentile
2	53%	60%	73%	67%	100%	113%
5	46%	54%	65%	58%	92%	104%
10	43%	49%	60%	51%	80%	91%
25	38%	44%	52%	46%	71%	81%
50	34%	39%	47%	42%	64%	73%
100	31%	37%	44%	38%	58%	65%
200	27%	32%	38%	33%	49%	56%

3.3 Estimate for an ungauged site using a proxy gauge (McLean Creek)

For ungauged locations, results from the single station frequency analysis for gauges which are nearby or located on the same stream or river can be used to determine site specific peak flow using basin area scaling. Characteristics of basins located on different streams should be compared to the ungauged basin to ensure that similarity between the two basins exist. The peak flows at the ungauged locations can be determined from the following equation:

$$Q_{ungauged} = Q_{gauged} \cdot \left(\frac{Area_{ungauged}}{Area_{gauged}} \right)^{b}$$

where b is a peak flow region scaling factor, $Area_{ungauged}$ is the drainage area of the ungauged location of interest, $Area_{gauged}$ is the drainage area of the gauge, and Q_{gauged} is the peak flow of interest of the gauged location.

An example of the application of basin area scaling using a proxy gauge is performed for McLean Creek at the Alaska Highway. The basin has a drainage area of 20 km^2 with a median elevation of 1078 m. Mean annual precipitation is 352 mm and mean annual temperature is -1.7°C. There is minimal storage within the basin with the surface area of lakes comprising less than 1% of the overall basin area. The basin is located within the Yukon Boreal peak flow region.

There are a very limited number of gauges of similar area with long term records in the region. Table 3.9 summarizes available gauges with drainage areas less than 200 km^2 and more than 10-years of instantaneous data. All three proxy gauges have higher basin elevation and mean annual precipitation than the McLean Creek catchment. The Wolf Creek basins also have greater lake storage than McLean Creek.

Table 3.9 Summary of potential proxy gauges for McLean Creek

Basin	Wolf Creek at Coal Lake	Granger Creek	Wolf Creek at Highway 1
Basin ID	29AB005	29AB007	29AB002
# of Instantaneous Peaks	11	19	27
# of Daily Peaks	21	19	27
Drainage Area (km^2)	74.3	7.8	184.3
Basin Elevation (m)	1445	1596	1290
Mean Annual Precipitation (mm)	506	529	438
Mean Annual Temperature (°C)	-2.5	-2.6	-1.9
% Lake	3%	0%	2%

The ungauged peak flows can be calculated using area based scaling using the three gauges for Wolf Creek and Granger Creek as proxy gauges. The user is cautioned in the application of these results as the proxy gauges are not a good match for the basin of interest. McLean Creek is located within the Yukon Boreal with a mean b scaling factor of 0.93 (Table 4.10 in NHC 2023). For the 100-year peak flow estimate scaled from Wolf Creek at Highway 1 this results in:

$$Q_{ungauged} = Q_{gauged} \cdot \left(\frac{Area_{ungauged}}{Area_{gauged}}\right)^{b} = 14.2\ cms \cdot \left(\frac{20}{184}\right)^{0.93} = 1.8\ cms$$

summarized in Table 2.10. Figure 3.3 shows the input and resulting output for scaling Wolf Creek at Highway 1 using the spreadsheet tool.

INPUT	
Table 1A: Basin Characteristics	
Ungauged Site	
Drainage Area (km^2)	*20*
Gauged Site	
Gauge ID	*29AB002*
Gauged Drainage Area (km^2)	184
Region	Yukon Boreal
b	*0.93*

OUTPUT					
Table 2A: ESTIMATED INSTANTANEOUS PEAK FLOWS					
Return Period (Year)	**Annual Exceedance Probability**	**Q_{gauged} (m^3/s)**	**$Q_{ungauged}$ (m^3/s)**	**90% Confidence Intervals (m^3/s)**	
				Lower	**Upper**
2	50.0%	5.2	0.7	0.6	0.8
5	20.0%	7.4	0.9	0.8	1.2
10	10.0%	9	1.1	0.9	1.5
25	4.0%	11	1.4	1.1	2
50	2.0%	13	1.6	1.1	2.5
100	1.0%	14	1.8	1.2	3.2
200	0.5%	16	2	1.2	3.9

Figure 3.3 Input (top) and output (bottom) for area based scaling for McLean Creek from the spreadsheet tool

The results using the b scaling factor of 0.93 are summarized in Table 3.10. Scaling results from Granger Creek are much higher than those from the two gauges on Wolf Creek. Granger Creek is a much higher elevation and smaller basin than the Wolf Creek basins and does not contain the same storage that may be attenuating peak flows in Wolf Creek. The sensitivity of the results to the scaling factor were examined, decreasing the scaling factor to 0.75. Values across the entire territory generally are greater than 0.70 (Figure 4.14 in NHC, 2023). The results were also compared to the regional regression for the Yukon Boreal. It is noted that the smallest basin used for the regression within this peak flow region was 74 km^2, and therefore the regression may not be accurate for a basin of this size.

Table 3.10 Scaled peak flows for McLean Creek based on proxy gauges

Return Period	Peak Flow Scaled from Granger Creek (29AB007) (m^3/s)		Peak Flow Scaled from Wolf Creek at Highway 1 (29AB002) (m^3/s)		Peak Flow Scaled from Wolf Creek at Coal Lake (29AB005) (m^3/s)		Peak Flow from Regional Regression (m^3/s)		
	b = 0.93	*b = 0.75*	*b = 0.93*	*b = 0.75*	*b = 0.93*	*b = 0.75*	*Peak Flow*	*Lower CI*	*Upper CI*
2	4.5	3.8	0.7	1	0.9	1.2	0.9	0.5	1.8
5	6.6	5.6	0.9	1.4	1.5	1.9	1.7	0.9	3.2
10	8	6.8	1.1	1.7	1.9	2.5	2.4	1.3	4.4
25	9.9	8.4	1.4	2.1	2.5	3.2	3.3	1.7	6.4
50	11	9.6	1.6	2.4	3	3.8	4.1	2.1	8.3
100	13	11	1.8	2.7	3.5	4.5	5.1	2.4	11
200	14	12	2	3	4.1	5.2	6.1	2.7	14

Overall, the results show a wide range of potential peak flows. Given the poor suitability of the proxy basins, as well as the basin area being outside the limits of the regional regression, another method such as the rational method should be used to further investigate peak flows for a basin of this size.

Climate change projections for the region indicate significant warming as well as an increase in precipitation between the historical period and mid- and end-of century timelines. Table 3.11 summarizes relative changes in temperature and precipitation expected from historic conditions from CMIP6 for the Yukon – Lake Laberge watershed (climatedata.ca, 2023).

Table 3.11 Relative changes in temperature and precipitation for the McLean Creek watershed based on CMIP6 SSP5-8.5

Time Horizon	Variable	SSP5-8.5 10th Percentile	SSP5-8.5 50th Percentile	SSP5-8.5 90th Percentile
Mid-Century (2041-2070)	Mean Temperature *(Delta °C)*	1.3	2.3	4.0
	Mean Precipitation *(% Increase)*	23%	25%	36%
End-Century (2071-2100)	Mean Temperature *(Delta °C)*	2.0	3.7	6.4
	Mean Precipitation *(% Increase)*	34%	41%	53%

An examination of seasonal trends indicate that temperature is expected to stay below 0°C between November and March, although the 90th percentile indicates temperatures slightly above freezing for November and march by the end-of-century. Precipitation is expected to increase through all months,

with the greatest increase in the Summer and Fall months. Based on the hydrographs of other nearby gauges, peak flows at McLean Creek likely occur due to both snowmelt and rainfall events. The combined change in precipitation and temperatures, could lead to an increased snowpack, increasing the magnitude of freshet peaks. However, with average temperatures potentially increasing in November and March, this could lead to an earlier, smaller freshet. The increase in precipitation in summer and fall months could also lead to higher rainfall generated peaks. An examination of climate change adjusted Intensity Duration Frequency Curves (IDF) for Whitehorse (climatedata.ca, 2023) indicate a potential increase of 47% for the 100-year 12-hour rainfall event.

To quantify the impacts of climate change on peak flows, the average annual temperature and precipitation was adjusted based on the 10th, 50th and 90th percentile for SSP5-8.5 for the mid- and end-of century and used within the regional regression equation. These results were then compared to the historical regression equations to get a relative change in peak flows. Table 3.12 summarizes the potential relative change in peak flows based on the SSP5-8.5 climate projections for mid- and end-of century timelines. Precipitation changes are within the range of values used to develop the regression equations, however temperature changes exceed the values used to develop the regression equations adding uncertainty to the results.

Table 3.12 Relative increases in peak flows for mid- and end-of-century based on SSP5-8.5 from CMIP6

Return Period	Mid-Century (2041-2070)			End-Century (2071-2100)		
	10th Percentile	50th Percentile	90th Percentile	10th Percentile	50th Percentile	90th Percentile
2	33%	33%	33%	44%	44%	56%
5	24%	24%	29%	35%	35%	41%
10	21%	21%	25%	29%	33%	38%
25	21%	21%	30%	30%	33%	39%
50	22%	22%	29%	32%	34%	39%
100	20%	20%	25%	27%	31%	37%
200	20%	20%	26%	28%	31%	38%

4 REFERENCES

climatedata.ca (2023). *CMIP6 Projections by Watershed*. [online] Available from: climatedata.ca.

Curran, J. H., Barth, N. A., Veilleux, A. G., and Ourso, R. T. (2016). *Estimating flood magnitude and frequency at gaged and ungaged sites on streams in Alaska and conterminous basins in Canada, based on data through water year 2012* (2016–5024). Report. Reston, VA. 58 pp. [online] Available from: http://pubs.er.usgs.gov/publication/sir20165024.

NHC (2023). *Yukon Regional Flow Frequency Analysis and Empirical Equation Development (DRAFT)* (3007020).

USGS (1982). *Guidelines for Determining Flood Flow Frequency, Bulletin #17B of the Hydrology Subcommittee*. Interagency Advisory Committee on Water Data, U.S. Department of the Interior, Geological Survey. 28 pp.

Wang, T., Hamann, A., Spittlehouse, D., and Carroll, C. (2016). Locally Downscaled and Spatially Customizable Climate Data for Historical and Future Periods for North America. *PLOS ONE*, 11(6), 1–17. doi:10.1371/journal.pone.0156720.

APPENDIX C

PREDICTION INTERVAL INFORMATION

Table 1 – Alaska Range – Instantaneous covariance matrices, model error variance, and degrees of freedom

Alaska Range - Instantaneous				
	X0	**Area**	**Model Error Variance**	**Degrees of Freedom**
$X0_2$	0.0216	-0.0106	0.0626	20
$Area_2$	-0.0106	0.0060		
$X0_5$	0.0194	-0.0096	0.0562	
$Area_5$	-0.0096	0.0054		
$X0_{10}$	0.0196	-0.0096	0.0565	
$Area_{10}$	-0.0096	0.0054		
$X0_{25}$	0.0212	-0.0104	0.0609	
$Area_{25}$	-0.0104	0.0059		
$X0_{50}$	0.0240	-0.0117	0.0685	
$Area_{50}$	-0.0117	0.0066		
$X0_{100}$	0.0275	-0.0135	0.0784	
$Area_{100}$	-0.0135	0.0076		
$X0_{200}$	0.0324	-0.0159	0.0925	
$Area_{200}$	-0.0159	0.0089		

Table 2 – Interior Alaska – Instantaneous covariance matrices, model error variance, and degrees of freedom

Interior Alaska – Instantaneous					
	Area	**MAP**	**MAT**	**Model Error Variance**	**Degrees of Freedom**
$Area_2$	0.0011	-0.0020	0.0015	0.0228	22
MAP_2	-0.0020	0.1464	-0.1931		
MAT_2	0.0015	-0.1931	0.2561		
$Area_5$	0.0010	-0.0018	0.0013	0.0206	
MAP_5	-0.0018	0.1331	-0.1756		
MAT_5	0.0013	-0.1756	0.2329		
$Area_{10}$	0.0012	-0.0021	0.0016	0.0239	
MAP_{10}	-0.0021	0.1552	-0.2048		
MAT_{10}	0.0016	-0.2048	0.2715		
$Area_{25}$	0.0016	-0.0028	0.0021	0.0322	
MAP_{25}	-0.0028	0.2096	-0.2765		
MAT_{25}	0.0021	-0.2765	0.3667		
$Area_{50}$	0.0021	-0.0036	0.0028	0.0418	
MAP_{50}	-0.0036	0.2710	-0.3575		
MAT_{50}	0.0028	-0.3575	0.4740		
$Area_{100}$	0.0025	-0.0044	0.0034	0.0509	
MAP_{100}	-0.0044	0.3295	-0.4346		
MAT_{100}	0.0034	-0.4346	0.5762		
$Area_{200}$	0.0031	-0.0054	0.0041	0.0622	
MAP_{200}	-0.0054	0.4019	-0.5301		
MAT_{200}	0.0041	-0.5301	0.7028		

Table 3 – Coast Mountains – Daily covariance matrices, model error variance, and degrees of freedom

Coast Mountains – Daily						
	Area	**MAP**	**MAT**	**% Lake**	**Model Error Variance**	**Degrees of Freedom**
$Area_2$	0.0059	0.0139	-0.0295	0.0042	0.0568	18
MAP_2	0.0139	0.0875	-0.1612	-0.3074		
MAT_2	-0.0295	-0.1612	0.3019	0.4554		
% $Lake_2$	0.0042	-0.3074	0.4554	11.5580		
$Area_5$	0.0056	0.0132	-0.0280	0.0040	0.0539	
MAP_5	0.0132	0.0831	-0.1530	-0.2919		
MAT_5	-0.0280	-0.1530	0.2866	0.4325		
% $Lake_5$	0.0040	-0.2919	0.4325	10.9707		
$Area_{10}$	0.0056	0.0131	-0.0277	0.0039	0.0534	
MAP_{10}	0.0131	0.0823	-0.1515	-0.2892		
MAT_{10}	-0.0277	-0.1515	0.2838	0.4286		
% $Lake_{10}$	0.0039	-0.2892	0.4286	10.8643		
$Area_{25}$	0.0057	0.0133	-0.0282	0.0039	0.0543	
MAP_{25}	0.0133	0.0838	-0.1543	-0.2948		
MAT_{25}	-0.0282	-0.1543	0.2891	0.4370		
% $Lake_{25}$	0.0039	-0.2948	0.4370	11.0649		
$Area_{50}$	0.0059	0.0139	-0.0295	0.0040	0.0568	
MAP_{50}	0.0139	0.0876	-0.1614	-0.3085		
MAT_{50}	-0.0295	-0.1614	0.3024	0.4574		
% $Lake_{50}$	0.0040	-0.3085	0.4574	11.5743		
$Area_{100}$	0.0062	0.0146	-0.0309	0.0042	0.0595	
MAP_{100}	0.0146	0.0918	-0.1691	-0.3233		
MAT_{100}	-0.0309	-0.1691	0.3168	0.4794		
% $Lake_{100}$	0.0042	-0.3233	0.4794	12.1250		
$Area_{200}$	0.0066	0.0156	-0.0331	0.0045	0.0636	
MAP_{200}	0.0156	0.0982	-0.1808	-0.3458		
MAT_{200}	-0.0331	-0.1808	0.3388	0.5129		
% $Lake_{200}$	0.0045	-0.3458	0.5129	12.9653		

Table 4 –Coast Mountains – Instantaneous covariance matrices, model error variance, and degrees of freedom

Coast Mountains – Instantaneous						
	Area	**MAP**	**MAT**	**% Lake**	**Model Error Variance**	**Degrees of Freedom**
$Area_2$	0.0040	0.0032	-0.0093	0.0262	0.0636	25
MAP_2	0.0032	0.0408	-0.0680	-0.3718		
MAT_2	-0.0093	-0.0680	0.1183	0.5130		
% $Lake_2$	0.0262	-0.3718	0.5130	14.3986		
$Area_5$	0.0040	0.0032	-0.0094	0.0263	0.0641	
MAP_5	0.0032	0.0412	-0.0686	-0.3748		
MAT_5	-0.0094	-0.0686	0.1193	0.5172		
% $Lake_5$	0.0263	-0.3748	0.5172	14.5080		
$Area_{10}$	0.0042	0.0033	-0.0097	0.0271	0.0661	
MAP_{10}	0.0033	0.0425	-0.0708	-0.3867		
MAT_{10}	-0.0097	-0.0708	0.1232	0.5338		
% $Lake_{10}$	0.0271	-0.3867	0.5338	14.9616		
$Area_{25}$	0.0043	0.0034	-0.0100	0.0280	0.0684	
MAP_{25}	0.0034	0.0441	-0.0735	-0.4009		
MAT_{25}	-0.0100	-0.0735	0.1278	0.5536		
% $Lake_{25}$	0.0280	-0.4009	0.5536	15.4981		
$Area_{50}$	0.0045	0.0036	-0.0104	0.0290	0.0712	
MAP_{50}	0.0036	0.0459	-0.0765	-0.4175		
MAT_{50}	-0.0104	-0.0765	0.1331	0.5767		
% $Lake_{50}$	0.0290	-0.4175	0.5767	16.1315		
$Area_{100}$	0.0047	0.0038	-0.0109	0.0302	0.0742	
MAP_{100}	0.0038	0.0479	-0.0799	-0.4356		
MAT_{100}	-0.0109	-0.0799	0.1390	0.6019		
% $Lake_{100}$	0.0302	-0.4356	0.6019	16.8222		
$Area_{200}$	0.0050	0.0040	-0.0116	0.0321	0.0788	
MAP_{200}	0.0040	0.0510	-0.0850	-0.4632		
MAT_{200}	-0.0116	-0.0850	0.1478	0.6401		
% $Lake_{200}$	0.0321	-0.4632	0.6401	17.8807		

Table 5 – Interior Mountains – Daily covariance matrices, model error variance, and degrees of freedom

Interior Mountains - Daily				
	X0	**Area**	**Model Error Variance**	**Degrees of Freedom**
$X0_2$	0.0141	-0.0042	0.0077	14
$Area_2$	-0.0042	0.0013		
$X0_5$	0.0143	-0.0042	0.0078	
$Area_5$	-0.0042	0.0013		
$X0_{10}$	0.0174	-0.0051	0.0094	
$Area_{10}$	-0.0051	0.0016		
$X0_{25}$	0.0222	-0.0065	0.012	
$Area_{25}$	-0.0065	0.0020		
$X0_{50}$	0.0271	-0.0080	0.0147	
$Area_{50}$	-0.0080	0.0024		
$X0_{100}$	0.0338	-0.0099	0.0183	
$Area_{100}$	-0.0099	0.0030		
$X0_{200}$	0.0423	-0.0124	0.0229	
$Area_{200}$	-0.0124	0.0038		

Table 6 – Interior Mountains – Instantaneous covariance matrices, model error variance, and degrees of freedom

Interior Mountains - Instantaneous				
	X0	**Area**	**Model Error Variance**	**Degrees of Freedom**
$X0_2$	0.0217	-0.0064	0.0114	12
$Area_2$	-0.0064	0.0020		
$X0_5$	0.0275	-0.0081	0.0144	
$Area_5$	-0.0081	0.0025		
$X0_{10}$	0.0332	-0.0098	0.0175	
$Area_{10}$	-0.0098	0.0030		
$X0_{25}$	0.0430	-0.0127	0.0226	
$Area_{25}$	-0.0127	0.0039		
$X0_{50}$	0.0529	-0.0156	0.0278	
$Area_{50}$	-0.0156	0.0048		
$X0_{100}$	0.0634	-0.0187	0.0333	
$Area_{100}$	-0.0187	0.0057		
$X0_{200}$	0.0763	-0.0225	0.0401	
$Area_{200}$	-0.0225	0.0069		

Table 7 – Yukon Boreal – Daily covariance matrices, model error variance, and degrees of freedom

Yukon Boreal – Daily						
	Area	**MAP**	**MAT**	**% Lake**	**Model Error Variance**	**Degrees of Freedom**
$Area_2$	0.0016	-0.0005	-0.0019	0.0004	0.0279	44
MAP_2	-0.0005	0.0262	-0.0353	-0.0489		
MAT_2	-0.0019	-0.0353	0.0518	0.0114		
% $Lake_2$	0.0004	-0.0489	0.0114	16.6903		
$Area_5$	0.0016	-0.0005	-0.0019	0.0004	0.0278	
MAP_5	-0.0005	0.0261	-0.0352	-0.0489		
MAT_5	-0.0019	-0.0352	0.0517	0.0114		
% $Lake_5$	0.0004	-0.0489	0.0114	16.6522		
$Area_{10}$	0.0017	-0.0005	-0.0020	0.0005	0.0323	
MAP_{10}	-0.0005	0.0270	-0.0365	-0.0507		
MAT_{10}	-0.0020	-0.0365	0.0536	0.0118		
% $Lake_{10}$	0.0005	-0.0507	0.0118	17.2212		
$Area_{25}$	0.0019	-0.0005	-0.0022	0.0006	0.0362	
MAP_{25}	-0.0005	0.0305	-0.0411	-0.0572		
MAT_{25}	-0.0022	-0.0411	0.0604	0.0134		
% $Lake_{25}$	0.0006	-0.0572	0.0134	19.4101		
$Area_{50}$	0.0021	-0.0006	-0.0025	0.0007	0.0402	
MAP_{50}	-0.0006	0.0342	-0.0461	-0.0642		
MAT_{50}	-0.0025	-0.0461	0.0678	0.0150		
% $Lake_{50}$	0.0007	-0.0642	0.0150	21.7672		
$Area_{100}$	0.0024	-0.0007	-0.0028	0.0008	0.0402	
MAP_{100}	-0.0007	0.0379	-0.0512	-0.0714		
MAT_{100}	-0.0028	-0.0512	0.0753	0.0167		
% $Lake_{100}$	0.0008	-0.0714	0.0167	24.1665		
$Area_{200}$	0.0027	-0.0007	-0.0032	0.0009	0.046	
MAP_{200}	-0.0007	0.0434	-0.0586	-0.0818		
MAT_{200}	-0.0032	-0.0586	0.0862	0.0192		
% $Lake_{200}$	0.0009	-0.0818	0.0192	27.6626		

Table 8 – Yukon Boreal – Instantaneous covariance matrices, model error variance, and degrees of freedom

Yukon Boreal – Instantaneous						
	Area	**MAP**	**MAT**	**% Lake**	**Model Error Variance**	**Degrees of Freedom**
$Area_2$	0.0018	-0.0002	-0.0027	0.0120	0.0257	41
MAP_2	-0.0002	0.0255	-0.0350	-0.0371		
MAT_2	-0.0027	-0.0350	0.0529	-0.0221		
% $Lake_2$	0.0120	-0.0371	-0.0221	15.8580		
$Area_5$	0.0017	-0.0001	-0.0026	0.0115	0.0246	
MAP_5	-0.0001	0.0245	-0.0336	-0.0357		
MAT_5	-0.0026	-0.0336	0.0508	-0.0209		
% $Lake_5$	0.0115	-0.0357	-0.0209	15.2042		
$Area_{10}$	0.0018	-0.0001	-0.0027	0.0118	0.0254	
MAP_{10}	-0.0001	0.0253	-0.0347	-0.0371		
MAT_{10}	-0.0027	-0.0347	0.0526	-0.0214		
% $Lake_{10}$	0.0118	-0.0371	-0.0214	15.7014		
$Area_{25}$	0.0020	-0.0001	-0.0030	0.0129	0.0278	
MAP_{25}	-0.0001	0.0277	-0.0381	-0.0408		
MAT_{25}	-0.0030	-0.0381	0.0577	-0.0231		
% $Lake_{25}$	0.0129	-0.0408	-0.0231	17.2013		
$Area_{50}$	0.0022	-0.0001	-0.0033	0.0145	0.0312	
MAP_{50}	-0.0001	0.0312	-0.0429	-0.0461		
MAT_{50}	-0.0033	-0.0429	0.0650	-0.0257		
% $Lake_{50}$	0.0145	-0.0461	-0.0257	19.3642		
$Area_{100}$	0.0025	-0.0002	-0.0038	0.0166	0.0356	
MAP_{100}	-0.0002	0.0356	-0.0489	-0.0527		
MAT_{100}	-0.0038	-0.0489	0.0741	-0.0291		
% $Lake_{100}$	0.0166	-0.0527	-0.0291	22.0718		
$Area_{200}$	0.0030	-0.0002	-0.0045	0.0193	0.0416	
MAP_{200}	-0.0002	0.0416	-0.0572	-0.0618		
MAT_{200}	-0.0045	-0.0572	0.0867	-0.0338		
% $Lake_{200}$	0.0193	-0.0618	-0.0338	25.8111		

Table 9 – Northern Region – Instantaneous covariance matrices, model error variance, and degrees of freedom

Northern Region - Instantaneous				
	X0	**Area**	**Model Error Variance**	**Degrees of Freedom**
$X0_2$	0.0082	-0.0028	0.0165	11
$Area_2$	-0.0028	0.0011		
$X0_5$	0.0146	-0.0050	0.0300	
$Area_5$	-0.0050	0.0020		
$X0_{10}$	0.0201	-0.0069	0.0413	
$Area_{10}$	-0.0069	0.0028		
$X0_{25}$	0.0284	-0.0098	0.0582	
$Area_{25}$	-0.0098	0.0040		
$X0_{50}$	0.0349	-0.0120	0.0714	
$Area_{50}$	-0.0120	0.0049		
$X0_{100}$	0.0424	-0.0146	0.0869	
$Area_{100}$	-0.0146	0.0059		
$X0_{200}$	0.0501	-0.0173	0.1027	
$Area_{200}$	-0.0173	0.0070		

APPENDIX D

DESIGN (SPREADSHEET) TOOL

APPENDIX E

SUPPLEMENTARY CLIMATE CHANGE INFORMATION

Yukon Regional Flow Frequency Analysis and Empirical Equation Development
Appendix E – Supplementary Climate Change Information

May 9, 2023
Final Report, Rev. 0

NHC Reference 3007020

TABLE OF CONTENTS

LIST OF FIGURES IN TEXT

1 INTRODUCTION

To support the understanding of potential climate change impacts to peak flows within the Yukon study area, NHC undertook a review of projected changes to permafrost coverage as well as a trend analysis of current climatic variables. Section 2 summarizes projected changes to permafrost based on published peer-reviewed articles. Section 3 provides an analysis of observed changes in observational temperature and precipitation data from long-term Yukon meteorological stations, as well as snow water equivalent (SWE). Warming has occurred throughout the Yukon since the mid-1970s and has been accompanied by increasing precipitation. As a result of the precipitation trend, SWE records for March, April and May also show statistically-significant rising trends. This information can be used by practitioners to help support their understanding of potential changes to peak flows of a specific project location.

2 PROJECTIONS OF PERMAFROST CHANGES

In this section the question is addressed of how future climate change might affect permafrost distribution in Yukon. Specifically, we are asking:

> *How are the projected changes in climate (presented in the Section 5 of the main report) expected to modify the spatial distribution of permafrost in Yukon?*

Higher air temperatures or increased winter precipitation may lead to the degradation of the relatively warm (close to 0°C) and sometimes thin "discontinuous permafrost" (Romanovsky et al., 2010; Smith et al., 2010). Given the impact of permafrost on hydrology and peak flows, the above question is important for estimating the timeline of applicability of the regional peak flow equations developed in this project[1].

To answer this question, the modeling results obtained by others for obtaining maps of permafrost probability (or percent of ground covered by permafrost) for different degrees of air temperature warming was reviewed. The model of permafrost probability is described in Section 2.1.1 and its climate-change projections are summarized in Section 2.1.2.

2.1.1 Model of permafrost probability (PP model)

The model of permafrost probability (PP model) reviewed in this report was developed by Bonnaventure et al. (2012) for the southern Yukon and northern British Columbia, and has been used to obtain future projections under scenarios of climate change (Bonnaventure and Lewkowicz, 2013). The PP model covers an area of nearly 500,000 km^2, comprised between 59°N and 65°N and between 141°W to 123.5°W. To the north of the 65°N domain boundary, Yukon is covered by continuous permafrost which, given its low temperatures, is least imminently threatened by climate change.

[1] Important consequences of permafrost degradation extend well beyond hydrology, however, and include compromise of infrastructure, limits to development, higher landslide risk, and the release of previously trapped greenhouse gases.

The PP model has high resolution (30m x 30m grid cells) and was built by combining seven local models, each of them consisting of the local empirical-statistical relationship between the measured wintertime basal temperature of snow (BTS) and the presence (or absence) of observed frozen ground in summer. The seven local models were merged and extended to grid cells that don't have BTS observations (which is the majority of grid cells) using a distance-decay power function that accounted for local terrain slope, potential incoming solar radiation, and an introduced variable called "equivalent elevation" that was developed by Lewkowicz and Bonnaventure (2011).

Calculation of the "equivalent elevation" of a grid cell required estimated local temperature lapse rates. In Yukon, temperature lapse rates vary greatly in space and, in regions situated away from maritime influence, inverted lapse rates (i.e., temperatures rising with elevation) predominate within the forested zone in winter. Most Yukon meteorological stations are located on valley floors, however, and measurement-based estimates of local lapse rates are limited. In the PP model, local lapse rates were estimated from a variable it was found to be strongly correlated with: the difference in mean monthly temperature between the warmest month (July) and the coldest month (January) (Kremer et al., 2011; Lewkowicz and Bonnaventure, 2011). Regions where this temperature difference is greater tend to have more positive (i.e., inverted) lapse rates, while regions with smaller thermal amplitude – which is the case of regions with a maritime influence – tend to have negative lapse rates.

The model results in Figure 2.1 compare well against observations, i.e., the predicted probability of permafrost in particular areas was similar to the percentage of sites observed to have permafrost, however, as noted by the authors (Bonnaventure et al., 2012), those same observational data had been used in model development. Independent verification with observations not used in model development, such as using a bootstrap methodology, was not conducted.

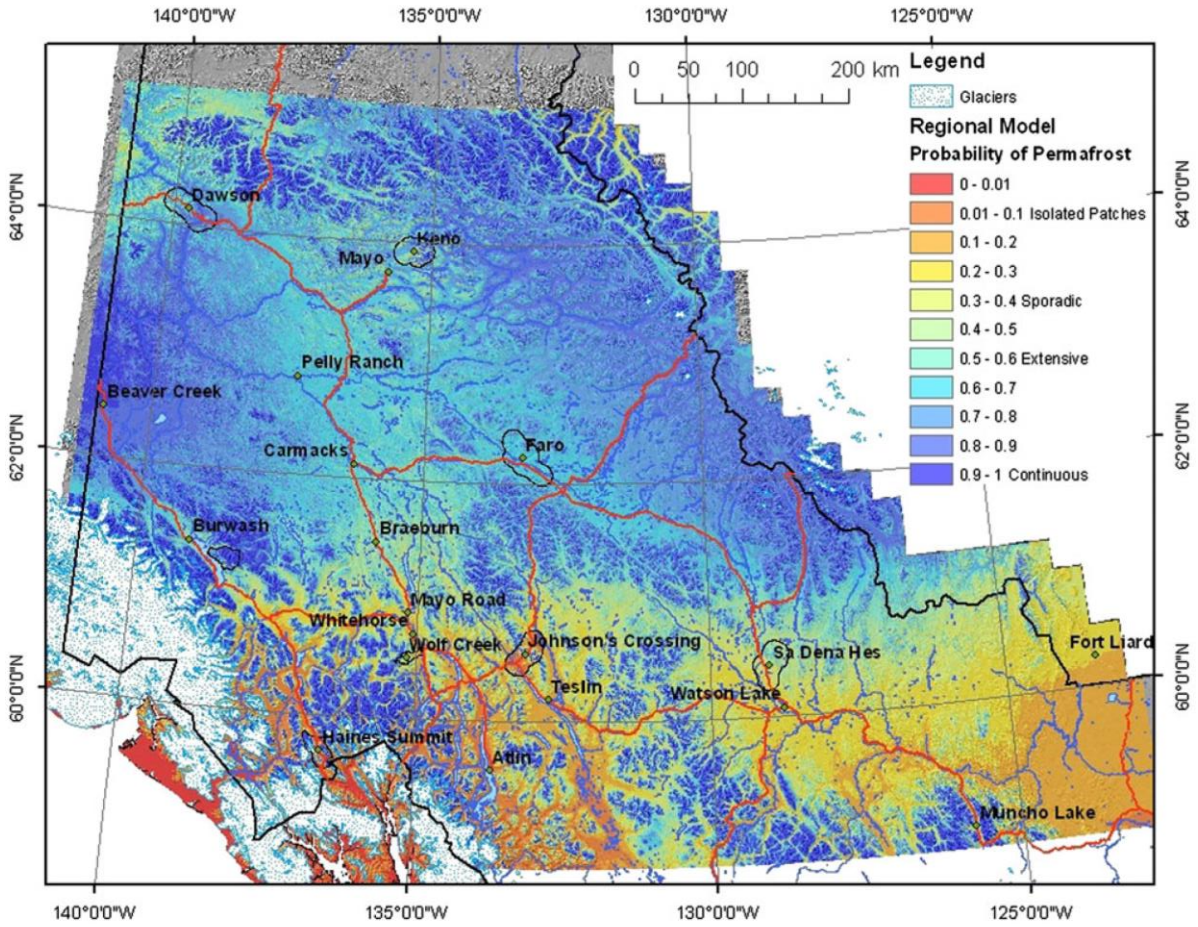

Figure 2.1 Regional model permafrost probability map with study area boundaries and locations of Environment Canada stations This figure and caption are reproduced from Bonnaventure et al. (2012)[2].

2.1.2 Projections of permafrost probability using the PP model

The PP model (described in the preceding section) has been used to simulate changes in the equilibrium response of permafrost probability to specific values of temperature rise that may occur at some future time as a result of anthropogenic climate change (Bonnaventure and Lewkowicz, 2013). This study is summarized in this section.

The projections of permafrost probability in Bonnaventure and Lewkowicz (2013) are based on perturbing the mean annual air temperature field in the PP model, which was developed to calculate the probability of permafrost under recent climatic conditions (1971-2000) (section 2.1.1). Scenarios of rising mean annual air temperature were studied, with rises of 1°C, 2°C, 3°C, 4°C and 5°C. A cooling

[2] Model results were also mapped as a classification based on traditional permafrost zones, as shown here: https://yukon.maps.arcgis.com/apps/webappviewer/index.html?id=534f141ffa5f4796954627dc98f82b99

scenario with -1°C was also studied, to represent conditions earlier in the 20th century. As noted by the authors (Bonnaventure and Lewkowicz, 2013), environmental factors other than air temperature also influence permafrost distribution in the discontinuous zones and are also projected to change in the future – especially snow and vegetation cover – but the PP model does not account for those changes.

Figure 2.2 (top panel), reproduced from Bonnaventure and Lewkowicz (2013), shows the subregions defined on the basis of surface temperature lapse rate (SLR). The entire study area encompasses the southern Yukon, northern British Columbia, and narrow bands in the Northwest Territories and Alaska. The projections by the PP model, shown in Figure 2.2 (bottom panel), reveal the change in areal extent and spatial distribution of permafrost in the study area after reaching equilibrium conditions with the new mean annual temperature. Results are shown for the entire study area (black dashed line) and each SLR subregion (by color, indicated in the figure legend). In the entire study region, permafrost area is considerably more extensive for the -1°C (cooler) scenario, representing past conditions (76%), compared to the reference period 1971-2000 (58%). A substantial loss of permafrost is predicted by the model for a +1°C warming (reduced to 38% over the study area), and greater losses are predicted for warmer scenarios. For a +5°C warming, only 9% of the study area remains underlain by permafrost, in isolated patches; and in the western regions (ESW) permafrost becomes restricted mostly to the highest peaks.

The authors (Bonnaventure and Lewkowicz, 2013) summarize the influence of local surface lapse rates (SLR) on the projected permafrost loss (or gain, in the case of the -1°C cooling scenario), which varies across the region in the forested area below treeline, as follows: *"Areas that are maritime exhibit SLRs characteristically similar above and below treeline resulting in low probabilities of permafrost in valley bottoms. When warming scenarios are applied, a loss front moves to upper elevations (simple unidirectional spatial loss). Areas where SLRs are gently negative below treeline and normal above treeline exhibit a loss front moving up-mountain at different rates according to two separate SLRs (complex unidirectional spatial loss). Areas that display high continentality exhibit bidirectional spatial loss in which the loss front moves up-mountain above treeline and down-mountain below treeline. The parts of the region most affected by changes in MAAT (mean annual air temperature) have SLRs close to [0°C km^{-1}] and extensive discontinuous permafrost, whereas the least sensitive in terms of areal loss are sites above the treeline where permafrost presence is strongly elevation dependent."*

+1°C

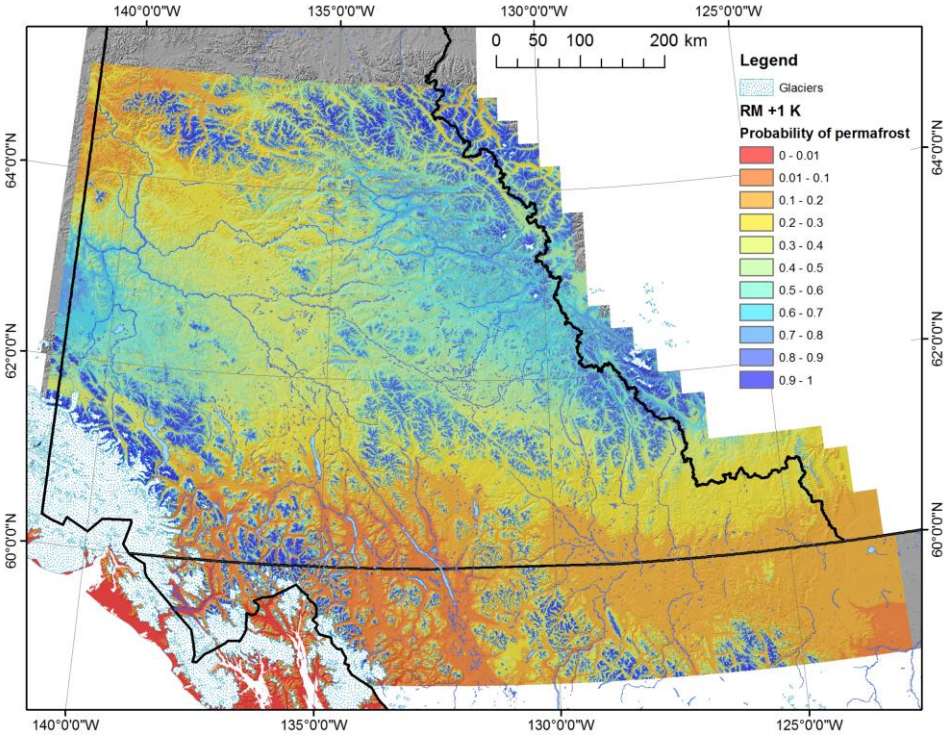

+2°C

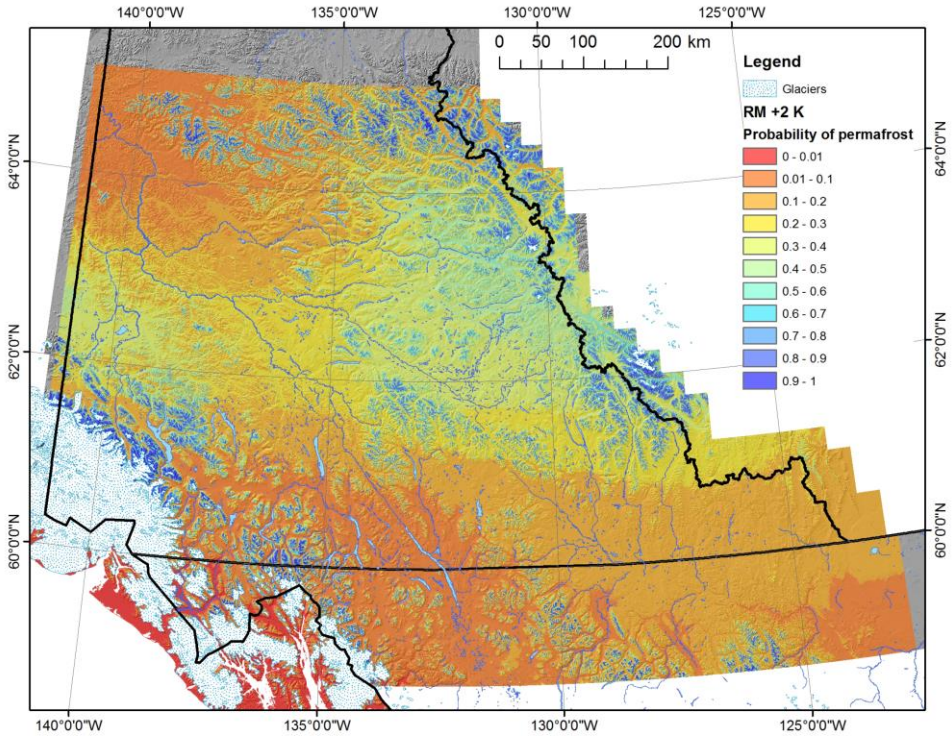

Figure 2.2 PP model permafrost probability map under warming scenarios These figure panels are reproduced from Bonnaventure and Lewkowicz (2013). (Figure continues on next page.)

+5°C

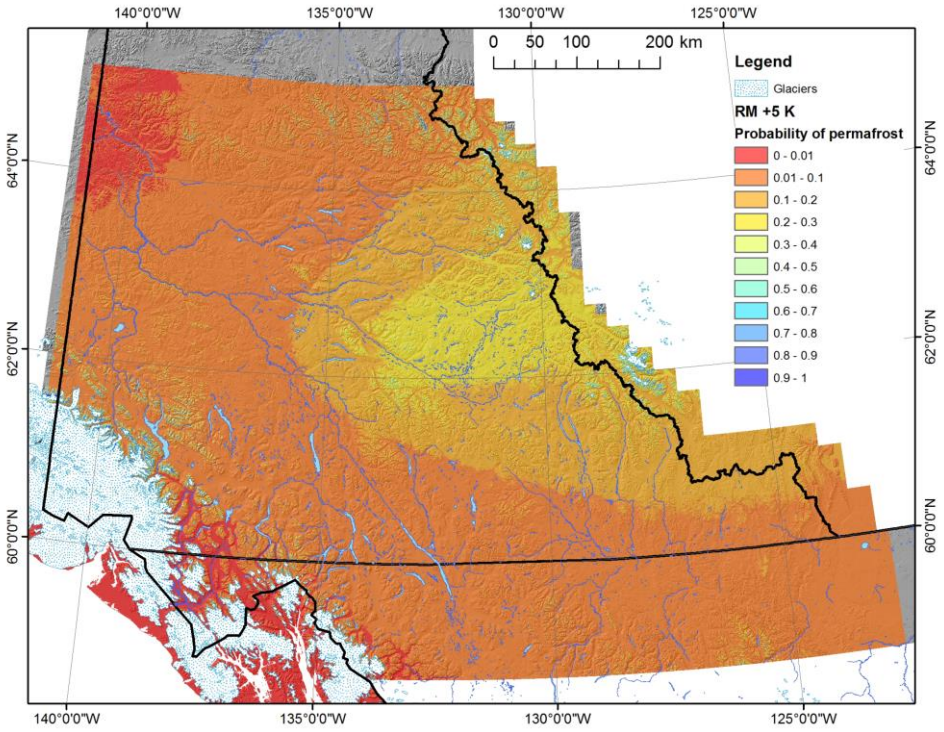

Figure 2.2 (continued)

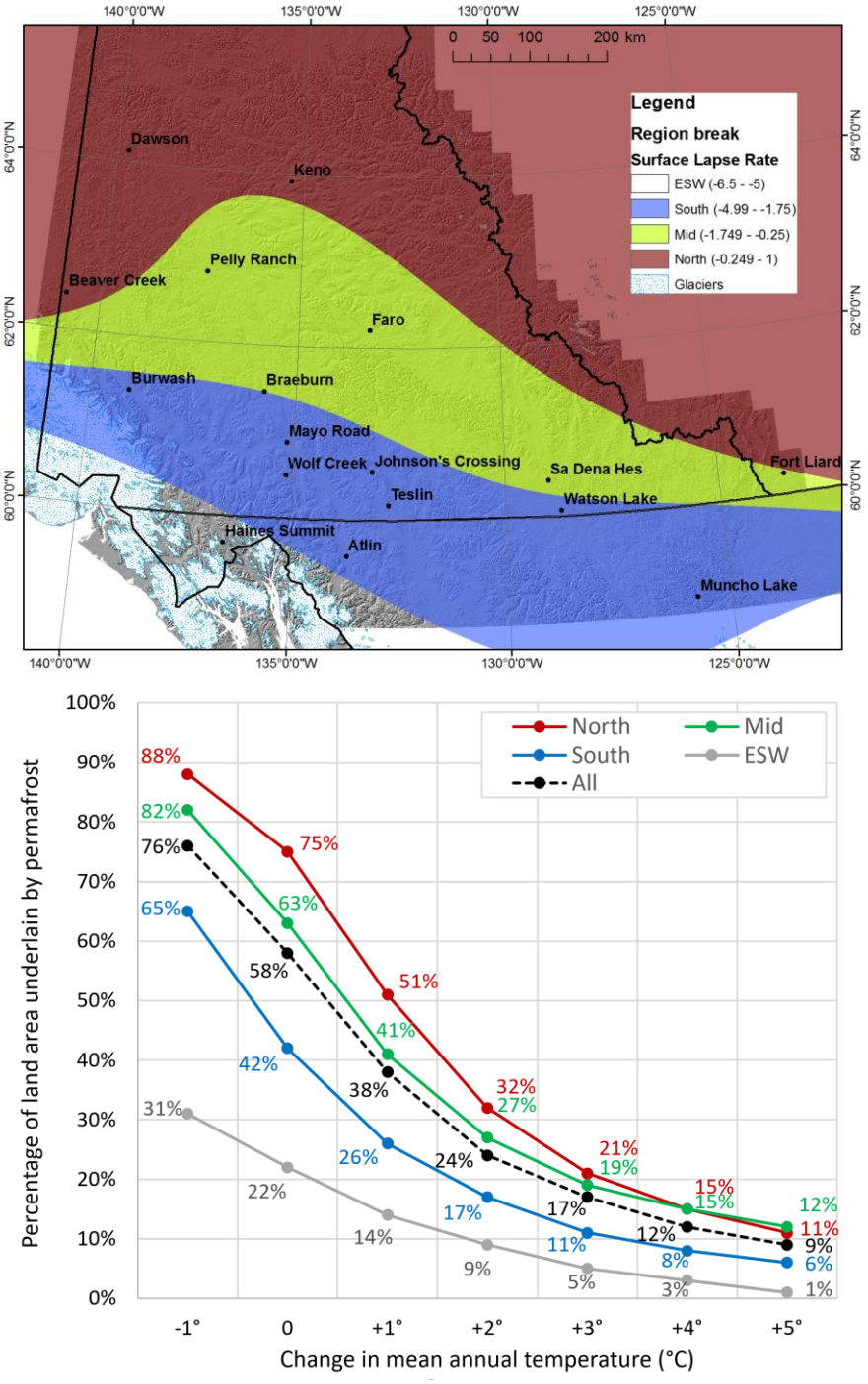

Figure 2.3 (Top) Subregions defined by surface temperature lapse rate intervals (in units of °C km^{-1}). (Bottom) Modeled percentage area underlain by permafrost under equilibrium conditions for the subregions in the top panel, and for the entire region, under the climate warming conditions indicated on the x axis. The top figure panel is reproduced from, and the bottom figure panel is redrawn from Bonnaventure and Lewkowicz (2013).

3 TRENDS IN OBSERVED CLIMATIC TIME SERIES

To support the understanding of climate change projections within the Yukon, an analysis of observed trends at long term climate stations was undertaken.

3.1 Analysis of temperature and precipitation meteorological station records

Figure 3.1 summarizes the temperature data available for Yukon meteorological stations, in the form of minimum and maximum temperature registered on each day (denoted Tmin and Tmax), and daily rainfall and snowfall. The number of stations is 22, a small number for this vast territory, and long continuous records are few. In this section, data from these stations are examined for trends over time using quantile regression, revealing that the lowest quantiles and highest quantiles of the distribution (i.e., the coldest and warmest days of each season) have often experienced trends of different intensity or even different sign.

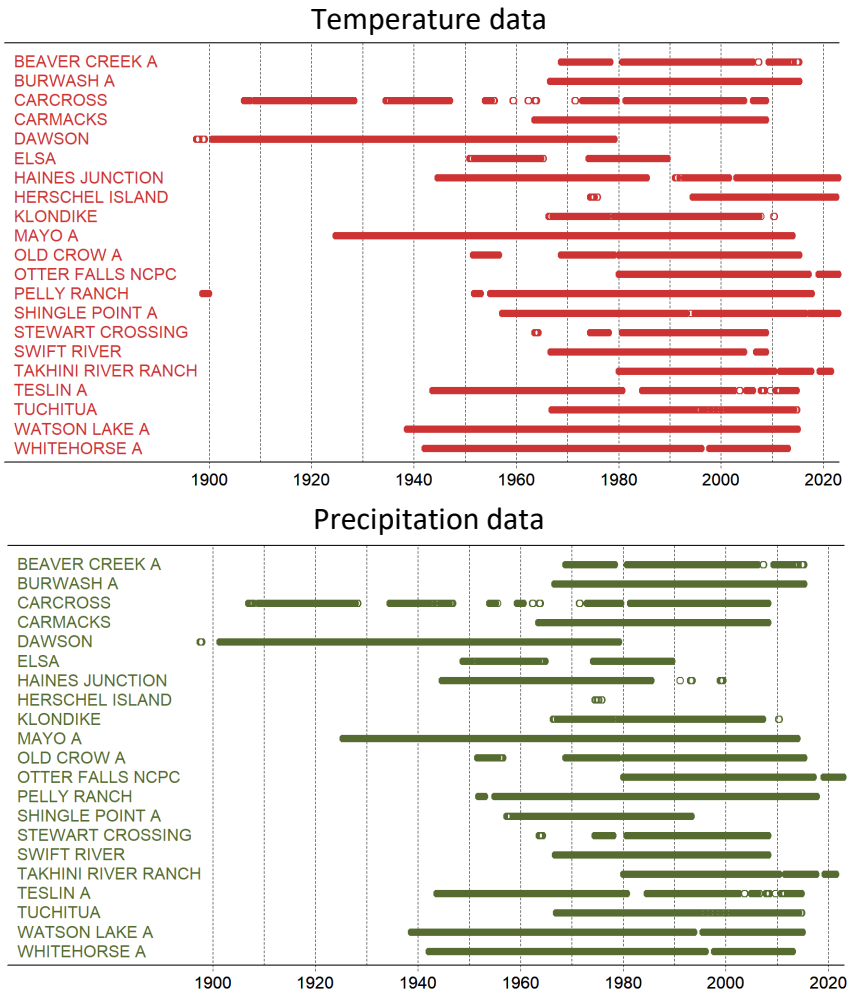

Figure 3.1 Availability of temperature (top panel) and precipitation data (bottom panel) for Yukon meteorological stations.

The longest temperature records are held by the following stations (Figure 3.1):

- Mayo Airport (in southeastern Yukon) (1924-2013);
- Watson Lake Airport (in mid-central Yukon) (1938-2014);
- Whitehorse Airport (in south-central Yukon) (1942-2012); and
- Dawson (in west-central Yukon) (1897-1979).

When first analyzing the long-term temperature trends in each of these stations, it was noted that the direction of trends at Dawson was markedly different from the other stations, showing cooling instead of warming on the lowest quantiles (i.e., on the coldest days) of fall and winter. Trying to find an explanation for Dawson being different, it was hypothesized that this might be due to its record ending in 1979. This led to the thought of analyzing, for each station, the evolution over time of cumulative deviations from the mean (Figure 3.2).

The graphs in Figure 3.2 are consistent with a change in behavior occurring at a break point around 1976. Prior to 1976, temperatures are predominantly below the long-term average (i.e., the slope of the cumulative deviations line is negative), while after 1976 temperatures are mostly above average (positive slope) at Mayo Airport or about average during 1976-1997 before rising above average after 1997 at Watson Lake Airport and Whitehorse Airport.

The Pettitt rank test of time series homogeneity was applied to the time series of mean annual temperature, and its U statistic is shown in Figure 3.3. (It is interesting to note that, since the U statistic is defined as a summation of the rank of each time series element, the result is that the U statistic graphs in Figure 3.3 are roughly similar to the graphs of cumulative deviations from the mean in Figure 3.2.) The probable break point identified by the Pettitt test is marked in red in each figure panel. However, whether the three series have truly different break points (as suggested by the Pettitt test) is not certain, and it appears likely that the year 1976 is a probable break point for all 3 of these long-term series.

The explanation for the (circa) 1976 break point in the temperature data is not known. Two explanations can be tentatively offered, but further analysis (and research on the history of station measurements) would be necessary before drawing any conclusions. The tentative explanations are:

(a) The well-known shift in the phase of the Pacific Decadal Oscillation that occurred about 1976, and/or,

(b) The inhomogeneity apparent in the time series reflected by less precision in the pre-1976 measurements compared to post-1976 (inclusive).

Regardless of the true explanation, which is not known, these temperature records were divided into a pre-1976 and a post-1976 (inclusive) period for separate trend analysis.

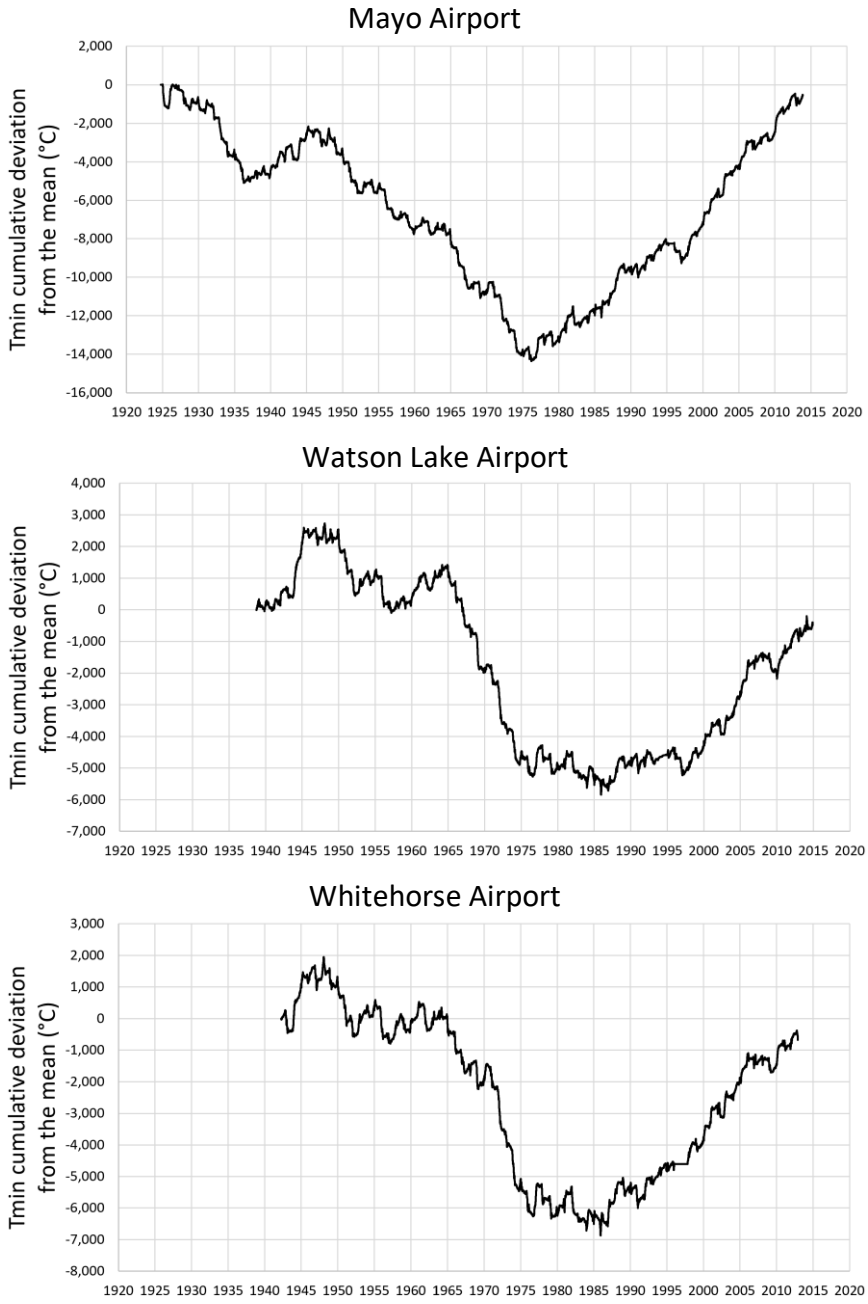

Figure 3.2 Cumulative deviations from the monthly mean for the daily Tmin record at the three long-term meteorological stations.

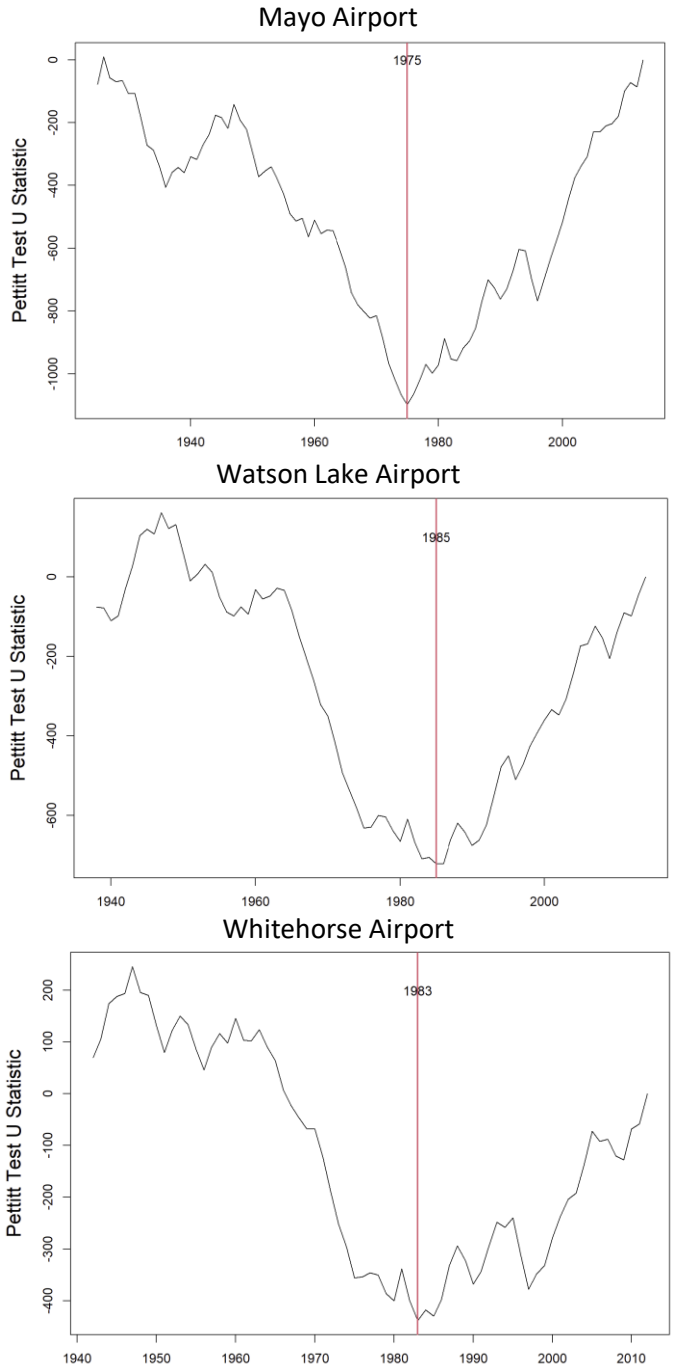

Figure 3.3 U statistic of the Pettitt rank test, and break points (marked by the red line) identified by the minimum value of U.

3.1.1 Quantile regression of temperature

In Figure 3.4 to Figure 3.11, trends estimated by quantile regression differ between these two major periods. In these figures, only Tmin is plotted because regression results obtained for Tmax (or Tave) are similar to those obtained for Tmin (not shown). Seasons are defined as follows: Fall is October-December, Winter is January-March, Spring is April-June and Summer is July-September. The left-hand figure panels display the data and the lines fitted by quantile regression, for cumulative probabilities of 0.05, 0.1, 0.15. 0.25, 0.35, 0.5, 0.65, 0.75, 0.85, 0.9 and 0.95. The right-hand figure panels indicate the slope of the fitted linear regressions for the quantile probabilities indicated in the x axis (points and solid line), with shading indicating the 90% confidence interval. The overall trend slope (all quantiles) is indicated by the red horizontal line, and the dashed red lines mark the 90% confidence interval.

In the left-hand figure panels for the spring and summer seasons, notice that the data contains many rounded values. This lack of precision offers low confidence in the regression results for these two seasons.

In fall and winter, the estimated temperature trends for the three long-term stations Mayo Airport, Watson Lake and Whitehorse Airport (Figure 3.4, Figure 3.6 and Figure 3.8), are roughly similar. For the period pre-1976, there were marked fall/winter cooling trends affecting especially the lower quantiles (i.e., the coldest days). Winter cooling trends were especially high, reaching -1°C/decade at Mayo Airport, -2°C/decade at Watson Lake and approaching -3°C/decade at Whitehorse Airport. At Dawson (Figure 3.10), there is cooling at the lower quantiles, and warming in some middle or upper quantiles.

For the period post-1976, the fall/winter experienced intense warming trends, especially in the fall season and especially affecting the lower quantiles of the distribution where trends lie between +1°C/decade and +2°C/decade. For the upper quantiles of the distribution, the post-1976 regression trend is more moderate and in some cases, it is negative (cooling). The overall slope for the entire temperature distribution in the post-1976 period (red line on the right-side figure panels) is in most cases positive (warming), and especially high in the fall season.

In spring and summer, the estimated temperature trends for the three long-term stations Mayo Airport, Watson Lake Airport and Whitehorse Airport (Figure 3.5, Figure 3.7 and Figure 3.9Figure 3.8) are different from fall and winter. The pre-1976 period shows some warming of the lowest quantiles, a bit stronger in spring than summer, at Mayo Airport and Watson Lake; but at Whitehorse Airport there is mostly a cooling trend except for the lowest quantile in spring where there is slight warming. At Dawson (Figure 3.11), warming trends predominate over most quantiles, especially in summer.

For the post-1976 period, the spring/summer experienced mixed trends depending on the station and quantiles. At Mayo Airport and Watson Lake Airport, there has been an overall warming trend, but the lowest quantiles in spring and the highest quantiles in summer show a cooling trend. At Whitehorse Airport, all quantiles have seen warming in the post-1976 period.

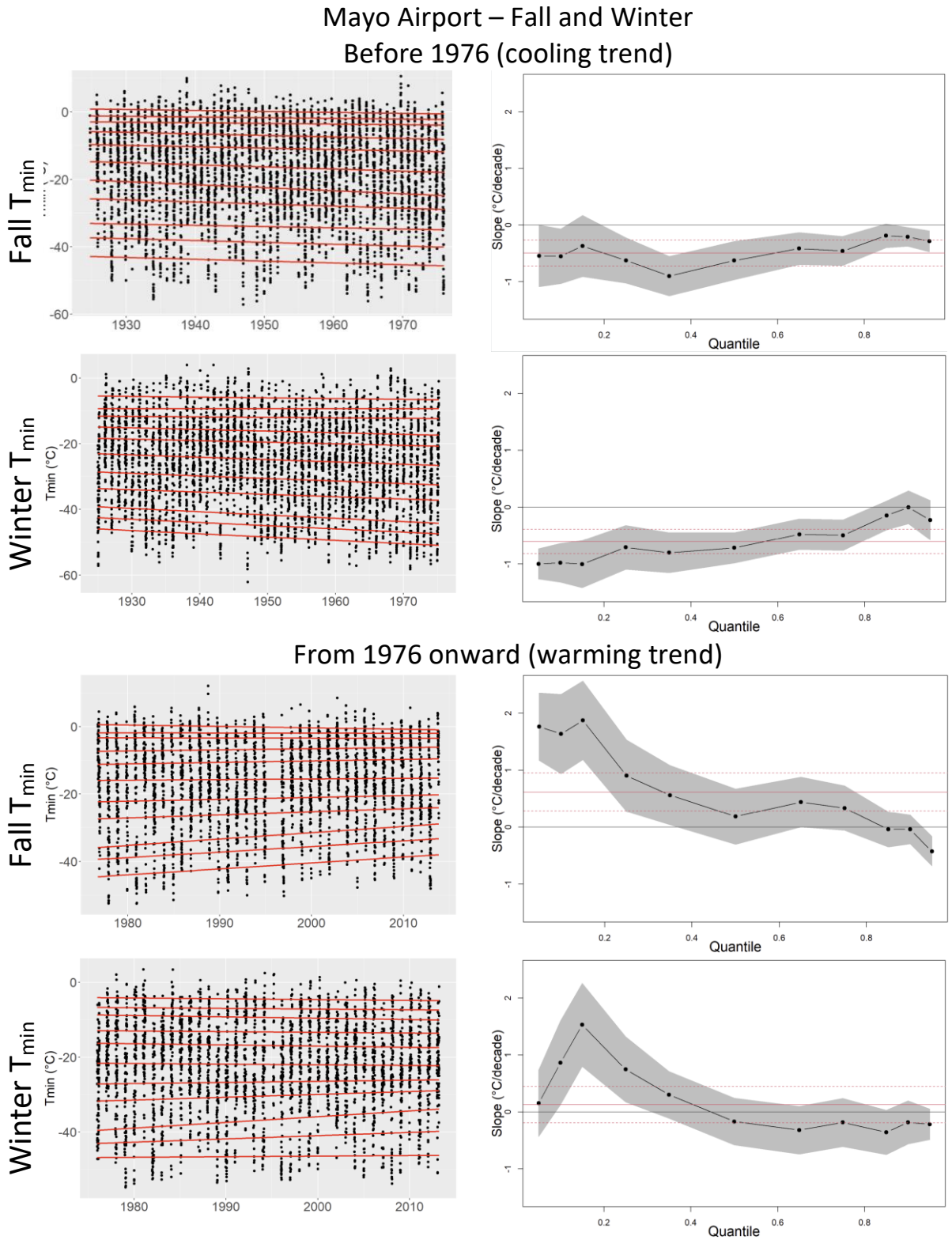

Figure 3.4 For Mayo Airport, temperature trends for fall (Oct-Dec) and winter (Jan-Mar) Negative slope values on the right-hand panels indicate a cooling trend, and vice-versa.

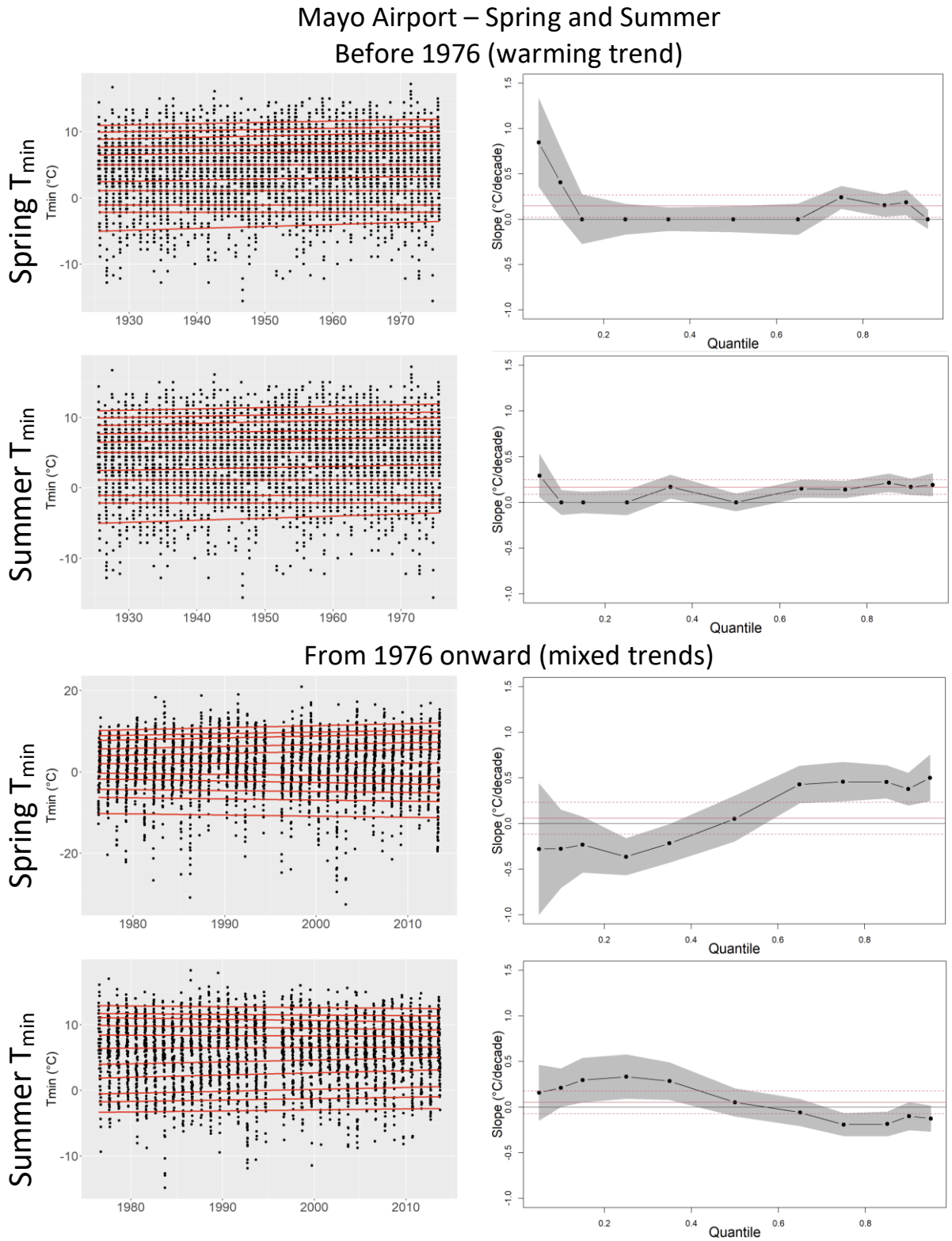

Figure 3.5 For Mayo Airport, temperature trends for spring (Apr-Jun) and summer (Jul-Sep).

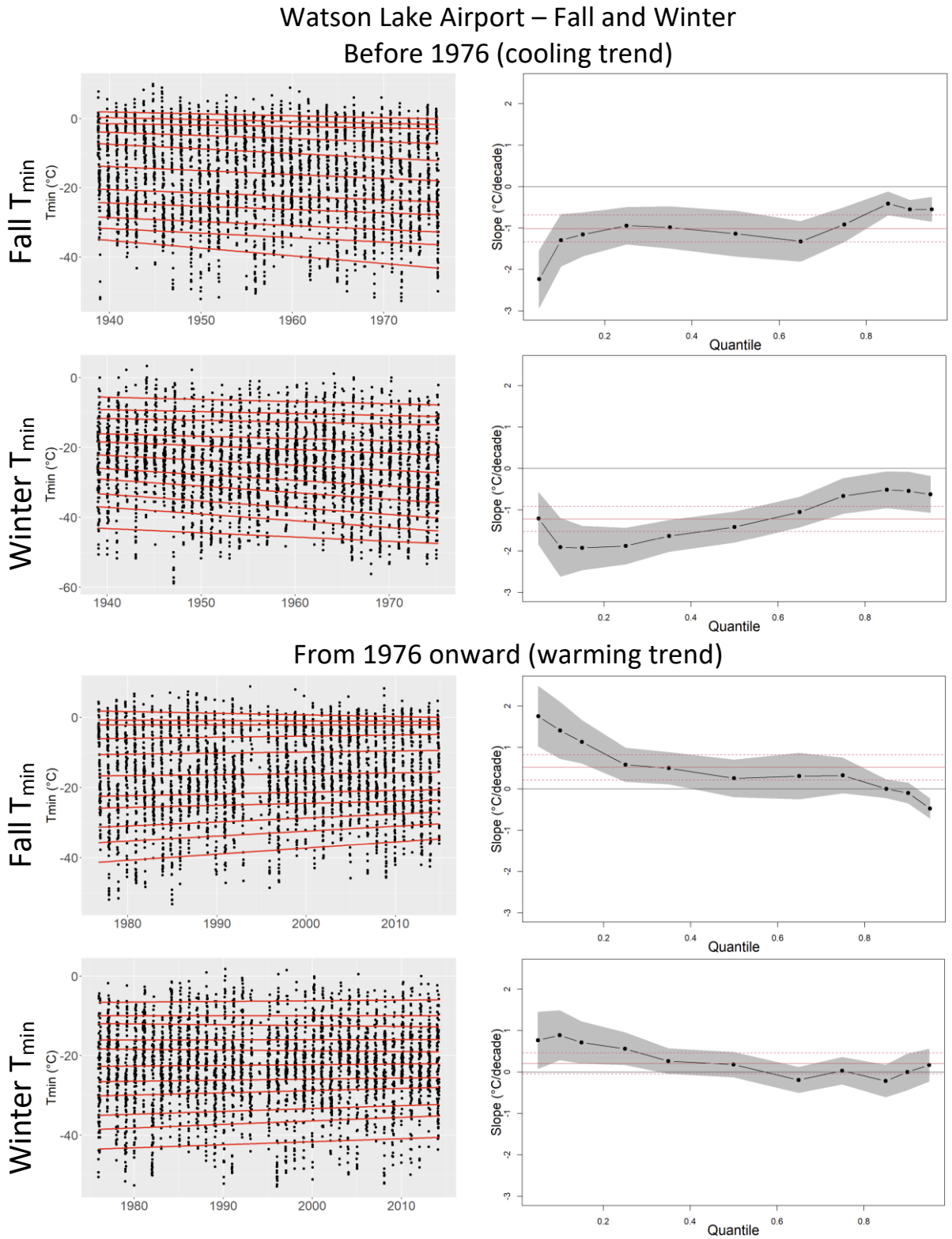

Figure 3.6 For Watson Lake Airport, temperature trends for fall (Oct-Dec) and winter (Jan-Mar).

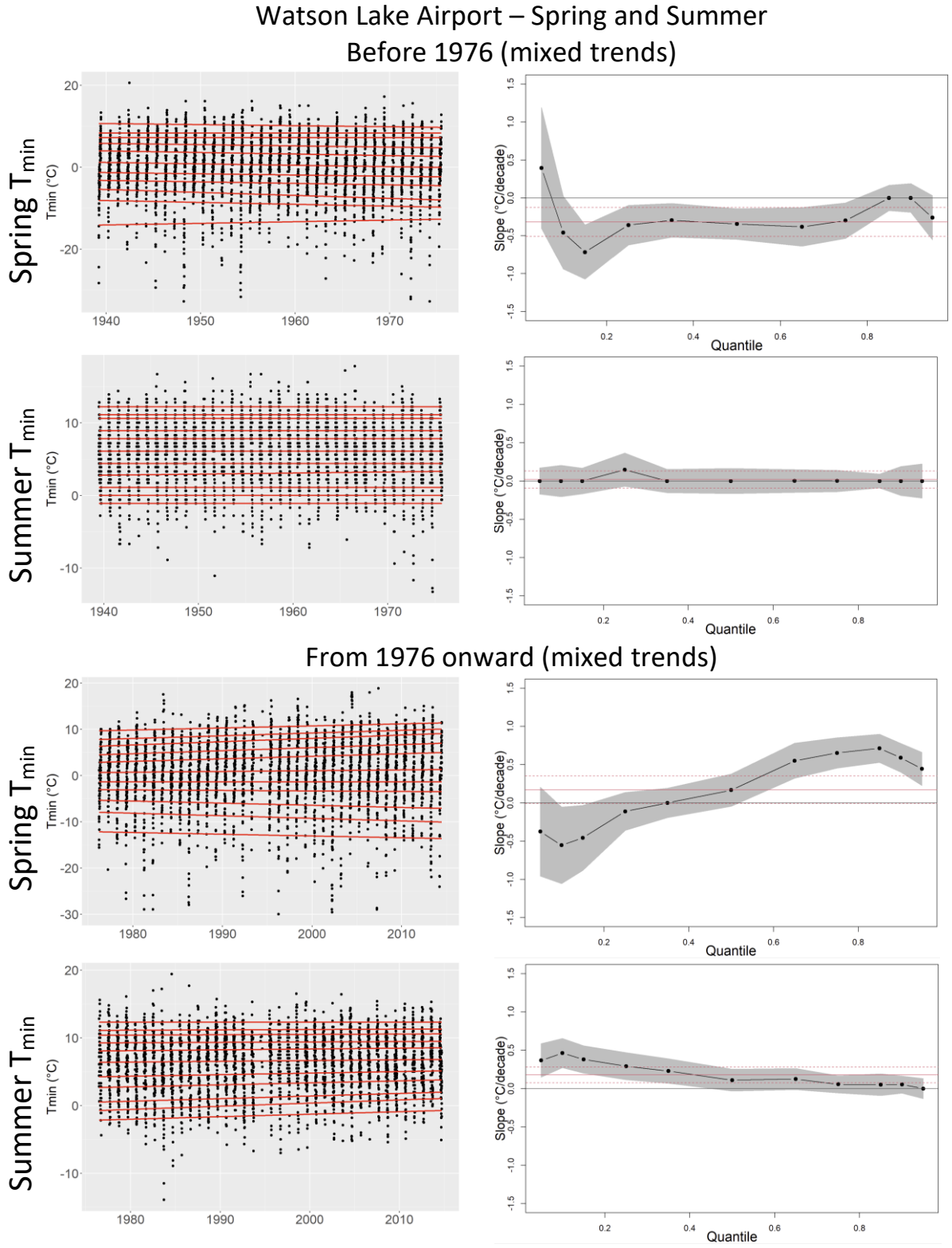

Figure 3.7 For Watson Lake Airport, temperature trends for spring (Apr-Jun) and summer (Jul-Sep).

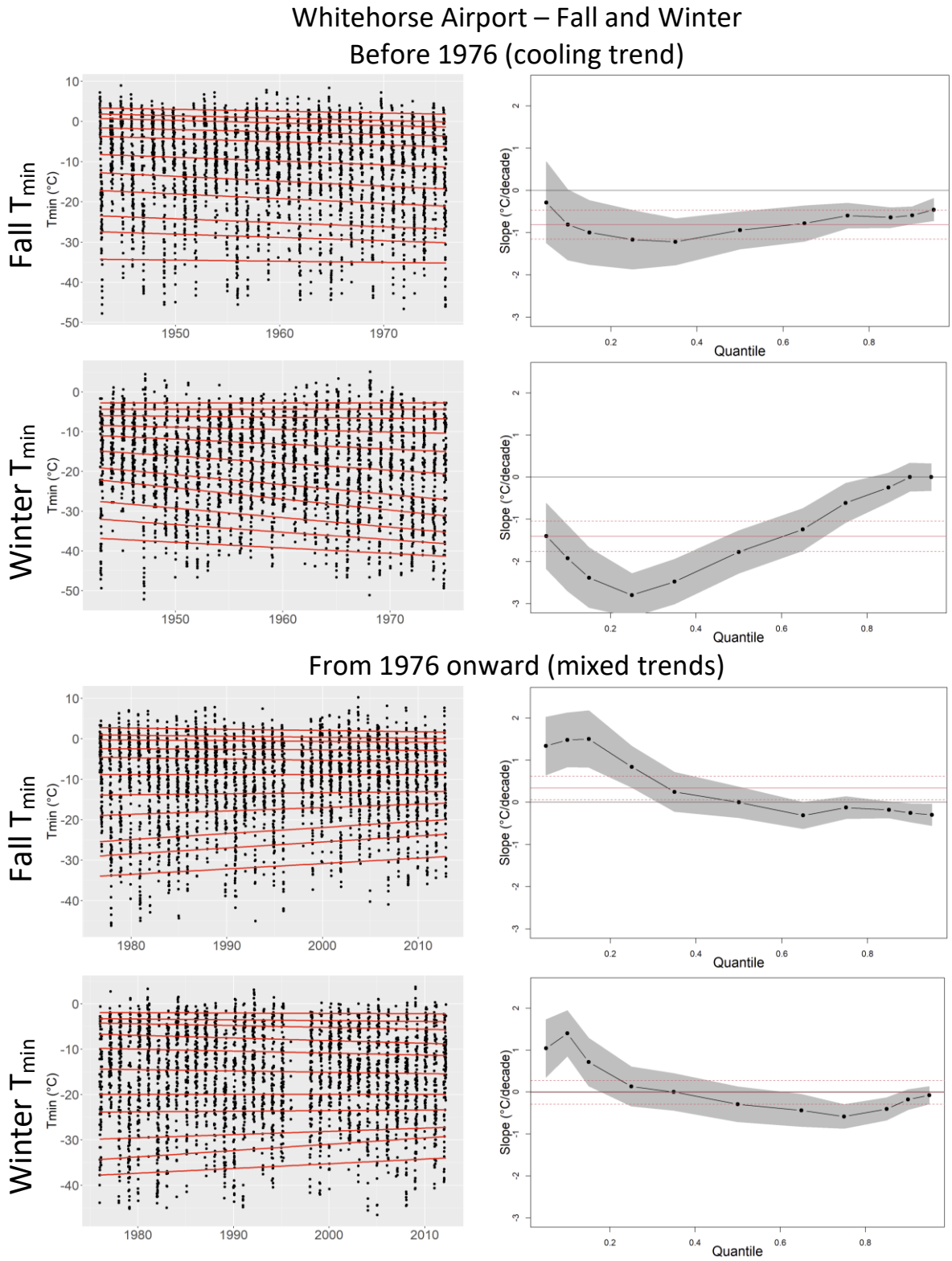

Figure 3.8 For Whitehorse Airport, temperature trends for fall (Oct-Dec) and winter (Jan-Mar).

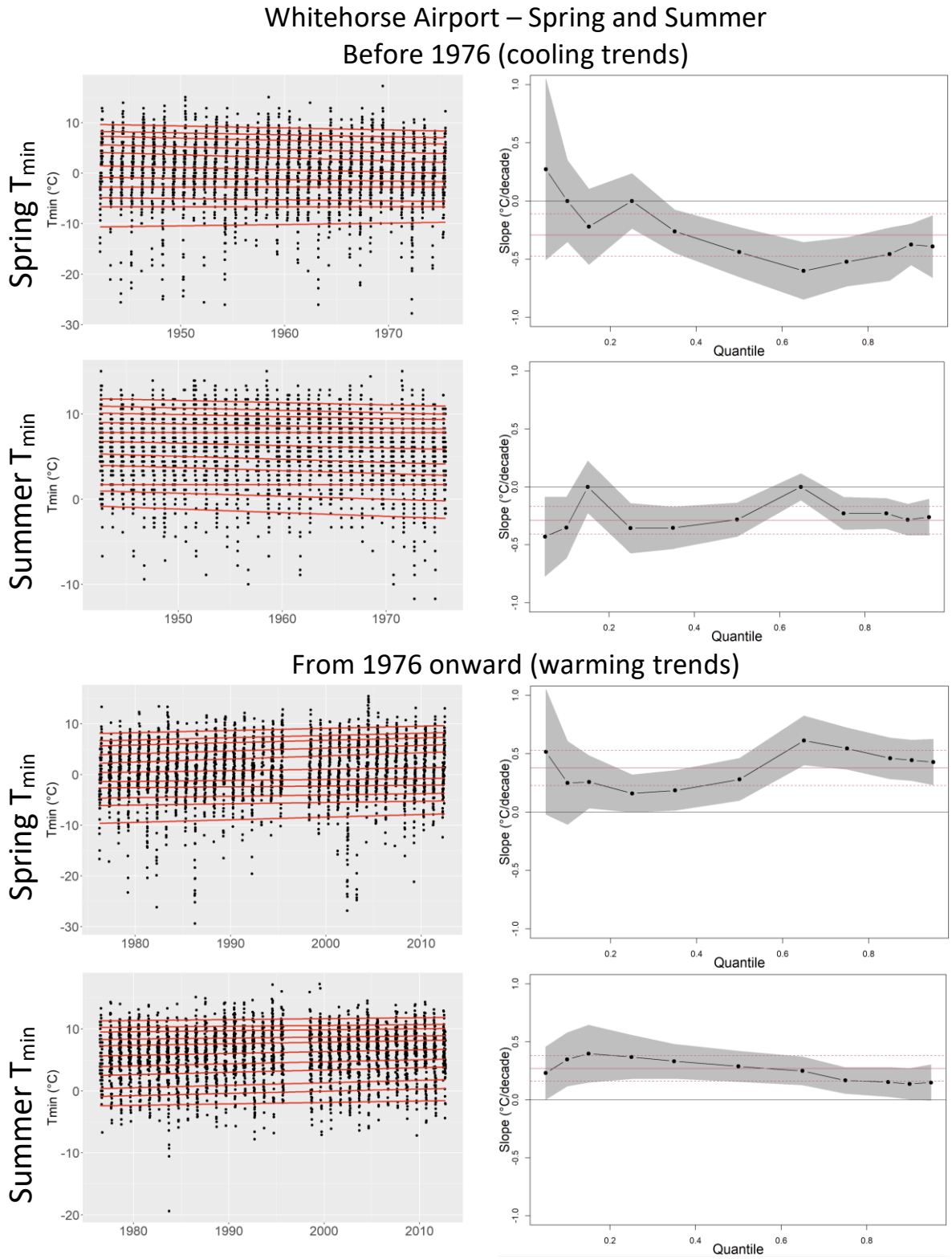

Figure 3.9 For Whitehorse Airport, temperature trends for spring (Apr-Jun) and summer (Jul-Sep).

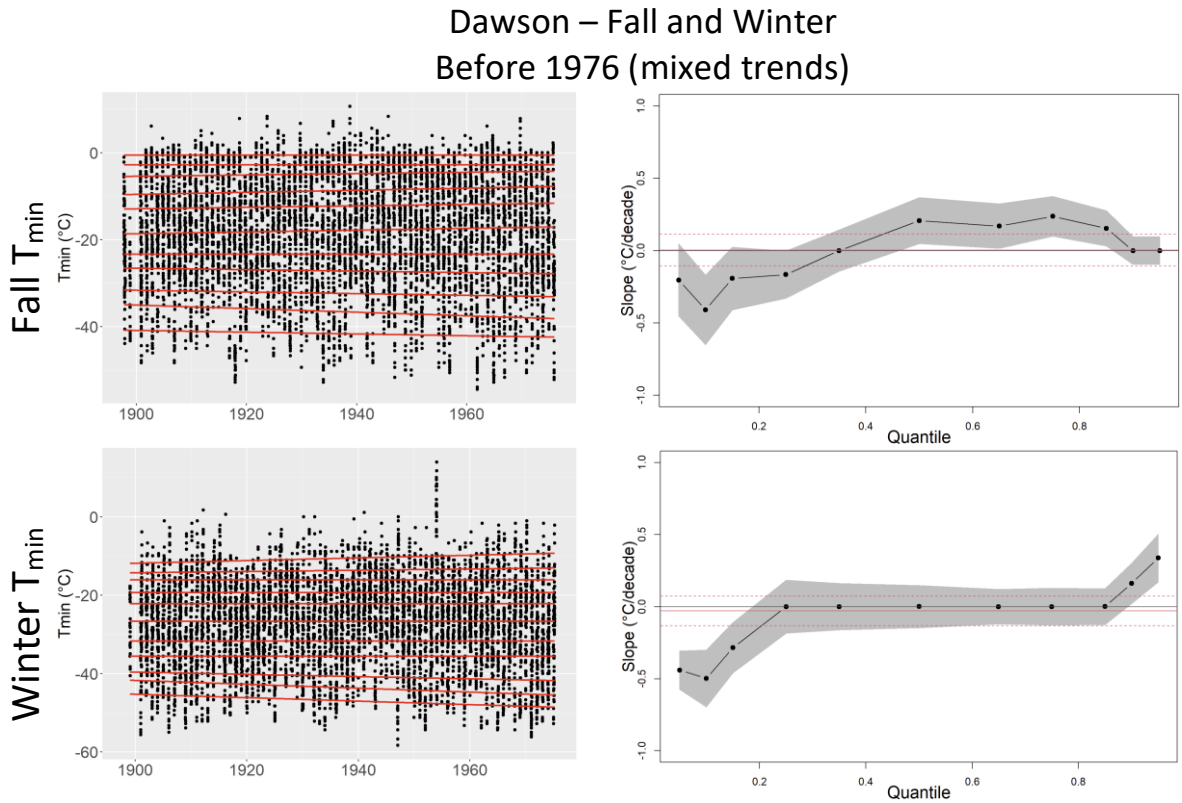

Figure 3.10 For Dawson, temperature trends for fall (Oct-Dec) and winter (Jan-Mar).

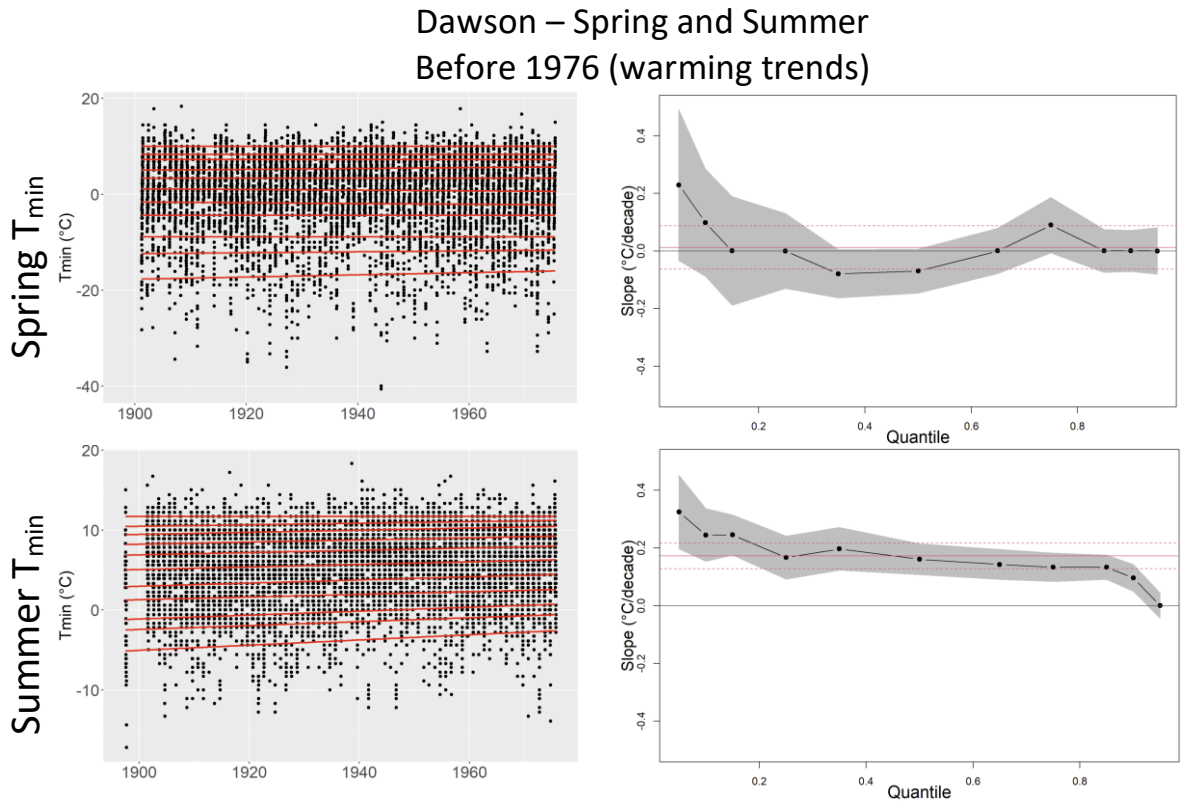

Figure 3.11 For Dawson, temperature trends for spring (Apr-Jun) and summer (Jul-Sep).

3.1.2 Trends in temperature

The Mann-Kendall test for trends was used to evaluate the statistical significance of trends. Specifically, the time series tested for each station were:

(a) the annual time series of mean Tmin seasonal temperatures,
(b) the annual time series of 5th percentile of Tmin temperatures, and
(c) the annual time series of Tmin 95th percentile.

Each of these three time series were tested for three time spans:

(i) the entire period of record,
(ii) only the pre-1976 period, and
(iii) only the post-1976 period (inclusive of 1976).

At the statistical significance level of 95%, the only trends identified as statistically significant – i.e., where the null hypothesis of no trend could be rejected with 95% confidence – were for (i) the entire period of record and only for the spring and summer seasons. Because the time series of spring and summer temperature data is clearly inhomogeneous, with rounded values in the pre-1976 period, it is possible that the significance of these trends is an artifact of the inhomogeneity.

Example results are shown for Mayo Airport in Figure 3.12 (entire record, 1925-2013) and in Figure 3.13

the post-1976 record (1976-2013).

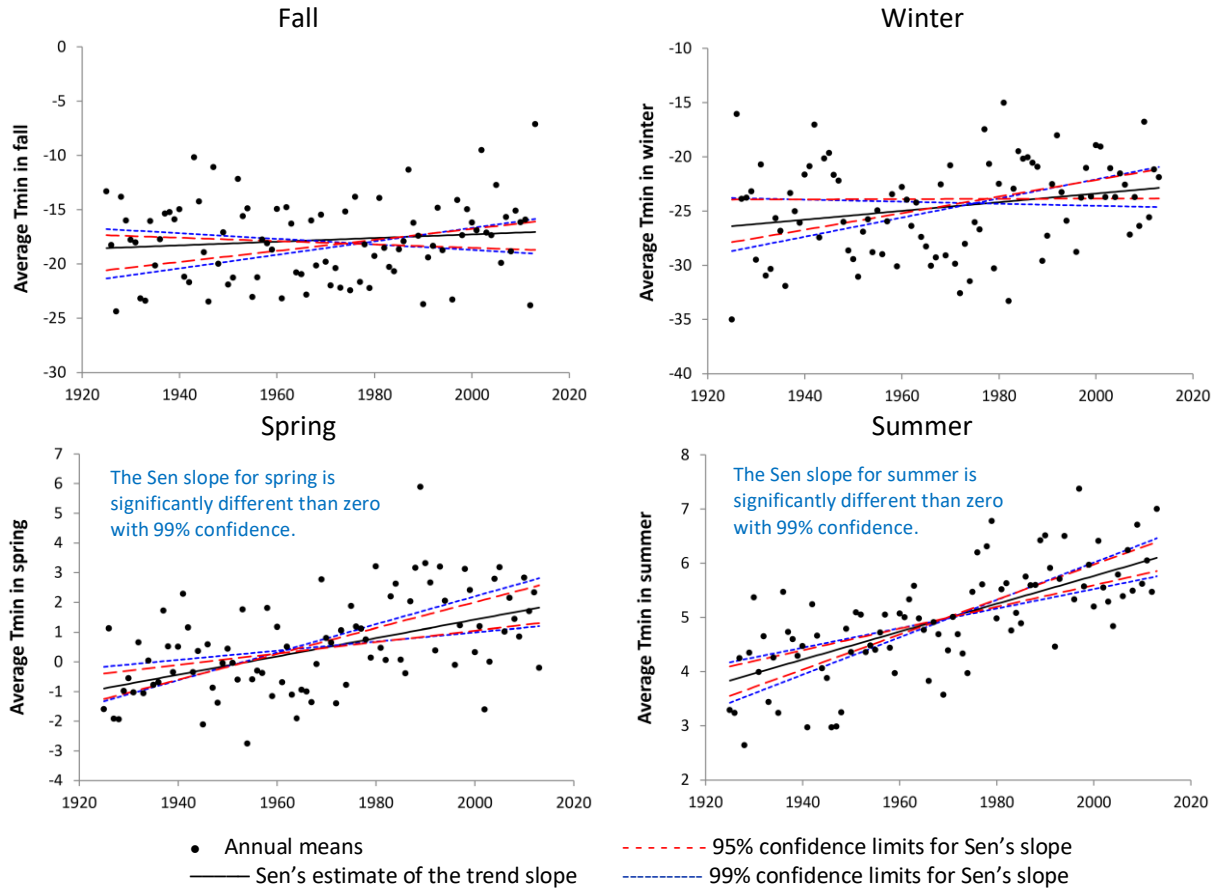

Figure 3.12 For Mayo Airport meteorological station (entire record, 1925-2013) annual time series of average seasonal Tmin, the Sen slope estimate and its confidence limits. Using the Mann-Kendall test for trends, the null hypothesis that there is no trend can be rejected (at 99% confidence level) for spring and summer, but not for fall or winter. The 95% confidence interval for the fall and winter Sen's slope includes the zero slope, therefore the null hypothesis cannot be rejected at the 95% confidence level (α=0.05). For spring and summer, it is possible that the slope significance could be a result of inhomogeneity in the time series (see text).

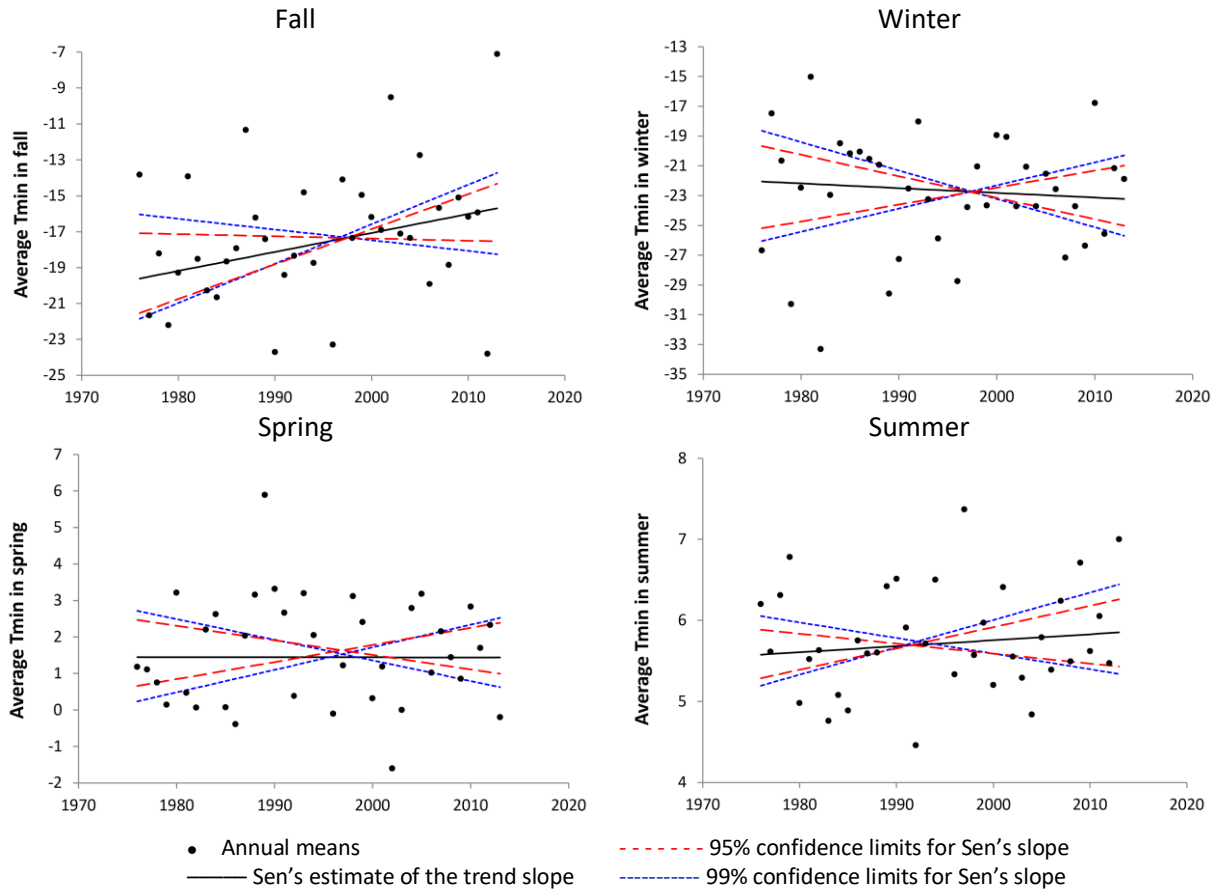

Figure 3.13 For Mayo Airport meteorological station (sub-period 1976-2013) annual time series of average seasonal Tmin, the Sen slope estimate and its confidence limits. Using the Mann-Kendall test for trends, the null hypothesis that there is no trend cannot be rejected (at 99% confidence level) for any of the seasons. For any season, the 95% confidence interval for the Sen's slope includes the zero slope, therefore the null hypothesis cannot be rejected at the 95% confidence level (α=0.05).

Analyzing the annual time series (1976-2013) of the 5th percentile of Tmin temperature, the null hypothesis that no significant trend exists cannot be rejected at the 95% confidence level (α=0.05) for any of the four seasons (Figure 3.14). The same is true of the 95th percentile (Figure 3.15). Similar results were obtained for Tmax and Tave, and for other meteorological stations (not shown).

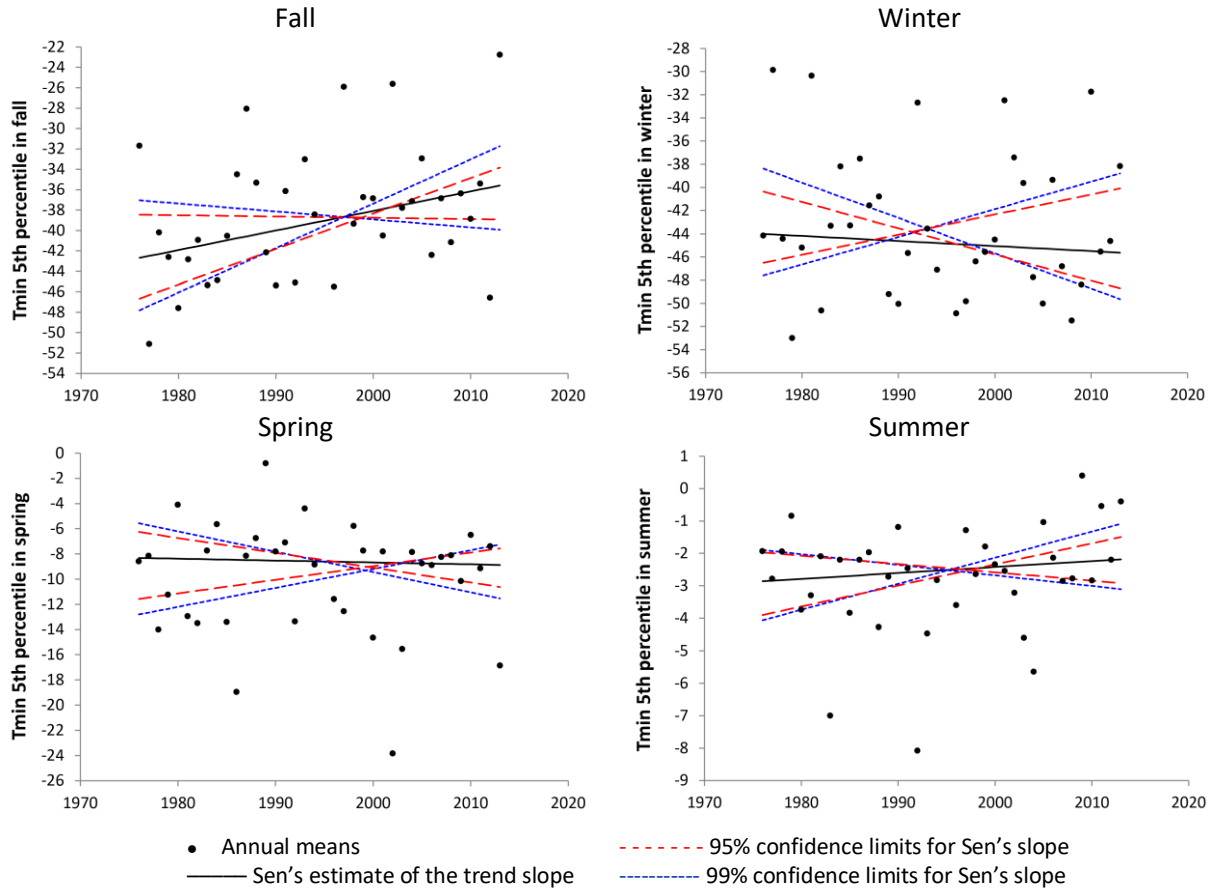

Figure 3.14 For Mayo Airport meteorological station (sub-period 1976-2013) annual time series of Tmin 5th percentile, the Sen slope estimate and its confidence limits. Using the Mann-Kendall test for trends, the null hypothesis that there is no trend cannot be rejected (at 99% confidence level) for any of the seasons. For any season, the 95% confidence interval for the Sen's slope includes the zero slope, therefore the null hypothesis cannot be rejected at the 95% confidence level (α=0.05).

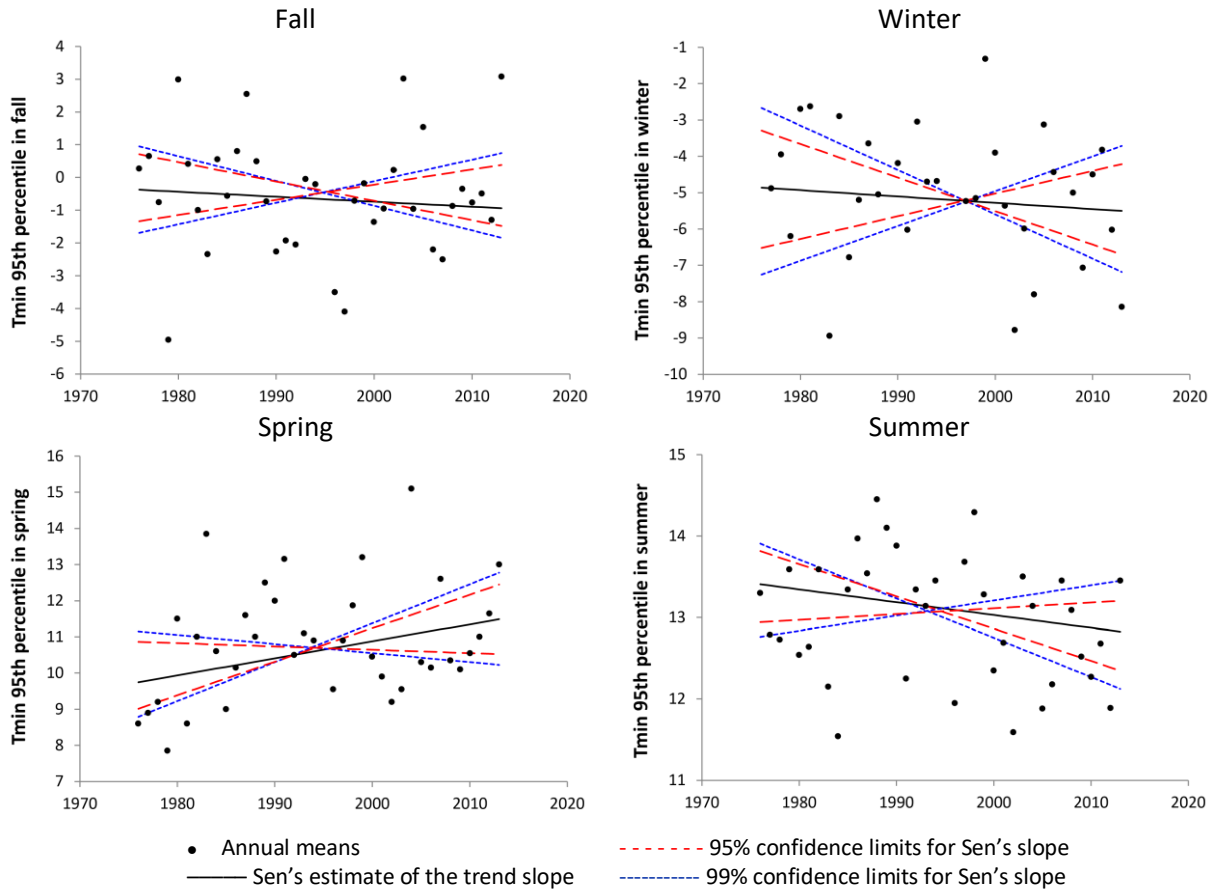

Figure 3.15 For Mayo Airport meteorological station (sub-period 1976-2013) annual time series of Tmin 95th percentile, the Sen slope estimate and its confidence limits. Using the Mann-Kendall test for trends, the null hypothesis that there is no trend cannot be rejected (at 99% confidence level) for any of the seasons. For any season, the 95% confidence interval for the Sen's slope includes the zero slope, therefore the null hypothesis cannot be rejected at the 95% confidence level (α=0.05).

3.1.3 Trends in precipitation and rain-to-snow ratio

The intense warming observed since about 1976 has not left a clear imprint over the rain-to-snow ratio recorded at the Mayo Airport meteorological station (Figure 3.16).

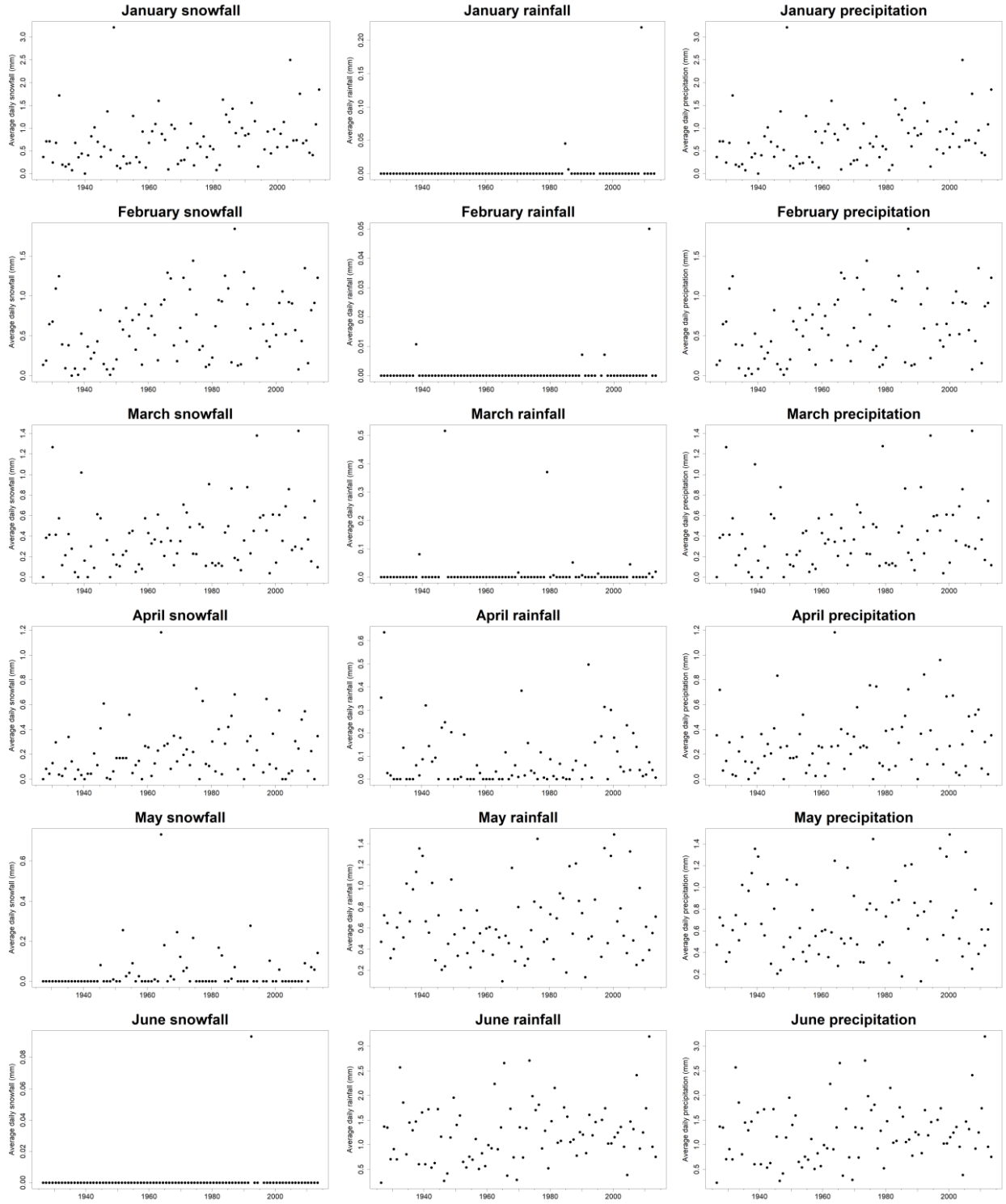

(Figure continues on the next page.)

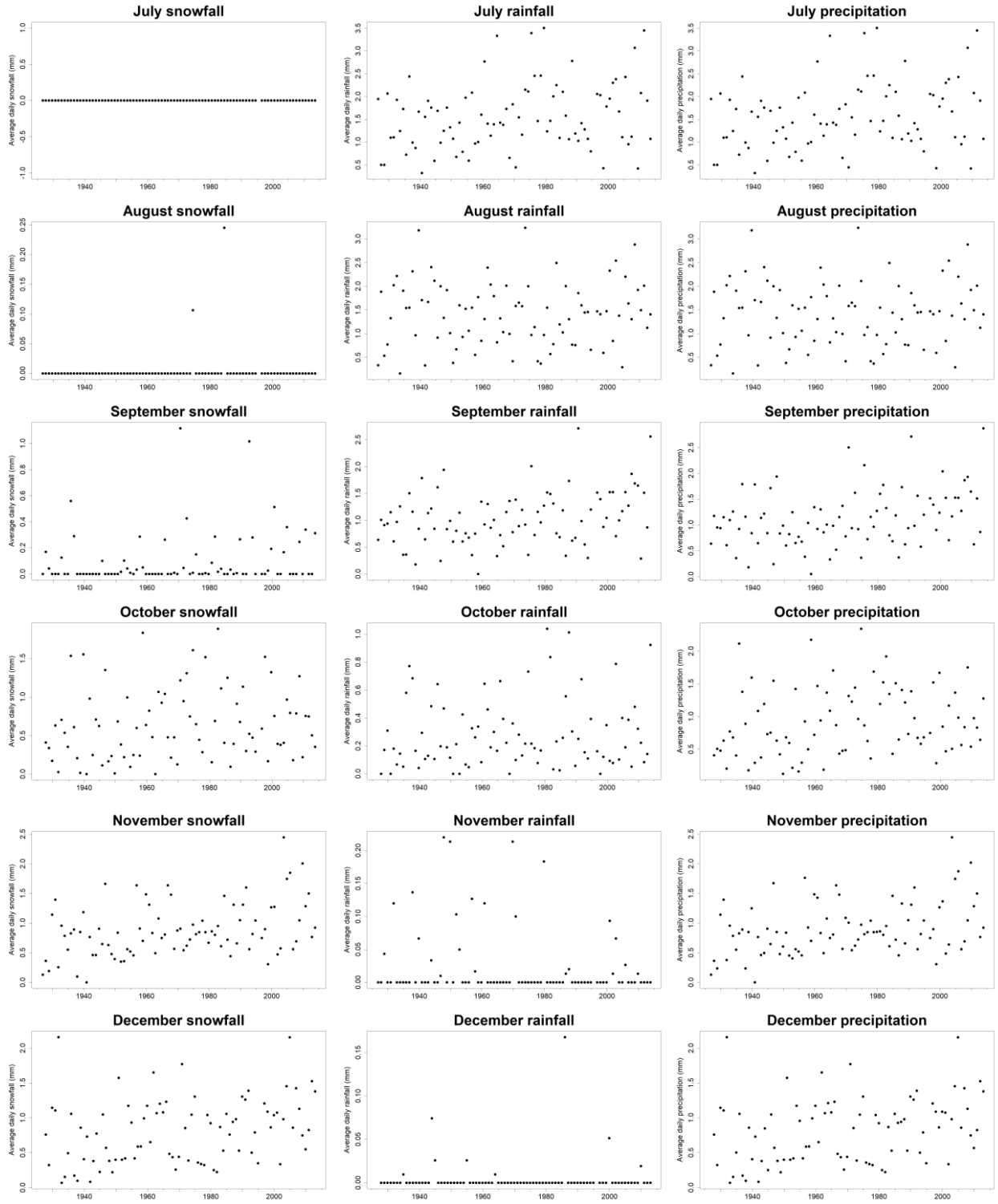

Figure 3.16 Snowfall, rainfall and total precipitation recorded at Mayo Airport meteorological station, for each month of the year. No increase in rainfall relative to snowfall is noted.

3.2 Trends in Snow Water Equivalent

Snow water equivalent (SWE) data at the start of March, February and April is available for 86 different stations across the Yukon and 51 of these stations have data extending from before 1990 until 2023 or 2022 (Figure 3.17). Most of these stations' records contain annual time series for the following three target dates:

- March 1 SWE
- February 1 SWE and
- April 1 SWE

Measurements are not generally taken on the exact target date but within 5 days (sometimes up to 10 days) prior or after the target date. For example, the March 1 target date may be represented by a measurement taken on February 25 or March 5, for example. Gaps are present but represent a small fraction of the data.

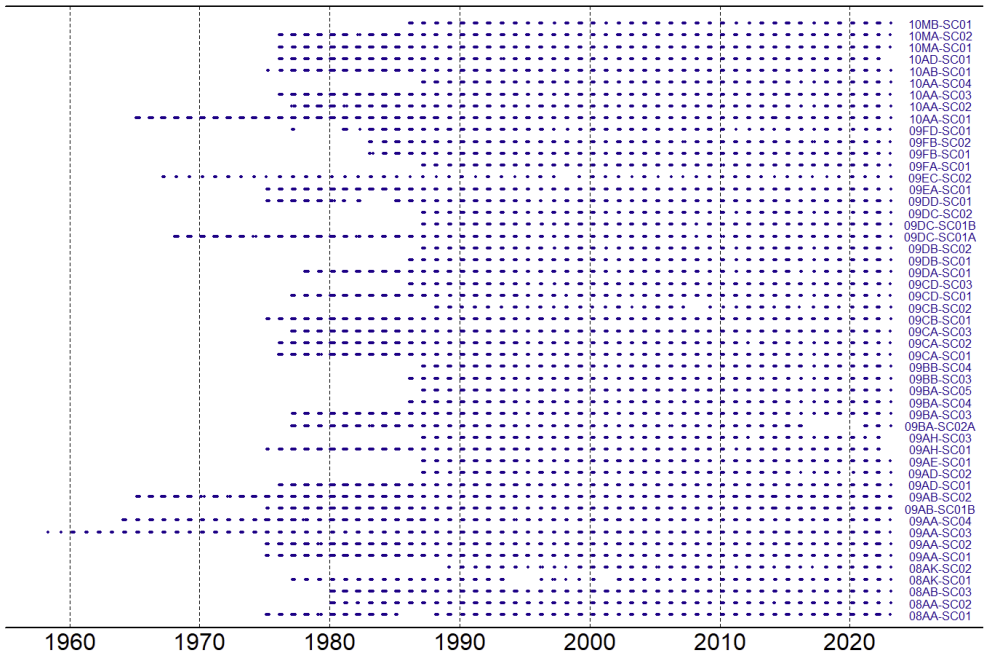

Figure 3.17 The 51 Yukon meteorological stations for which monthly SWE data is available since before 1990. The SWE data is for target dates March 1, April 1 and May 1.

The Mann-Kendall test for trends was used to determine whether any of the stations in Figure 3.17 have statistically significant trends. The number of stations found to have significant trends is: 13 stations for March 1, 12 stations for February 1 and 14 stations for April 1. All of the statistically significant trends are positive, indicating an increase in SWE for the given month, as given by Sen's slope. All but one of the 51 stations had a positive Sen's slope, and all of the statistically significant trends were positive. Stations with statistically significant trends are located in different regions of the Yukon or just across one of its borders (Figure 3.18).

Figure 3.19 shows examples of stations with statistically significant trends in monthly SWE.

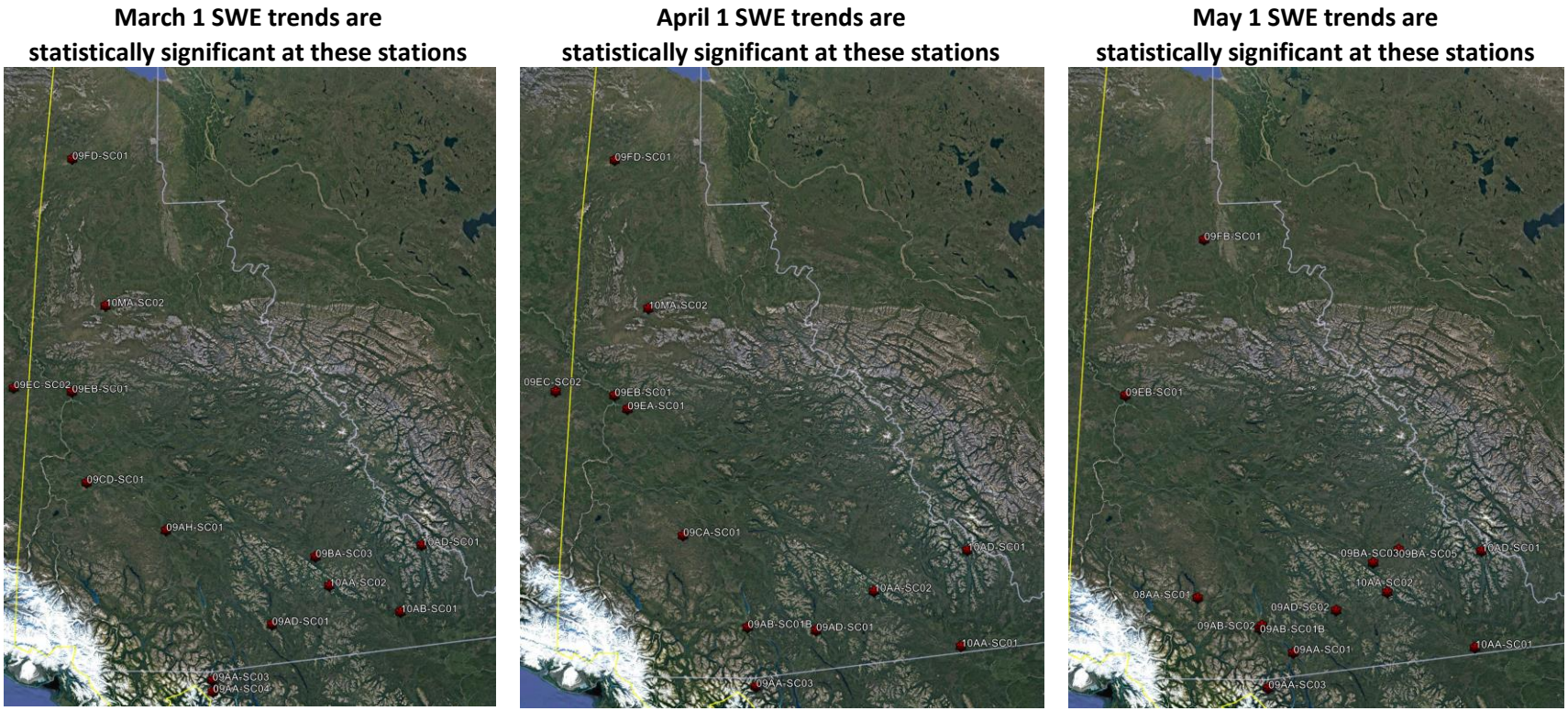

Figure 3.18 Yukon meteorological stations for which trends are statistically significant for (left panel) March 1 SWE, (central panel) April 1 SWE, and (right panel) May 1 SWE. The SWE data is for target dates March 1, April 1 and May 1.

	March 1 SWE trend	April 1 SWE trends	May 1 SWE trends
09FD-SC01	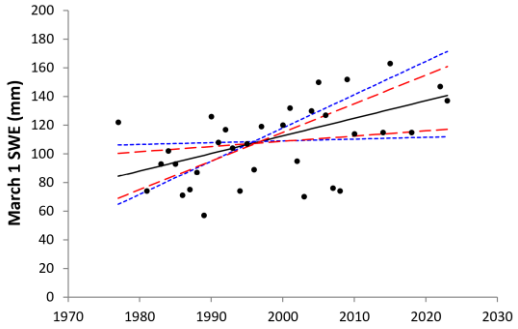	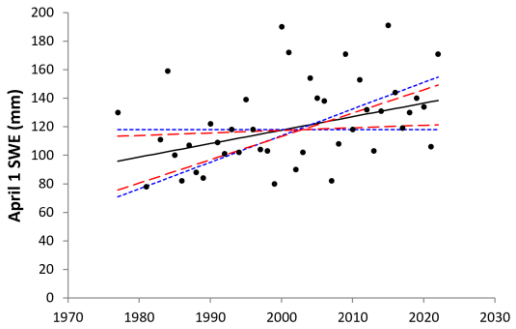	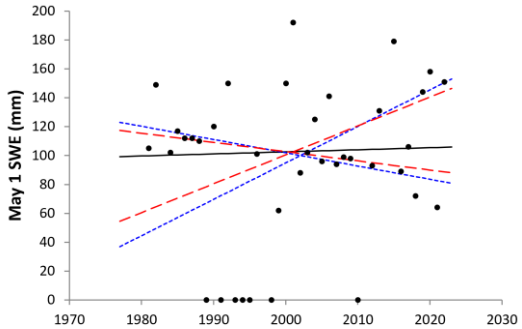
	H_0 rejected with 99% confidence. Q=1.227 mm/yr.	H_0 rejected with 99% confidence. Q=0.944 mm/yr.	H_0 cannot be rejected with 90% confidence.
10MA-SC02	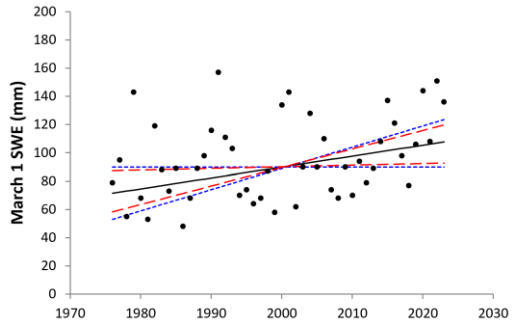	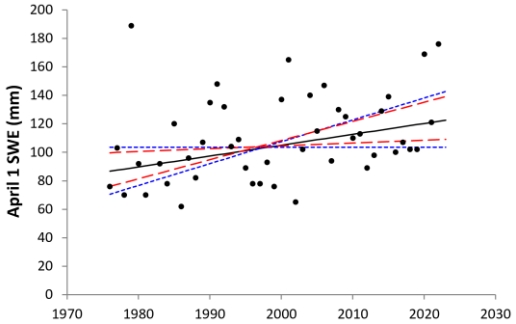	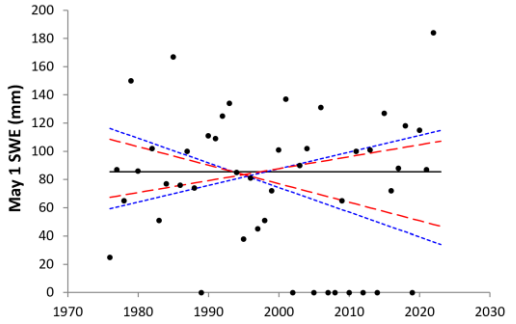
	H_0 rejected with 95% confidence. Q=0.775 mm/yr.	H_0 rejected with 95% confidence. Q=0.763 mm/yr.	H_0 cannot be rejected with 90% confidence.
09EB-SC01	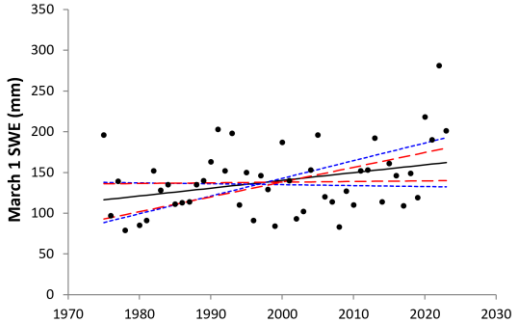	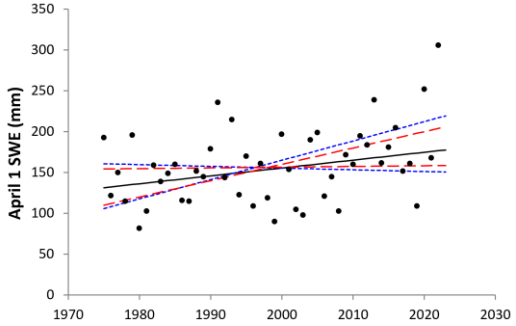	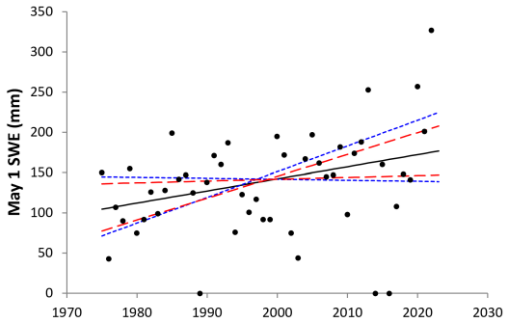
	H_0 rejected with 95% confidence. Q=0.954 mm/yr.	H_0 rejected with 95% confidence. Q=0.962 mm/yr.	H_0 rejected with 95% confidence. Q=1.500 mm/yr.

(Figure continues on the next page.)

	March 1 SWE trend	April 1 SWE trends	May 1 SWE trends
10AD-SC01	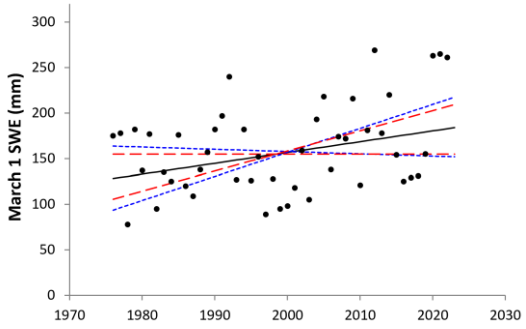	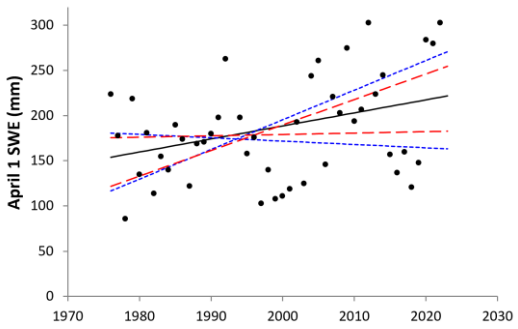	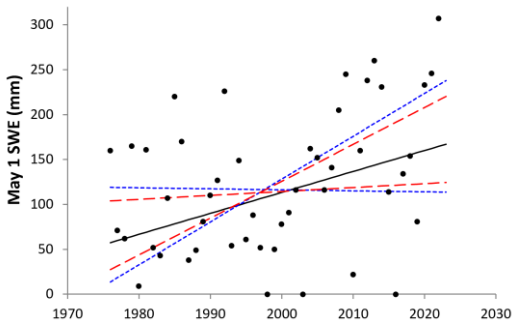
	H_0 rejected with 95% confidence. Q=1.184 mm/yr.	H_0 rejected with 95% confidence. Q=1.444 mm/yr.	H_0 rejected with 95% confidence. Q=2.333 mm/yr.
10AA-SC02	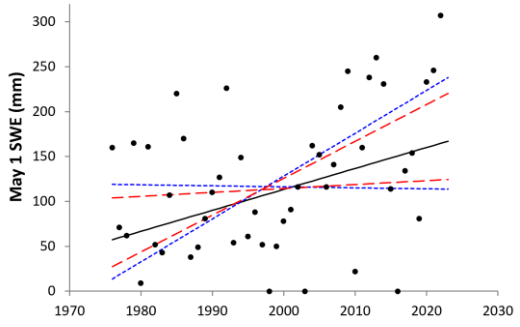	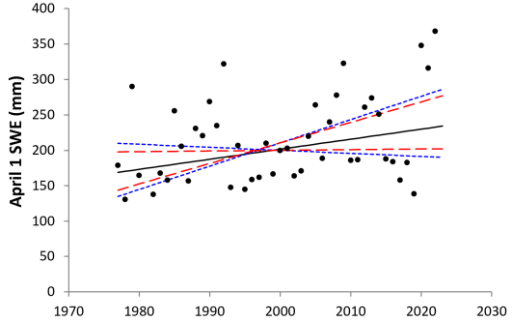	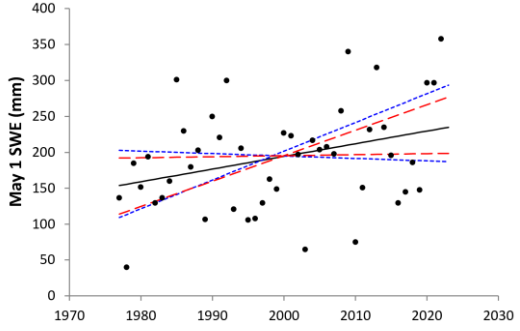
	H_0 rejected with 99% confidence. Q=1.933 mm/yr.	H_0 rejected with 95% confidence. Q= 1.142 mm/yr.	H_0 rejected with 95% confidence. Q= 1.762 mm/yr.
09BA-SC03	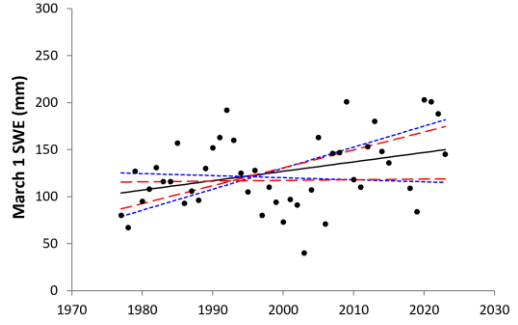	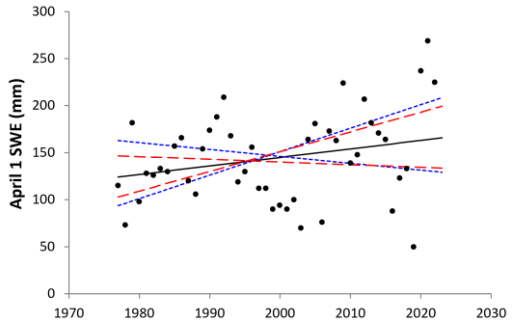	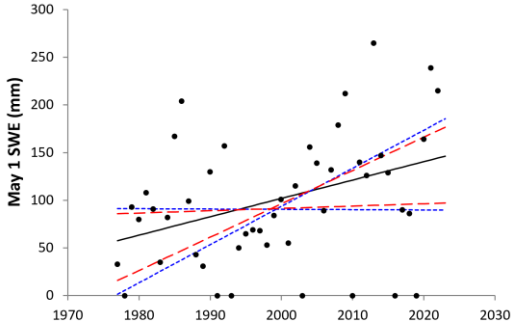
	H_0 rejected with 95% confidence. Q= 1.000 mm/yr.	H_0 cannot be rejected with 90% confidence.	H_0 rejected with 95% confidence. Q= 1.926 mm/yr.

(Figure continues on the next page.)

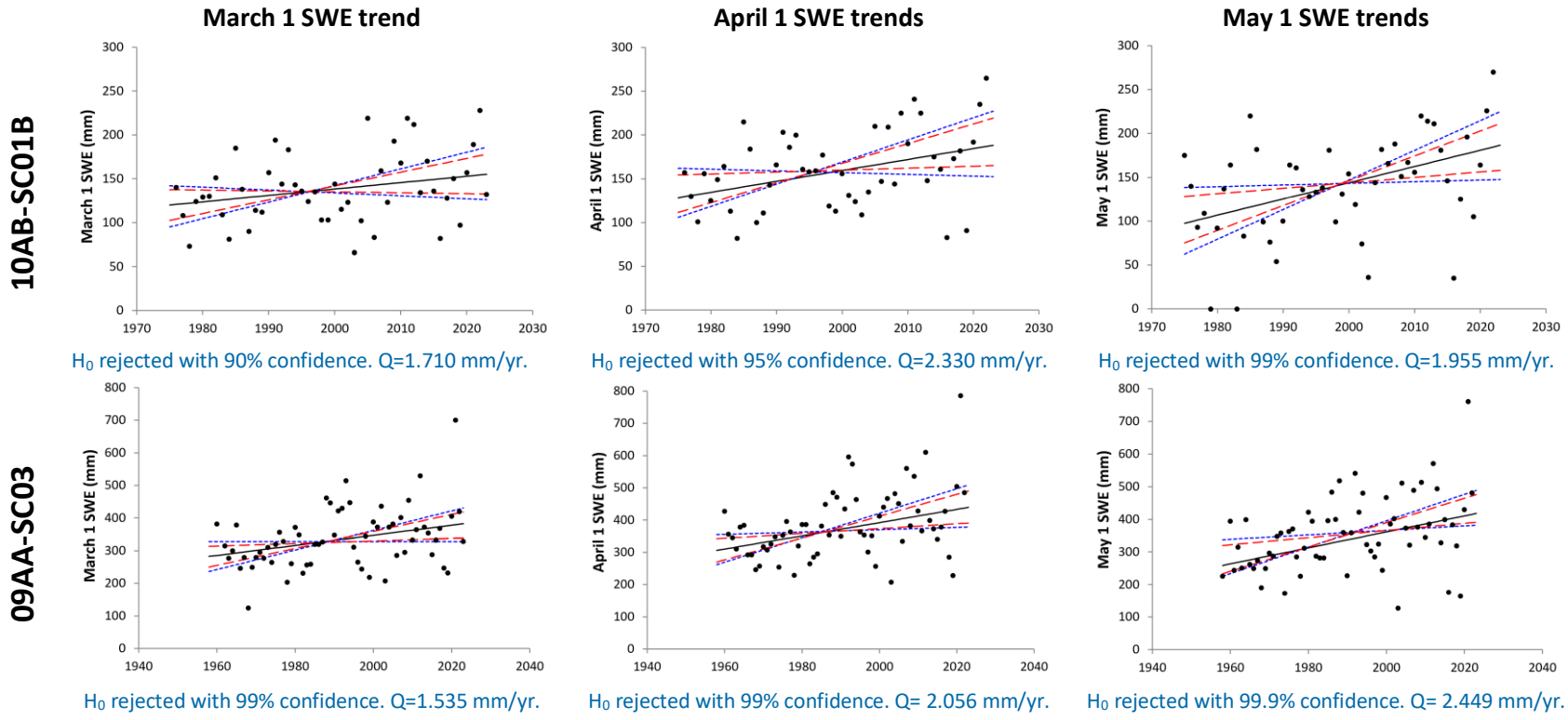

Figure 3.19 For different meteorological stations (named on the left column) the annual time series of SWE in March 1, April 1 and May 1 are plotted, and the Sen slope estimate and its confidence limits are shown. Using the Mann-Kendall test for trends, the null hypothesis that there is no trend can be rejected (at 99% confidence level) for both these months.

4 REFERENCES

Bonnaventure, P. P., and Lewkowicz, A. G. (2013). Impacts of mean annual air temperature change on a regional permafrost probability model for the southern Yukon and northern British Columbia, Canada. *The Cryosphere*, 7, 935–946. doi:10.5194/tc-7-935-2013.

Bonnaventure, P. P., Lewkowicz, A. G., Kremer, M., and Sawada, M. C. (2012). A Permafrost Probability Model for the Southern Yukon and Northern British Columbia, Canada. *Permafrost and Periglacial Processes*, 23, 52–68. doi:10.1002/ppp.1733.

Kremer, M., Lewkowicz, A. G., Bonnaventure, P. P., and Sawada, M. C. (2011). Utility of classification and regression tree analyses and vegetation in mountain permafrostmodels, Yukon Territory, Canada. *Permafrost and Periglacial Processes*. doi:10.1002/ppp.719.

Lewkowicz, A. G., and Bonnaventure, P. P. (2011). Equivalent elevation: a new method to incorporate variable lapse rates into mountain permafrost modelling. *Permafrost Periglacial Processes*, 22, 153–162. doi:10.1002/ppp.720.

Romanovsky, V. E., Smith, S. L., and Christiansen, H. H. (2010). Permafrost thermal state in the polar northern hemisphere during the International Polar Year 2007–2009: a synthesis. *Permafrost and Periglacial Processes*, 21, 106–116. doi:10.1002/ppp.689.

Smith, S. L., Romanovsky, V. E., Lewkowicz, A. G., Burn, C. R., Allard, M., Clow, G. D., Yoshikawa, K., and Throop, J. (2010). Thermal state of permafrost in North America: a contribution to the International Polar Year. *Permafrost and Periglacial Processes*, 21, 117–135. doi:10.1002/ppp.690.